

**SEISMIC PERFORMANCE EVALUATION  
OF REINFORCED CONCRETE STRUCTURES USING  
MULTI-DIRECTIONAL POLYGONAL 3D LATTICE MODEL**

**Mauro Ricardo Simão**

Supervisor: Associate Professor Tomohiro Miki

A thesis submitted to the  
Faculty of the Graduate School of  
Kobe University in partial fulfillment of  
the requirements for the degree of  
**DOCTOR OF PHILOSOPHY IN ENGINEERING**

Department of Civil Engineering  
Kobe University  
Kobe, Japan

January 2017

The thesis entitled  
Seismic Performance Evaluation of Reinforced Concrete Structures  
Using Multi-Directional Polygonal 3D Lattice Model  
written by Mauro Ricardo Simão  
has been submitted to the Department of Civil Engineering  
of Kobe University

Supervisor:

Associate Professor Tomohiro Miki

Supervising Committee:

Professor Shinichi Akutagawa

Professor Hidenori Morikawa

Professor Takashi Nagao

## **ABSTRACT**

Recently, with the advance of research and improved design methods, a big overflow of design procedures of reinforced concrete (RC) structures has been proposed in the context of performance based design. These design procedures are in many cases based on concrete mechanics and are applied by the nonlinear analysis. On the other hand, with recent seismic events and developments in the field of earthquake engineering, a new shift in the seismic evaluation of RC structures has occurred and the specifications in many countries try to keep up with the most recent developments in this field.

With the advent of three dimensional (3D) analytical methods, the seismic performance in can now consider the effects of combination of bilateral bending, shear and torsion that actual structures are subjected to during actual earthquakes. However with all these developments little attention has been paid to geometrical particularities of RC members such as circular cross-section geometry. On the other hand, is seismic design, while the new keywords revolve around performance evaluation, there is lack of clarity on the meaning of performance based design in some cases, and especially when performance is based on the numerical verification of damage conditions.

With the above in mind, the aim of this study is to generally propose the 3D lattice model which has been enhanced from a 2D lattice model to assess the seismic performance of RC structures. In order to do that, two conceptual categories were used: first is the development of a 3D lattice model aimed at circular-cross section columns. In this conceptual part, issues of performance are evaluated based on response of RC members and analysis of criteria related to force and displacement. In order to achieve that, a multi-directional polygonal 3D lattice model is proposed and the applicability to discretize and correctly represent the structural response is verified by performing static and dynamic analyses in RC columns.

In seismic events, after cracking of concrete, there is a change in the gross shear resisting area capacity of concrete as well as degradation of stiffness. In the modeling using the multi-directional polygonal 3D lattice model these two important issues are studied .The applicability of the multi-directional polygonal 3D lattice model is further extended to perform cumulative seismic damage evaluation in RC columns. In seismic events, RC structures are subjected in many times to multiple sequences of motion; therefore it is important to study this effect from the force and displacement point of view, as well as understanding the effect of residual displacement in every new loading of RC structures, and in this study that is carried out by the multi-directional polygonal

3D lattice model.

On the other hand in this study, performance evaluation of RC structures under seismic motion is evaluated from the energy approach. A numerical verification method of performance of RC structures in seismic analysis is proposed by performing damage evaluation of existing RC structures from the material point of view. One of the key points from the fracture mechanics is that the global structural behavior of a structure is affected first and foremost by the material behavior. On the other hand in the mechanics of solids it is said that the strain energy density of the material can inform us about the nature and behavior of the material, whether that is a brittle material or ductile. In this study based on that a choice was made to perform damage evaluation from the material point of view based on the energy dissipation criteria.

One of the key characteristics about the way the discretization of structure is performed using the lattice model is that it allows the individual analysis of stress-strain relationship of each element. That means that the strain energy density can be evaluated individually and from that the global behavior of structure understood. Based on that, a damage index can be proposed from the stress-strain relationship of each one of these elements.

The way the proposed damage index works, is by establishing a ratio between ultimate energy dissipation capacity of a RC member and the accumulated energy dissipation that is captured from the response under seismic motion. In the analysis special attention is given to concentration of damage in the RC structures. The method is verified by performing numerical verification of RC columns that have been subjected to cyclic loading and also by performing dynamic analysis of RC column that has been tested by a shake-table test.

In order to extend the concept of energy based damage evaluation proposed in this study, the nonlinear analysis using the 3D dynamic lattice model is performed on actual RC structures. The target used in the analysis is actual rigid-frame RC viaducts damaged at 1995 Hyogo-ken Nanbu Earthquake. This RC viaduct has slight damage with diagonal cracks and the buckling of longitudinal reinforcement. The results of dynamic analysis are compared with actual damages of RC viaducts. The comparison reveals the reliability of the 3D dynamic lattice model at the structural system level. It is also found that the analysis can predict the damage conditions.

## **ACKNOWLEDGEMENTS**

First and foremost I would like to express my deep gratitude to my supervisor Associate Professor Tomohiro Miki for his superb guidance and unconditional support during the 6 years in which I have been a member of the structural concrete laboratory. For that, a lifetime of gratefulness will never be enough to express my gratitude towards my Professor and I am forever indebted to him.

I would like express my gratitude to Professor Shinichi Akutagawa, Professor Hidenori Morikawa and Professor Takashi Nagao, members of the supervising committee, for taking the time to be in the committee and contributing to the refinement of this work.

My sincere words of thanks go to Professor Satoru Oishi, Professor Hideyuki Kita, Associate Professor Yasuko Kuwata and Associate Professor Toshimori Otazawa for the immeasurable kindness and advice throughout all these years of graduate studies.

I would like to acknowledge Professor Óscar Mário Cavele my undergraduate professor of structural mechanics, who recently passed away, for early on strongly encouraging me to pursue my interest in structural engineering and for patiently teaching me the fundamentals of engineering mechanics.

I would like to acknowledge the members of Professor Miki's Laboratory and Professor Kuwata's Laboratory past and present for the great atmosphere and shared sense of duty and for always helping me out with Japanese language.

I want to thank my family, especially my father *Engenheiro* Amândio Santos Simão for bringing engineering into our household and unconditionally supporting my vision.

I want to thank my friends in Japan and Mozambique, especially Dr. Nader Al-Juma'I from Kwansei Gakuin University with whom I have shared this journey from day one.

I want to thank Dr. Letícia Sarmiento dos Muchangos from Osaka University, my fellow engineer, my best friend and my life partner for all the love, continuous debate of ideas, support and the years of her life she has been giving me. Our journey has just begun.

## TABLE OF CONTENTS

ABSTRACT .....	I
ACKNOWLEDGEMENTS .....	III
1. GENERAL INTRODUCTION .....	1
1.1. BACKGROUND .....	1
1.2. LITERATURE REVIEW.....	3
1.2.1. 3D nonlinear analysis of concrete structures.....	3
1.2.2. Damage Evaluation of RC Structures.....	4
1.2.3. Seismic Design Philosophies of RC Structures.....	6
1.3. SCOPE AND OBJECTIVES .....	8
1.4. CONTENTS OF THE THESIS .....	9
REFERENCES OF CHAPTER 1.....	10
2. ANALYTICAL MODEL.....	13
2.1. INTRODUCTION.....	13
2.2. OUTLINES OF 2D LATTICE MODEL .....	13
2.3. MATERIAL MODELS.....	15
2.3.1. Compressive stress-strain relationships for concrete.....	15
2.3.2. Tensile stress-strain relationships of concrete .....	17
2.3.3. Reinforcement model .....	18
2.4. OUTLINES OF 3D LATTICE MODEL .....	19
2.4.1. Configuration of elements .....	21
2.5. NONLINEAR ANALYSIS PROCEDURE .....	24
2.6. CYCLIC ANALYSIS OF RC COLUMNS USING 2D LATTICE MODEL.....	25
2.6.1. Outline of experiment and analysis .....	25
2.6.2. Lateral force-displacement characteristics of RC column.....	26
2.7. STATIC ANALYSIS OF RC COLUMNS SUBJECTED TO BILATERAL LOADING USING 3D LATTICE MODEL .....	28
2.7.1. Outline of experiment and analysis .....	28
2.7.2. Analytical results and discussion.....	29
REFERENCES OF CHAPTER 2.....	32
3. DEVELOPMENT AND APPLICATION OF MULTI-DIRECTIONAL POLYGONAL 3D LATTICE MODEL.....	34
3.1. INTRODUCTION.....	34

3.2. MODELING AND GEOMETRY OF MEMBERS .....	34
3.3. CROSS-SECTIONAL AREA OF LATTICE MEMBERS .....	36
3.3.1. Cross-sectional area of arch members .....	37
3.3.2. Cross-sectional area of truss members .....	39
3.4. PARAMETRIC ANALYSIS OF RELATIONSHIP BETWEEN ARCH AND TRUSS MEMBERS	40
3.4.1. Introduction .....	40
3.4.2. Effect of value of $t$ .....	40
3.5. LINEAR-ELASTIC ANALYSIS OF CIRCULAR-CROSS SECTION RC COLUMNS.....	42
3.5.1. Introduction .....	42
3.5.2. Outline of analytical target .....	42
3.5.3. Discretization of target .....	42
3.5.4. Analytical results and discussion.....	43
3.6. STATIC ANALYSIS OF CIRCULAR RC COLUMNS SUBJECTED TO CYCLIC LOADING.	44
3.6.1. Outline of analysis .....	44
3.6.2. Analytical results and discussion.....	46
3.7. DISCRETIZATION METHOD ANALYSIS OF CIRCULAR RC COLUMNS.....	47
3.7.1. Introduction .....	47
3.7.2. Outline of analysis .....	47
3.7.3. Analytical results and discussion.....	49
3.8. CUMULATIVE SEISMIC DAMAGE ASSESSMENT IN CIRCULAR RC COLUMNS.....	52
3.8.1. Introduction .....	52
3.8.2. Outline of analysis .....	53
3.8.3. Analytical results and discussion.....	55
REFERENCES OF CHAPTER 3.....	59
4. NUMERICAL VERIFICATION OF SEISMIC PERFORMANCE OF CIRCULAR RC COLUMNS USING MULTI-DIRECTIONAL POLYGONAL 3D LATTICE MODEL.....	60
4.1. INTRODUCTION.....	60
4.2. ENERGY DISSIPATION CAPACITY IN RC COLUMNS .....	61
4.2.1. Introduction .....	61
4.2.2. Hysteretic energy dissipation.....	61
4.2.3. Elemental energy dissipation.....	62
4.3. DAMAGE RANGE EVALUATION .....	63
4.3.1. Introduction .....	63
4.3.2. Evaluation of seismic damage using damage index .....	64

4.4. NUMERICAL VERIFICATION OF SEISMIC PERFORMANCE .....	65
4.4.1. Analytical frame-work.....	65
4.4.2. Evaluation of performance states .....	67
4.5. NUMERICAL VERIFICATION OF SEISMIC PERFORMANCE OF RC COLUMN SUBJECTED TO CYCLIC LOADING.....	68
4.5.1. Outline of analysis .....	68
4.5.2. Analytical results and discussion.....	69
4.6. PERFORMANCE EVALUATION OF RC COLUMNS SUBJECTED TO SEISMIC MOTION DESIGNED ACCORDING TO 2002 JRA SPECIFICATIONS .....	71
4.6.1. Outlines of Analysis .....	71
4.6.2. Analytical results and discussion.....	72
REFERENCES OF CHAPTER 4.....	75
5. PERFORMANCE EVALUATION OF RC VIADUCT .....	77
5.1. INTRODUCTION.....	77
5.2. DAMAGE DISTRIBUTION IN RC VIADUCTS BASED ON ENERGY DISSIPATION.....	78
5.2.1. Outline of target structure.....	78
5.2.2. Configuration of lattice model.....	79
5.2.3. Damage distribution of Hansui R5 viaduct .....	81
5.3. NUMERICAL VERIFICATION OF SEISMIC PERFORMANCE OF HANSUI R5 VIADUCT .	84
5.4. SEISMIC DESIGN AND RETROFIT CONSIDERATIONS BASED ON 3D LATTICE MODEL .....	87
REFERENCES IN CHAPTER 5.....	88
6. CONCLUSIONS AND RECOMMENDATIONS FOR FUTURE RESEARCH .....	89
6.1. GENERAL CONCLUSIONS .....	89
6.2. RECOMMENDATIONS FOR FUTURE RESEARCH .....	91
6.3. FURTHER CONTRIBUTIONS AND DISCUSSION.....	92



# **1. GENERAL INTRODUCTION**

## **1.1. Background**

In the last few decades, a considerable number of very strong earthquakes have occurred in many parts of the world. That has been the case in the United States of America with the Loma Prieta Earthquake in 1989 and the Northridge Earthquake in 1994. In the People`s Republic of China the 2008 Sichuan Earthquake caused great damage to social infrastructure, in New-Zealand the Christchurch Earthquake in 2011 caused great social and financial damage and in japan, a country very vulnerable to earthquakes, a number of strong seismic events such as the Great Hanshin Earthquake (Kobe Earthquake) in 1995, the Great Eastern Japan Earthquake (Tohoku Earthquake) in 2011 and more recently the Kumamoto Earthquake in 2016 exposed the vulnerabilities that social infrastructures are subjected to in the event of strong seismic actions.

With such potential to cause financial damage and destruction of social infrastructure, the effect earthquakes have on public infrastructures such as water and gas pipelines, roads and viaducts should be object of close attention to the Civil Engineering community. In the event of earthquakes, reinforced concrete (RC) structures are very vulnerable to damage in general, but that is particularly the case of RC bridges and viaducts. Because of the complexity of different earthquakes and the response that different RC structural members tend to show under seismic excitation, the study and analysis of seismic response is inherently highly nonlinear. In recent times, design engineers are encouraged by design codes to address these nonlinearities during the design process. In japan the benchmark to this shift in the design process occurred after the Great Hanshin Earthquake in 1995. For structural design, the standard specifications for seismic performance verification of concrete structures (JSCE 2002) have been extensively revised. The core concept in this revision was that considerable inelastic deformation of RC structures is possible after the longitudinal reinforcement yield. This concept moved from the previous consideration of only the elastic behavior when the structure is subjected to strong earthquake motion. Furthermore in these revisions, the ductility design criterion is adopted, replacing the criterion for load carrying capacity to determine the deformation capacity of RC structures. It is also noteworthy that under these revisions, the designers are required to perform verifications using dynamic analysis. The applicability of this requirement has been greatly enhanced by the recent developments in the field of earthquake engineering, which allowed the use of the input ground motion that has been recorded during actual earthquakes.

The upgrade in the design requirements of concrete structures has been made possible by important contributions in analysis technology and methods. For example the structural response in dynamic analysis for RC columns is considered analyzing the principal axes of structural systems, but in reality the actual ground-motion is applied in three-dimensional (3D) way in the actual structures from different directions of its principal axes. Under these conditions, the behavior becomes more complex than under uniaxial motion and 3D analysis is indispensable to clarify the seismic performance of RC columns subjected to multi-directional ground motion (Miki 2004). In the current research for advanced analytical technology where 3D constitutive models with special focus on cracking of concrete applied to nonlinear analysis are the target, nonlinear finite element analysis using the solid element has been proposed (Hauke et al. 2000, Maekawa et al. 2001, Tsuchiya et al. 2002) and nonlinear analysis using three-dimensional lattice model (Miki and Niwa 2004) has also been proposed. The principal merit of the mentioned analysis tools is that they can reliably capture the response of RC structures. However the 3D finite solid element analysis requires powerful computational capability and the computation times is quite large due to the large number of degrees of freedom, which contrasts with the nonlinear analysis using three-dimensional lattice model where due to its simple and efficient 3D numerical approach the analysis difficulties are tackled with more ease.

Based on the outcome of recent research on design of RC structures, a new era is inaugurated which is focus on the notion of performance based design of structures. Many propositions have been made. At the core of it are the damage evaluation models, which generally state that performance verification of RC structures is realized through the evaluation of seismic damage of RC structures. Early models tended to evaluate seismic damage in terms of deformation capacity, but notably Park and Ang (1985) conveyed that seismic damage on a structure is centered around the earthquake energy input and the structural mechanical dissipated energy, therefore in their proposition, the Park-Ang damage model, damage is evaluated by a combination of excessive deformation and a ratio of plastic strain energy. More and more the research on the performance evaluation of RC structures under seismic motion recognizes the importance of energy based criteria for analysis as well as the need to reduce the complexities of analysis by combining efficient but powerful analytical tools for the analysis of the behavior of RC structures with simple but practical methods to perform damage evaluation of RC structures under seismic motion and ultimately performance evaluation and performance based design.

## **1.2. Literature Review**

### **1.2.1. 3D nonlinear analysis of concrete structures**

In order to perform structural analysis of concrete structures, the target structure should be discretized using one of many modeling tools currently developed. On the modeling process it is important to clarify the scale or level in which the discretization takes place. Generally three levels are recognized in the analytical modeling that is: macro-level, meso-level and micro-level. Furthermore in recent literature, a very strong focus on 3D modeling has emerged. In these 3D models two major issues are at the center: the first is treating structural members in 3D space which has implications in geometry of the structures and loading conditions and second is expressing the stress field by means of full 3D solid elements. Below a brief description of 3D nonlinear analysis research is given.

#### **(a) Fiber model**

According to Feng et al. (2012) in fiber-based models, materials have only uni-directional strength and stiffness whose behavior is defined in terms of its stress-strain response. Fiber sections are assumed to remain plane throughout the analysis. In reinforced concrete structures, the fiber section is assembled with pre-defined concrete and steel materials. The section is divided into a number of concrete patches where the steel fiber will be located. Strain compatibility between reinforcement and surrounding concrete is assumed. The sectional reactions under force and moment are in terms of axial strain at mid-section and curvature. A unique solution of this deformation combination will be obtained based on the moment-curvature analysis of the section. Spacone et al. (1996a, 1996b) proposed the formulation of a fiber beam-column element for nonlinear static and dynamic analysis of RC frames. In their work flexibility-based formulations that allowed a more accurate description of the force within the element have been presented. The flexibility-based model offers a clear and reliable procedure for their implementation in finite element analysis.

#### **(b) Finite element analysis of concrete structures**

The finite element method is a powerful computational tool, which allows complex analyses of the nonlinear response of RC structures to be carried out in a routine fashion. In their study Ngo and Scordelis (1967) analyzed with a finite element model simple beams in which concrete and reinforcing steel were represented by constant strain triangular elements, and a special bond link element was used to connect the steel to the concrete and describe the bond-slip effect. Nilson (1972) introduced nonlinear material

properties for concrete and steel and a nonlinear bond-slip relationship into the analysis and used an incremental load method of nonlinear analysis. Four constant strain triangular elements were combined to form a quadrilateral element by condensing out the central node. Cracking was accounted for by stopping the solution when an element reached the tensile strength, and reloading incrementally after redefining a new cracked structure. More recently Hauke and Maekawa (2000) have presented a 3D constitutive model for nonlinear finite element analysis of RC members with special attention to cracking. In their research, post-cracking formulations derived from uniaxial tension tests are generalized into spatially arbitrarily inclined cracks in multiple directions. The development of computing allowed more recently the performance of nonlinear 3D analysis using solid elements and Noguchi et al. (2001, 2002) conducted the 3D finite element analysis for performance verification of steel beam-RC joints. These analyses are largely dependent of the computational capabilities due to large degree of degrees of freedom. From that the lattice model (Niwa et al. 1995, Miki et al. 2003a, 20003b) has been proposed, based on decreased degrees of freedom which shortens computing time and is also more practical while remaining accurate in the prediction of RC structural behavior considering material nonlinearity.

### **1.2.2. Damage Evaluation of RC Structures**

Structural damage characterization under seismic loading has extensively been studied in recent years and many models with different concepts have been proposed. One of the relatively simplest one was the prediction of damage in terms of ductility demands. Although much effort has been spent on estimation of damage with ductility demand in reinforced concrete frames, there is still a large gap between the ductility demand and actual observed damage in experiments. Eventually, researchers constructed more realistic damage models with different parameters. In the light of these findings, different models have been proposed by researchers using either the classical definition of low-cycle fatigue or energy dissipation of a member during its inelastic response, or stiffness deterioration under reversed cyclic loading.

#### **(a) Damage models based on ductility concepts**

The development of damage models starting from the ductility concept led to the development of the first damage models. Newmark and Rosenblueth (1971), proposed the ductility factor as a mean to assess damage. The factor can be expressed either as a function of curvature, rotation or displacement. Using a similar approach as Newmark and Rosenblueth (1971), Lybas and Sozen (1977) came up with a similar damage

concept which correlates the initial elastic stiffness and maximum elastic stiffness do produce a damage index. Using the stiffness based damage index, Banon et al. (1981) presented a flexural damage index, computed according to the relation between the ultimate bending moment as resulting from a pushover analysis, maximum bending moment and corresponding curvatures. In this approach, considerations of ultimate displacement capacity, softening due to the buckling of longitudinal reinforcement are considered as shown in **Figure 1.1**.

**(b) Damage models based on energy concepts**

The benchmark moment in which energy based damage models became widely proposed is a study by Park and Ang (1985) which proposed a damage index as the linear combination of the maximum displacement and the dissipated energy namely. The Park and Ang index can take into account both maximum plastic displacement and plastic dissipated energy and is supported by a wide correlation with observed damage. Tembulkar and Nau (1987) carried out an analytical study on inelastic structures modelled as SDOF systems with two different hysteretic models, in order to investigate the role of models on seismic energy dissipation. They have stated that damage attained by a reinforced concrete member under dynamic action cannot be predicted adequately by response spectrum concepts. Therefore, a well-constructed hysteresis model should be constructed as a tool for the damage assessment of concrete structural members.

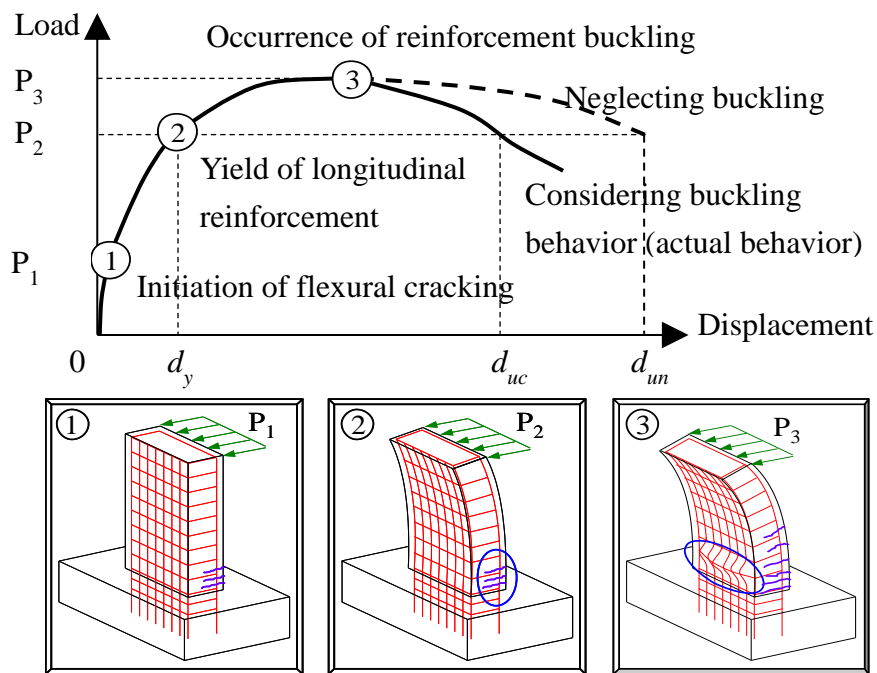


**Figure 1.1** Load-displacement relationship of a RC column

Stojadinovic and Thewalt (1996) proposed a pair of energy balanced hysteresis models based on experiments that were conducted on knee joint sub-systems. The proposed models were piecewise linear and segments on envelope curves were defined by some special points such as first crack, yield and ultimate resistance.

### **1.2.3. Seismic Design Philosophies of RC Structures**

#### **(a) Japan**

The Great Hanshin Earthquake in 1995, marked a turning point in terms of prescribed seismic design specifications in Japan due to elevated degree of damage sustained by RC structures. The most evident result of that was the publication of the Standard Specifications for Concrete Structures- Seismic Performance Verification (2002) by the Japan Society of Civil engineers (JSCE). In these specifications, the concept of performance-based design is nuclear which represented a major change from the specifications published in 1986 which was based on the limit state design method. In these new specifications, two levels of design earthquake ground motion are prescribed: Level 1 corresponds to an earthquake that is likely to occur a few times within the life of a structure and level 2 corresponds to a very rare strong earthquake. The Seismic performance level of a structure is verified considering three seismic performance levels: in seismic performance level 1 function of the structure is maintained without any repair after the earthquake, in seismic performance level 2 function of the structure can be restored within a short period after the earthquake and in seismic performance level 3 there is no overall collapse of the structure, however it does not remain functional after the earthquake. With that seismic design should be carried out so that the structure satisfies seismic performance 1 against level 1 earthquake ground motion and seismic performances 2 or 3 against level 2 earthquake ground motion.

#### **(b) United States of America**

In the United States of America a considerable number of design specifications exist from the federal level to the state level. However with all its diversity, the AASHTO Bridge Design Specifications (2012) and Caltrans (2015) give a very informative outlook on the design philosophies of RC Structures in the USA. The design philosophies of Caltrans (2013) are centered on the contributions of AASHTO Bridge Design Specifications (2012). In the design, the Load and Resistance Factor Design (LRFD) method is prescribed. With focus on seismic design of RC structural members, Caltrans (2013) states that columns, shafts, Pile/Shaft groups in soft or liquefiable soils,

pier walls, and pile/pile-extensions in slab bridges designed and detailed to behave in a ductile manner are designated as seismic-critical members. Seismic-critical members may sustain damage during a seismic event without leading to structural collapse or loss of structural integrity. Other bridge members such as dropped bent cap beams, outrigger bent cap beams, “C” bent cap beams, and abutment diaphragm walls shall be designed and designated as seismic-critical if they will experience any seismic damage as determined by the Project Engineer and approved during Type Selection. All other components not designated as seismic-critical shall be designed to remain elastic in a seismic event.

For structural applications, seismic demand is represented using an elastic 5% damped response spectrum. In general, the Design Spectrum (DS) is defined as the greater of: a probabilistic spectrum based on a 5% in 50 years probability of exceedance (or 975-year return period); a deterministic spectrum based on the largest median response resulting from the maximum rupture of any fault in the vicinity of the bridge site and a statewide minimum spectrum defined as the median spectrum generated by a Magnitude 6.5 earthquake on a strike-slip fault located 12 kilometers from the bridge site.

### **(c) Europe**

In the context of the European Union (EU), member countries of the EU have umbrella codes which are the Eurocodes. On a country local level, the specifications are subject to adjustment; however the Eurocodes prescribes the global design philosophy in the EU space. According to Eurocode 8 (2004) which deals with seismic design of structures, the design of earthquake resistant concrete structures shall provide the structure with an adequate capacity to dissipate energy without substantial reduction of its overall resistance against horizontal and vertical loading.

Structures in seismic regions shall be designed and constructed in such a way that the following requirements are met: No collapse requirement - the structure shall be designed and constructed to withstand the design seismic action without local or global collapse. Damage limitation requirement - the structure shall be designed and constructed to withstand a seismic action having a larger probability of occurrence than the design seismic action, without the occurrence of damage and the associated limitations of use. Seismic action is considered dividing the territories in seismic zones. The earthquake motion at a given point on the surface is represented by an elastic ground acceleration response spectrum called elastic response spectrum.

### **1.3. Scope and Objectives**

Currently, in the field of 3D nonlinear analysis of RC structures the 3D finite solid element analysis tends to be a dominant force. Constitutive models focused on cracking of concrete are applied to finite element analysis, with very accurate results. Although these developments mean more accuracy and better performance prediction, the fact of the matter is that the process remains very complex and sensitive to changes in the analytical input information, as well as the ability of the design engineer to deal with often complex FEM packages, which means that a simpler and yet effective method to perform nonlinear seismic performance analysis of RC structures in 3D space is indispensable.

On the other hand the JSCE standard specifications for concrete structures state very important principles when it comes to seismic design and can be resumed as being important to carry seismic design not only to ensure the safety of structures throughout the occurrence of an earthquake, but also ensure the prevention of fatal damage affecting human life, on a social point of view and on an engineering point of view Miki (2004) refers that in order to obtain good performance of structures during earthquakes, it is essential to analyze in detail the dynamic characteristics of the actual 3D structural system, and clearly address the subjective nature of observations of seismic performance.

Miki et al. (2004) developed the 3D lattice model concept for nonlinear analysis of RC structures, based on the 2D lattice model presented by Niwa et al. (1995), in order to enhance its capabilities. This 3D lattice developed, offers reasonable prediction of the shear carrying capacity of RC structural members, and by discretizing a RC structural member into truss elements, internal stress flows are easy to determine.

With that, the main objective of this study is performance evaluation of existing RC structures subjected to seismic excitation using the 3D lattice model. In a more specific way, three conceptual phases are developed: one, detailed development of a 3D lattice model analysis for circular cross-section RC columns, two investigate and propose appropriate quantitative damage measurement index to induced seismic damage on an existing structures and three propose a seismic performance evaluation method for RC structures using the 3D Lattice model.



#### **1.4. Contents of the Thesis**

The study is divided in six chapters. In chapter 1 background of the study is discussed including the most recent advances in the nonlinear analysis of RC structures subjected to seismic motion as well as major seismic design philosophies in Japan, United States of America and Europe.

Chapter two presents the analytical model used in the study. In this study the lattice model is used. In this review the initial development of 2D lattice model is briefly presented, followed by a more detailed focus of the development of 3D lattice model. Here, material considerations as well as geometry properties are presented. The constitutive models of concrete and reinforcement are explained.

Chapter three presents the full development and application of the multi-directional polygonal 3D lattice model. In this chapter full consideration of the application of the model is given to static analysis of RC columns subjected to cyclic loading. On the other hand analysis of methodology of discretization of circular cross section columns based on circular to rectangular equivalence are compared to a more realistic representation of geometry using the multi-directional polygonal 3D lattice model. Cumulative seismic damage evaluation of RC columns is performed.

In chapter four the numerical evaluation of seismic performance of RC structures is performed. Here the energy approach is explained and a damage index is proposed based on the strain energy of the lattice model elements. To perform the analysis, the multi-directional polygonal 3D lattice model is used and the applicability of the method is verified by performing analysis in RC column subjected to cyclic loading and dynamic analysis of RC column tested by shake table test,

In chapter five the damage evaluation using energy dissipation is subject to an expansion of scope. An actual viaduct is analyzed. This is a viaduct that suffered damage during the Hyogo-ken Nanbu earthquake. The damage is compared to the actual registered damage in the structure.

Finally chapter six includes conclusions based on the study and the multiple aspects of it and from that a few recommendation for a future study on the topic discussed in this thesis.

## References of Chapter 1

AASHTO LRFD Design Specifications (2012): American Association of State Highway and Transportation Officials Specifications for Bridge Structures, Washington, DC.

Banon, H., Biggs J.M., Irvine H.M. (1981): Seismic Damage in Reinforced Concrete Frames, *Journal of ASCE- Structural Division*, vol. 107, pp. 1713-1729.

CALTRANS (2013): Seismic Design Criteria-2013, California Department of transportation.

Eurocode 8 (2004): Design of structures for earthquake resistance – Part 1: General rules, seismic actions and rules for buildings, December

Feng, Y., Kowalsy, M. J. and Nau, Y.M (2012): Fiber-Based Modeling for Investigating the Effect of Load History on the Behavior of RC Bridge Columns, *15 WCEE Proc.*, Lisboa.

Hauke, B. and Maekawa, K. (2000): Three-Dimensional Modeling of Reinforced Concrete with Multi-Directional Cracking, *Concrete Library of JSCE*, No.36, pp.181-206, December.

JSCE (2002): Standard Specifications for Concrete Structures-2002, *Seismic Performance Verification*, December.

Lybas, J.M. and Sozen, M.A. (1977): Effect of Beam Strength and Stiffness on Dynamic Behavior of Reinforced Concrete Coupled walls, *Technical Report on Civil Eng. Studies*, No. 444, University of Illinois, Urbana.

Maekawa, K., Fukuura, N., and An. X. (2001): 2D and 3D Multi-directional Cracked Concrete Model under Reversed Cyclic Stresses, *Modeling of Inelastic Behavior of RC Structures Under Seismic Loads*, ASCE, pp.56-78.

Miki, T. (2004): *Nonlinear Analysis of Reinforced Concrete Structures Subjected to Seismic Loading by Using Three-dimensional Lattice Model*, Doctoral thesis, Tokyo Institute of Technology, February.

Miki, T. and Niwa, J. (2004): Nonlinear Analysis of RC Structural Members Using 3D Lattice Model, *Journal of Advanced Concrete Technology*, JCI, Vol. 2, No.3, pp.343-358, October.

Miki, T., Niwa, J., and Lertsamattiyakul, M. (2003a): Earthquake Response Analysis for RC Bridge Piers Considering Reinforcement Buckling Behavior, *Journal of Materials, Concrete Structures and Pavements*, JSCE, No.732/V-59, pp.225-239, May. (in Japanese)

Miki, T., Niwa, J., and Lertsamattiyakul, M. (2003b): Numerical Evaluation of Seismic Performance of Reinforced Concrete Bridge Piers Using Dynamic Lattice Model, *Concrete Library of JSCE*, Vol.41, pp.49-64, June.

Newmark, N.M and Rosenblueth, E. (1971): Fundamentals of Earthquake Engineering, Prentice-Hall, Englewood Cliffs, New Jersey.

Ngo, D. and Scordelis, A.C. (1967): Finite Element Analysis of Reinforced Concrete Beams, *Journal of ACI*, Vol. 64, No. 3, pp. 152-163.

Nilson, A. H. (1972): Internal Measurement of Bond Slip, *Journal of ACI*, Vol. 69, No. 7, pp 439-441.

Niwa, J., Choi, I. C., and Tanabe, T. (1995): Analytical Study for Shear Resisting Mechanism Using Lattice Model, *Concrete Library of JSCE*, No.26, pp.95-109, December.

Noguchi, H., Kashiwazaki, T., Uchida, K., and Nozaki, Y. (2001): FEM Analysis for Structural Performance Design of Concrete Structures, *Modeling of Inelastic Behavior of RC Structures under Seismic Loads*, ASCE, pp.257-275.

Noguchi, H., Zhang, D, and Kashiwazaki, T. (2002): Three-dimensional Finite Element Analysis of RC Beam-column Joints Reinforced by New Reinforcing Way, *Proceedings of the JCI*, Vol.24, No.2, pp.397-402. (in Japanese)

Park, Y. J. and Ang, A.H.S (1985): Mechanistic Seismic Damage Model for Reinforced Concrete, *Journal of the Structural Division*, ASCE, Vol. 111, No. 4, pp. 722-739.

Tembulkar, J.M. and Nau, J.M. (1987): Inelastic Modeling and Seismic Energy Dissipation. *Journal of Structural Engineering*, ASCE, Vol. 113, No. 6, pp. 1373-1377.

Stojadinovic, B. and Thewalt, C.R. (1996): Energy Balanced Hysteresis Models, *Report No. UCB/EERC-96/01*, Earthquake Engineering Research Center, University of California, Berkeley

## 2. ANALYTICAL MODEL

### 2.1. Introduction

It is fundamental that the performance of RC structures can be simulated using nonlinear analytical models that are both objectively simple to handle and accurate. In seismic analysis of RC structures, many nonlinearities related to geometry and the material require that the analysis criteria is handled with appropriate analogies, and the most essential methods in order to do this treat the structure as a 2 dimensional (2D) element. However in a seismic event, actual ground motions imposed on RC structures work against the actual 3 dimensional (3D) structures from different directions along the principal axis. With that it is important to be able to carry the nonlinear analysis of RC structures in 2D and 3D spaces with a method that is both accurate and objective while preserving a sensible need for calculation time and CPU processing power. To meet these requirements, in this study the lattice model first proposed by Niwa et. al (1995) for 2D space and enhanced by Miki and Niwa (2004) for 3D space is focused. This model predicts the shear carrying capacity of RC members based on arch and truss analogy to treat concrete as a material. In this chapter the formulations of 2D lattice model and 3D lattice model which are described.

### 2.2. Outlines of 2D Lattice Model

The lattice model consists of members representing concrete and reinforcement. **Figure 2.1** schematically shows the lattice model of RC column. In the lattice model, arch action and truss action are considered as the shear resisting mechanism of a structural member is. For the 2D lattice model, a RC member in 3D is presented as the 2D model based on the plane stress condition. The concrete is modeled into flexural compression members, flexural tension members, diagonal compression members, diagonal tension members, vertical members, or arch members. For RC column, longitudinal and transverse reinforcement are modeled into horizontal and vertical member, respectively.

The diagonal compression members and the diagonal tension members represent the truss action of shear resistance mechanism in the lattice model. The 2D lattice model is categorized as a fixed angle truss model in which the diagonals are assuming as the 45° angle of inclination trusses. By incorporating the arch member to represent the arch action, the lattice model can be used to estimate the changing direction of internal compressive stress flows after diagonal cracking. For the lattice model, the arch part should be located along the compressive stress flows inside a RC member.

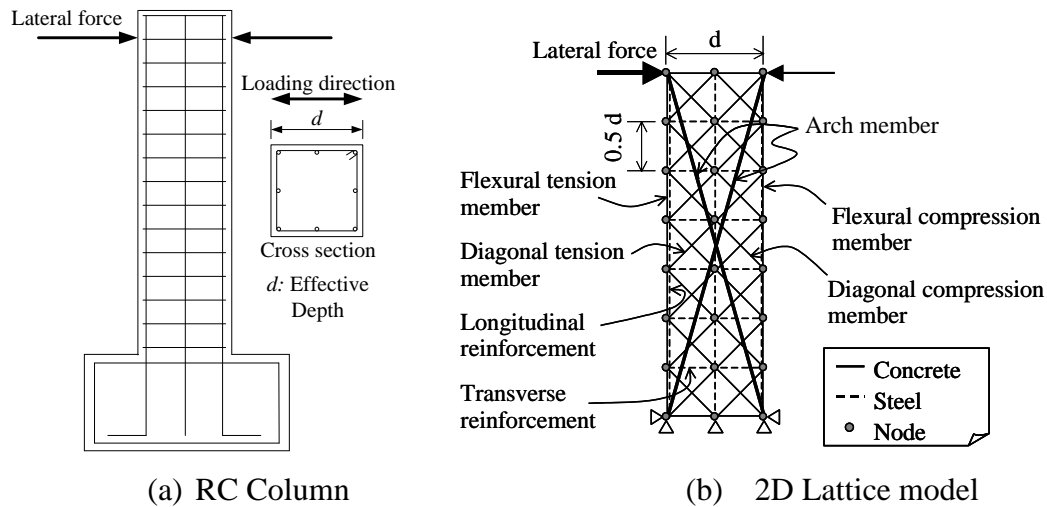


**Figure 2.1** Outline of 2D lattice model (Miki 2004)

The arch and truss analogy allows the consideration of shear resisting mechanism. In other words, in the discretization process the concrete is divided into truss and arch members. When the value of  $t$  is defined as the ratio of the width of the arch part to the width of cross section  $b$ , the widths of the arch part and the truss part are given by  $bt$  and  $b(1 - t)$ , respectively, where  $0 < t < 1$ . The value of  $t$  is determined based on the theorem of the minimization of the total potential energy for the 2D lattice model with the initial elastic stiffness. **Figure 2.2** shows a detailed diagram of cross section of RC column modeled using 2D lattice model.

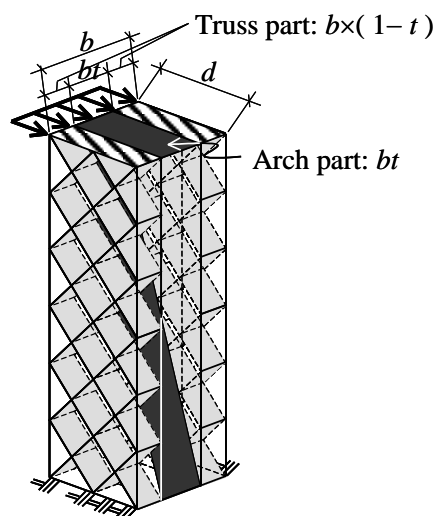


**Figure 2.2** Cross section of RC member modeled by 2D lattice model (Miki 2004)

In the modeling due to the existence of reinforcing bars for flexural tension members the concrete still contributes to tensile resistance even after cracking. In that manner the cross-sectional area of concrete flexural members, for simplicity, is determined by considering the bond effect between concrete and reinforcing bars, and the cross-sectional area of the flexural tension or compression member is assumed to be the product of the double depth of cover concrete and the width of cross section.

## 2.3. Material Models

### 2.3.1. Compressive stress-strain relationships for concrete

In this study, in order to take into account the confinement effect by transverse reinforcement that is observed when a suitable amount of transverse reinforcement is used to confine the concrete, the stress-strain relationship proposed by Mander et al. (1988) as expressed by **Equation 2.1** and illustrated in **Figure 2.3**, is used as a material model for the diagonal compression members and the arch members. Under these circumstances a significant increase in both compressive strength and ductility can be expected

$$\sigma_c' = \frac{f_{cc}' x^r}{r-1+x^r} \quad (2.1)$$

where

$$x = \frac{\varepsilon_c'}{\varepsilon_{cc}'} \quad (2.2)$$

$$f_{cc}' = f_{c0}' \left( -1.254 + 2.254 \sqrt{1 + \frac{7.94 f_l'}{f_{c0}'}} - 2 \frac{f_l'}{f_{c0}'} \right) \quad (2.3)$$

$$f_l' = K_e \rho_w f_{wy} \quad (2.4)$$

$$\varepsilon_{cc}' = \varepsilon_{c0}' \left\{ 1 + 5 \left( \frac{f_{cc}'}{f_{c0}'} - 1 \right) \right\} \quad (2.5)$$

$$r = \frac{E_{c0}}{E_{c0} - E_{\text{sec}}} \quad (2.6)$$

$$E_{c0} = 5000 \sqrt{f_{c0}'} \quad (2.7)$$

$$E_{\text{sec}} = \frac{f_{cc}'}{\varepsilon_{cc}'} \quad (2.8)$$

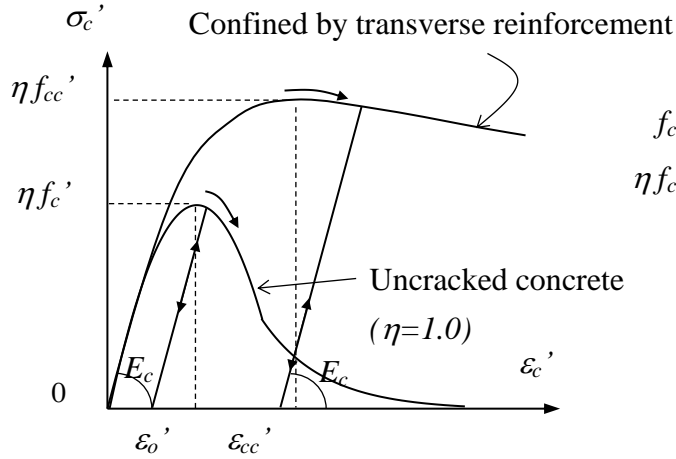


**Figure 2.3** Compressive model of concrete

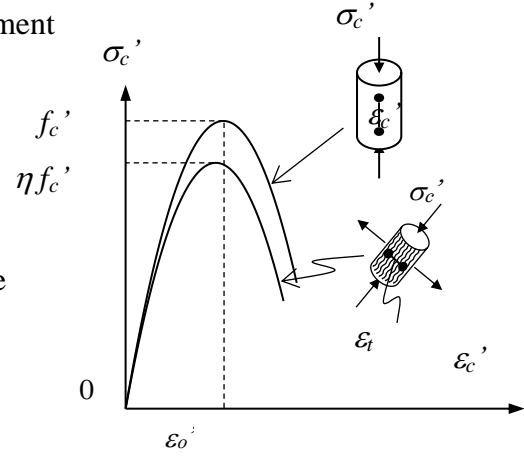


**Figure 2.4** Reduction in compressive strength of cracked concrete

where,  $f_c'$  is the uniaxial compressive strength of the concrete,  $r_w$  is the transverse reinforcement ratio ( $= A_w / b_w s$ ),  $A_w$  is the cross-sectional area of the transverse reinforcement,  $b_w$  is the width of web concrete of a RC member,  $s$  is the transverse reinforcement spacing, and  $f_{wy}$  is the yield strength of the transverse reinforcement.

Moreover Vecchio and Collins (1986) demonstrated that the compressive stress of diagonally cracked concrete decreases as the transverse tensile strain,  $\varepsilon_t$ , increases, as shown in **Figure 2.4**. Therefore, the value of  $\varepsilon_t$ , for the diagonal tension members, which are normal to the diagonal compression members, is used to determine the coefficient to express concrete compressive softening,  $\eta$ . The behavior of the cracked concrete in compression is then characterized by **Equation 2.9**. For the arch member, the transverse tensile strain of the diagonal tension member near the loading point is used.

$$\eta = \frac{1.0}{0.8 - 0.34 \left( \frac{\varepsilon_t}{\varepsilon_o} \right)} \leq 1.0 \quad (2.9)$$

where  $\varepsilon_o'$  is equal to 0.002. The tensile strain  $\varepsilon_t$  of the diagonal tension members, which is the normal direction to the diagonal compression member, is used to determine the coefficient of the compressive softening of concrete  $\eta$ .



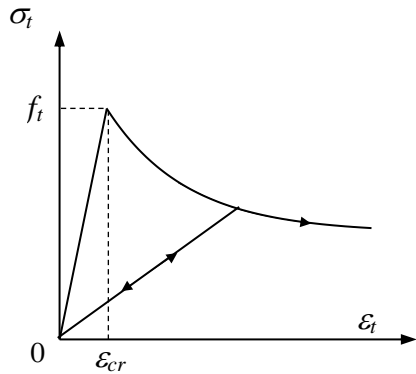


**Figure 2.5** Tension stiffening model

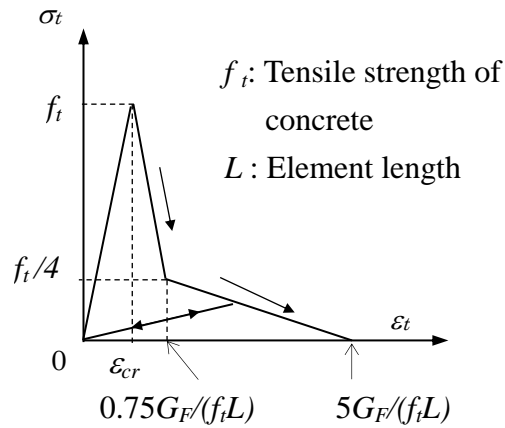


**Figure 2.6** Tension softening model (1/4 model)

Conversely for flexural compression members including the cover concrete, the quadratic stress-strain relationship illustrated in **Figure 2.3** that has been proposed by Vecchio and Collins (1986) is adopted as **Equation 2.10** shows.

$$\sigma_c = -\eta \cdot f_c \left\{ 2(\varepsilon_c / \varepsilon_0) - (\varepsilon_c / \varepsilon_0)^2 \right\} \quad (2.10)$$

In the case of flexural compression members, because the direction of compression stress is assumed to correspond to the direction of the principal tensile strain, the effect of compressive softening behavior represented by the **Equation 2.10** is neglected, thus  $\eta = 1.0$ .

### 2.3.2. Tensile stress-strain relationships of concrete

For the flexural tension members prior to cracking, a linear-elastic relationship is applied, while the tension stiffening curve proposed by Okamura and Maekawa (1991) defined by **Equation 2.11** and illustrated in **Figure 2.6** is applied after cracking. The strain at crack initiation,  $\varepsilon_{cr}$  is assumed to be 0.0001 (100  $\mu$ ).

$$\sigma_t = f_t (\varepsilon_{cr} / \varepsilon_t)^{0.4} \quad (2.11)$$

where,  $f_t$  is the uniaxial tensile strength of concrete.

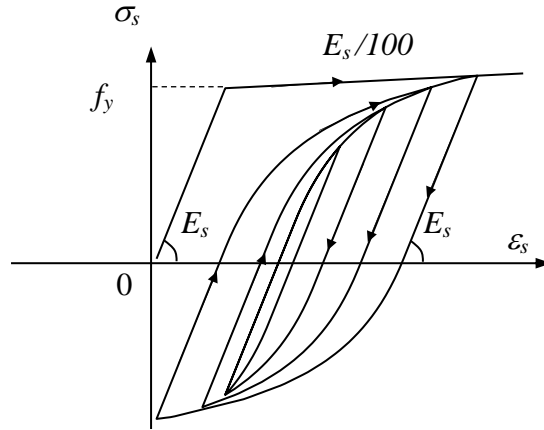


**Figure 2.7** Stress-strain relationship of reinforcement under cyclic loading

The diagonal tension members exhibit elastic behavior prior to cracking. However, once a crack occurs, concrete is assumed to exhibit tension softening behavior. In this study, softening behavior, expressed by the 1/4-model (Uchida et al. 1991) shown in **Figure 2.7** and **Equations 2.12** and **2.13**, is applied to the diagonal tension members

$$\varepsilon_1 = \varepsilon_{cr} + 0.75G_F / (f_t \cdot L) \quad (2.12)$$

$$\varepsilon_2 = \varepsilon_{cr} + 5.0G_F / (f_t \cdot L) \quad (2.13)$$

where,  $f_t$  is the splitting tensile strength of concrete and  $L$  is the element length. Here, the fracture energy of concrete,  $G_F$ , is assumed to be standard value of 0.1 N/mm.

### 2.3.3. Reinforcement model

The stress-strain relationship of the reinforcement is expressed as an elasto-plastic model under monotonic loading. As shown in **Figure 2.7**, the stress-strain relationship of the reinforcement is bi-linear, having a tangential stiffness after yielding of  $E_s/100$  (where  $E_s$  indicates the elastic modulus of reinforcement). The unloading and reloading paths are also shown. After yielding, the *Bauschinger* effect which is when the stiffness of the reinforcement decrease as the stress state moves from tension to compression, while similar behavior is observed when the stress changes from compression to tension. is incorporated into the analysis using the model proposed by Fukuura et al. (1997).

## 2.4. Outlines of 3D Lattice Model

The discretization of a RC structure using a 3D model allows the consideration of geometries and loading conditions that cannot be expressed by a 2D model. In this study, the extension from the 2D lattice model to the 3D lattice model presented is based on the concept of the conventional 2D lattice model which has been proved by previous studies that can appropriately predict the 2D response of RC structural members subjected to the monotonic or reversed cyclic loading (Niwa et al. 1995, Miki et al. 2003a, 2003b).

The detailed development of the 3D lattice model for RC columns is described by Miki and Niwa (2004) and furthermore by Miki (2004). Since in the lattice model, the shear resisting mechanism is divided into arch action and truss action, to represent the truss action, it is assumed that 3D space is comprised of an orthogonal coordinate system that is defined by three planes, such as x-y plane, y-z plane, and z-x plane. Two crossed truss members are located on each truss plane so that unit element consists of 12 truss members in six truss planes as shown in **Figure 3.1 (a)**. In each truss plane, the in-plane 2D constitutive law of concrete, with the consideration of the softening of compressive strength of diagonally cracked concrete depending on the transverse tensile strain (Vecchio and Collins 1986).

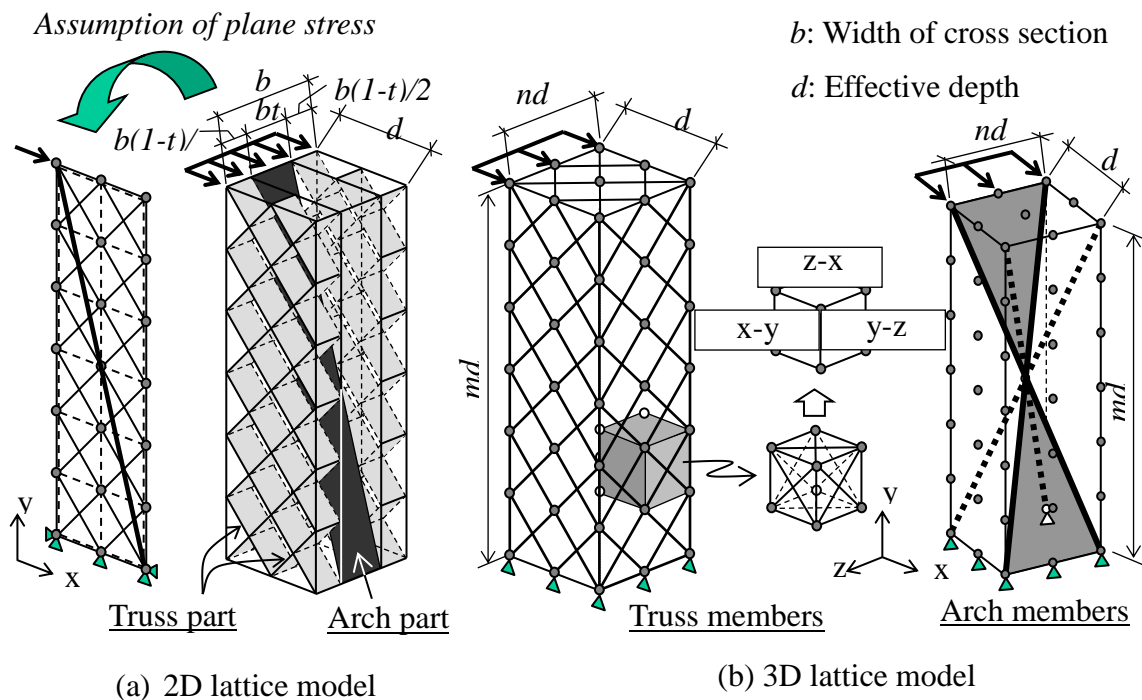


**Figure 3.1** Discretization for 2D and 3D lattice models (Miki 2004)

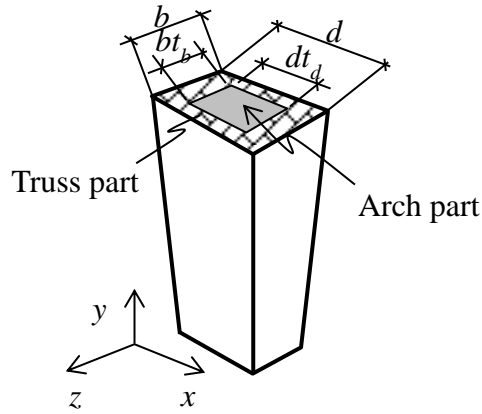


**Figure 3.2** Partition of cross section in 3D lattice model (Miki 2004)

In order to represent the arch action in the 3D lattice model for RC column, four arch members are arranged by connecting between the top and the bottom of the column at the opposite corners. The resisting mechanism of a RC column subjected to one certain load consists of two arch members crossing each other. The stiffness of these arch members is assumed to be equivalent to one of two arch members in the 2D lattice model. Two pairs of arch members are incorporated into the model symmetrically. When lateral load is applied on the RC column from the diagonal direction of the section, it is assumed that the corner-to-corner arch action (from the loading point to the bottom of a column at opposite corner) inside the RC member is idealized as a compressive strut.

The value of  $t$  is defined by the ratio of the arch part width to the cross-sectional width of a RC member in the 2D lattice model as mentioned previously. Assuming the global stiffness of 3D lattice model to be equivalent to that of 2D lattice model, the cross-sectional area of the arch member can be identified. The schematic representation about the division of cross-section of the 3D lattice model is shown in **Figure 3.3**. Here, the ratios of the arch part width to the width,  $b$  and the depth,  $d$  in the cross section of the column are defined by  $t_b$  and  $t_d$ , respectively.

With the determination of value of  $t$  in the 3D lattice model, both the cross-sectional width of the column and the cross-sectional depth of the column are evaluated in preliminary analysis. According to the 2D lattice model, the values of  $t_b$  and  $t_d$  in the 3D lattice model are determined based on the theorem of minimization of the total potential energy.

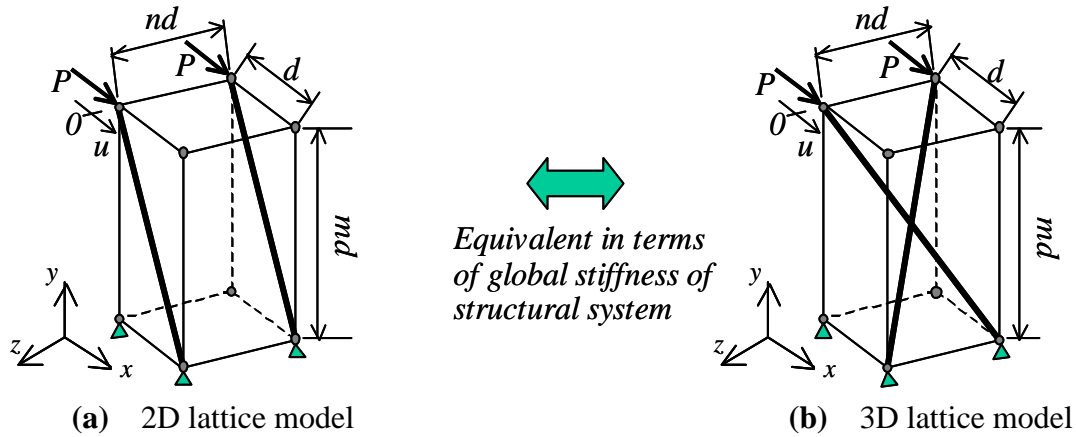


**Figure 3.3** Arch members in 2D and 3D lattice model (Miki 2004)

### 2.4.1. Configuration of elements

#### (a) Concrete Elements

##### Arch members

The arch members assumed in the 2D lattice model and 3D lattice model are illustrated in **Figure 3.3**. The global stiffness of 2D lattice model and 3D lattice model are compared with each other, in that way the cross-sectional areas of arch member are presented in **Equation 3.1** and **Equation 3.2** as follows:

$$A_{arch-3D} = \left( \frac{1+m^2+n^2}{1+m^2} \right)^{3/2} \times A_{arch-2d} \quad (3.1)$$

$$A_{arch-2D} = \frac{1}{2} b t_b \cdot d t_d \cdot \sin \theta \quad (3.2)$$

where  $A_{arch-3}$  is the cross-sectional area of arch members in the 3 lattice model,  $_{arch-2D}$  is the cross-sectional area of arch members in the 2D lattice model. The values of  $m$ ,  $n$  are determined in which  $md$  and  $nd$  correspond to the width of cross section and the height of the column in the model, respectively. Here,  $d$  is the effective depth of cross-section. In the modeling, the height of the lattice model is not always equal to the height of the column because the horizontal or vertical distance of two adjoining nodes is determined based on the half of the effective depth  $d$ . Hence, the height and the width of the 3D lattice model are set on the dimensions of the structure comparatively close to actual dimensions.

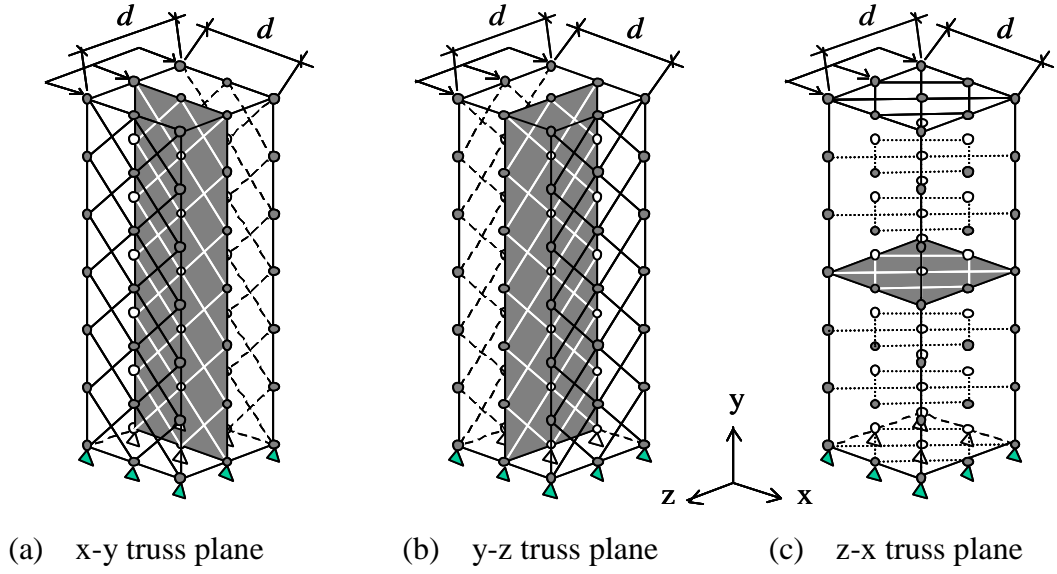


**Figure 3.4** Truss planes in 3D lattice model (Miki 2004)

#### Truss members

In the 3D lattice model the horizontal or vertical distance of two adjoining nodes is equal to  $0.5d$ , and then the thickness of the truss members on the side view of the column is equal to  $0.5d \cdot \sin 45^\circ$ . In order to represent the truss mechanism along the principal direction in 3D space, it is assumed that the cross-sectional area of truss members inside a RC column is a half of that at the surface of the column. The cross-sectional areas of truss members in x-y plane, y-z plane, and z-x plane illustrated in **Figure 3.4** by hatching are expressed as the following equations (**Equations 3.21 to 3.23**).

$$A_{truss-xy} = \frac{b(1-t_b)}{2} \cdot \frac{d}{2} \sin 45^\circ \quad (3.21)$$

$$A_{truss-yz} = \frac{h(1-t_d)}{2} \cdot \frac{d}{2} \sin 45^\circ \quad (3.22)$$

$$A_{truss-zx} = \frac{a}{2n} \cdot \frac{d}{2} \sin 45^\circ \quad (3.23)$$

where,  $A_{truss-xy}$ ,  $A_{truss-yz}$ , and  $A_{truss-zx}$  are the cross-sectional areas of truss members in x-y plane, y-z plane, and z-x plane, respectively.  $b$ ,  $h$ , and  $a$  represent the cross-sectional width, the cross-sectional height, and the shear span of the column, respectively.

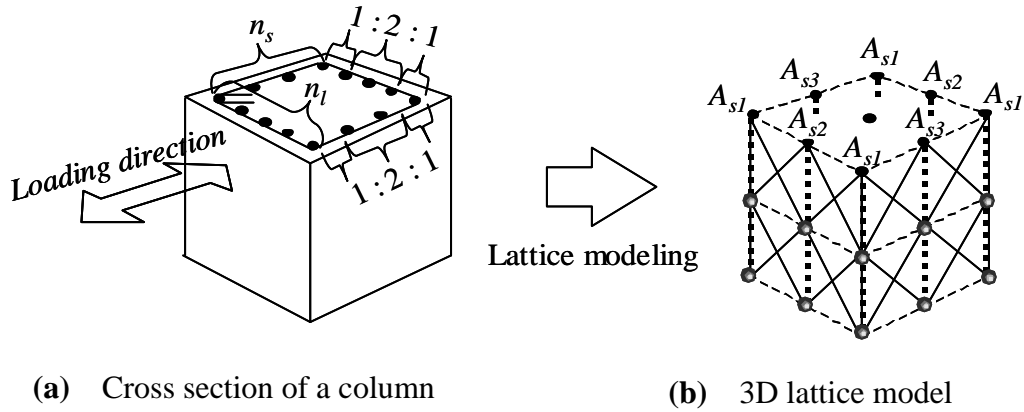


**Figure 3.5** Arrangements of longitudinal and transverse reinforcements with single layer (Miki 2004)

### (b) Reinforcement Elements

For longitudinal reinforcement and transverse reinforcement, horizontal and vertical members are used. Each reinforcement member is determined based on the actual cross section and actual location of reinforcements. **Figure 3.5** shows the example of the arrangements of longitudinal and transverse reinforcements at the single layer in which there are no intermediate ties. Here, the longitudinal reinforcement is divided into eight elements in one layer as illustrated in **Figure 3.5 (b)**. It is assumed that the cross-sectional areas of reinforcement along the side perpendicular or parallel to laterally loading direction are divided at a ratio of 1:2:1 (**Figure 3.5 (a)**). The cross-sectional areas of members of longitudinal reinforcement are expressed as the following equations (**Equations 3.24 to 3.26**).

$$A_{s1} = \left( \frac{n_l}{4} + \frac{n_s}{4} - 1 \right) \times A_l \quad (3.24)$$

$$A_{s2} = \frac{n_l}{2} \times A_l \quad (3.25)$$

$$A_{s3} = \frac{n_s}{2} \times A_l \quad (3.26)$$

where,  $A_{s1}$ ,  $A_{s2}$ , and  $A_{s3}$  are the cross-sectional areas at the corner of section, at the middle of tension extreme fiber, and at the middle of the side parallel to laterally loading direction, respectively. Similarly,  $A_l$  is the cross-sectional area of longitudinal reinforcement. Here,  $n_l$  and  $n_s$  are the number of longitudinal reinforcement along with

the side perpendicular and parallel to laterally loading direction, respectively.

In the lattice model, the transverse reinforcement is arranged at intervals of  $0.5d$  throughout the model uniformly so that the actual transverse reinforcement ratio equals the model transverse reinforcement ratio. The transverse reinforcement ratio,  $r_w$  of an actual RC structural member is calculated by the following equation:

$$r_w = \frac{A_w}{b_w s} \quad (3.27)$$

where  $A_w$  is the cross-sectional area of a couple of transverse reinforcements,  $b_w$  is the width of the cross section of the RC member, and  $s$  is the transverse reinforcement spacing.

## 2.5. Nonlinear Analysis Procedure

The nonlinear analysis procedure is done based on computer programs that have been developed to facilitate the process (Miki et al.2004). The static analysis case is performed for a monotonic and cyclic loading, and the dynamic analysis is done assuming that the mass equivalent to the self-weight of the structure is distributed over all the nodal points. Moreover it is assumed that a concentrated mass having the weight of superstructure applies uniformly on the nodal points at the top of the structure.

The numerical procedure implemented in the computer program is explained below. The equations of motion are formulated to satisfy the equilibrium condition for the structure. Then, prior to time integration, nodal displacements of the lattice model are converted into those in the generalized coordinates by using the mode shape vector. The mode shape vector of vibration is obtained as the solution for the free vibration equations neglecting the damping. The mode of vibration can be obtained by solving the Eigen problem. In this study, the subspace iteration method is used to solve the Eigen problem.

The stiffness matrix,  $K$  can be obtained from the tangent stiffness considering the material nonlinearities of concrete and reinforcement. The damping is assumed to be proportional to a combination of the mass and the stiffness matrices, so-called the Rayleigh damping. However, this damping formulation has no physical meaning and



may lead to the damping with unexpected vibration mode shapes. From a previous studies (Hilber et al.1977, Sing et al.1991), it was pointed out that when the factor in the Newmark method,  $\gamma$  was given as the value that was present, and consequently it was possible to attain unconditionally stability and a favorable energy dissipation property if  $\beta \geq 1/4(\gamma + 0.5)^2$ . Therefore, in the analysis, it is assumed that the viscous damping is neglected ( $h = 0$ ). In addition, the numerical damping of the Newmark method with factors  $\beta = 0.36$  and  $\gamma = 0.70$  is used as time integration (committee 311 2002). Here a time interval is set as 0.01 sec. Moreover, since the nonlinear responses appear when RC structures are subjected to large ground motions, it is necessary to iterate the calculation until a sufficiently converged solution is obtained. In this study, the Newton-Raphson iteration method is used to iterate until an adequately converged solution is obtained.

In order to check the convergence, the out-of-balance force and the energy increment are compared with each initial value during the iteration. The convergence tolerances for the out-of-balance force and energy are set at 0.001 and 0.01, respectively (Miki.2004).

## **2.6. Cyclic Analysis of RC Columns Using 2D Lattice Model**

In order to demonstrate the applicability of 2D lattice model, analysis of RC column in static case under cyclic loading is performed and compared the analytical results to experimental results on RC column experimentally loaded laterally and expected to fail either in flexure or shear. An analysis previously carried by Miki (2004) is here presented to demonstrate the applicability of the 2D lattice model.

### **2.6.1. Outline of experiment and analysis**

The experiment was carried out by Takemura et al. (1997) on RC bridge piers subjected to static reversed cyclic loading are analytical target. The specimen and arrangement of reinforcement are illustrated in **Figure 4.1**. The specimen is a cantilever RC bridge pier with a cross section of 400 mm by 400 mm. The reversed cyclic loading was applied by controlled horizontal displacement at a point 1,245 mm above the base of the pier. The uniaxial compressive strength of concrete was 35.7 MPa, yield strength of longitudinal reinforcement is 363 MPa and nominal diameter SD295 D13 and yield strength of transverse reinforcement is 368 MPa and nominal diameter SD295 D6.

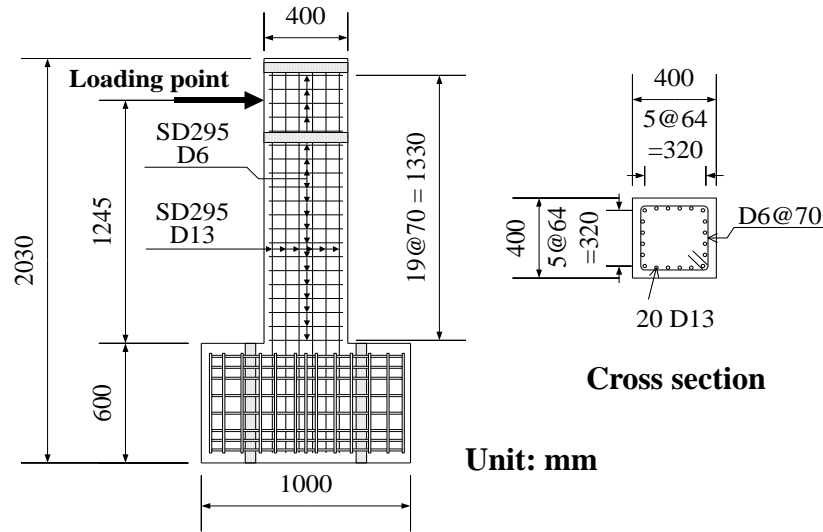


**Figure 4.1** Specimen details and test setup (Takenuma et al. 1997)

In the experiment, the displacement amplitude was increased stepwise in the increments of  $n\delta_y$  ( $n = 1, 2, 3, \dots$ ) at each cyclic loading step. Here,  $\delta_y$  is the lateral displacement at the initial yielding of longitudinal reinforcement at the bottom of the pier and is taken as  $\delta_y = 6\text{ mm}$ . During the test, a constant axial compressive load of 156.7 kN was applied at the top of the pier; this is equal to an applied axial compressive stress of 0.98 MPa.

The specimen subjected to cyclic loading is analyzed by the 2D static lattice model. In **Figure 4.2** analytical model is presented. To simulate RC piers subjected to reverse cyclic loading, the flexural compression members and flexural tension members are assumed to have the same cross-sectional area. In addition, since the specimen is a cantilever RC pier, two intersecting arch members connecting the loading points at the top of the pier and the opposite pier-footing connections are provided. Here, from the results of pre-analysis already described, the value of  $t$  is obtained as 0.20. The applied axial compressive load at the top of the pier is uniformly distributed over the top three nodes.

### 2.6.2. Lateral force-displacement characteristics of RC column

The lateral force-lateral displacement relationships obtained in the experiment and static lattice model analysis are shown in **Figure 4.3**. The experimental result shows that the longitudinal reinforcement initially yields on the flexural tension side at the bottom of the RC bridge pier.

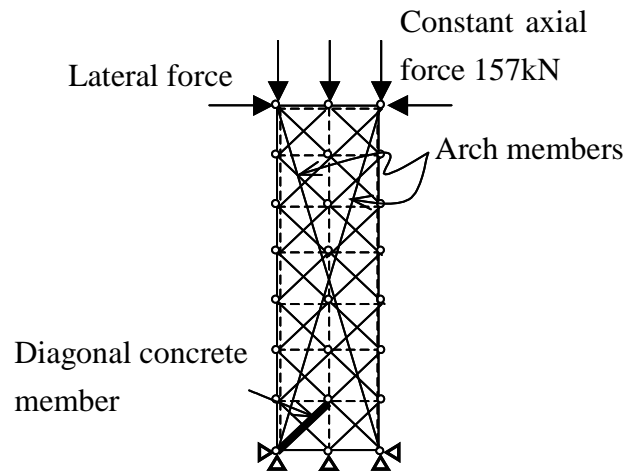


**Figure 4.2** Static lattice model

As the lateral displacement increases gradually after reversing the loading direction, the longitudinal reinforcement behaves plastically and deforms laterally outwards in a process referred to as buckling. Ultimately, the lateral load-lateral displacement curve reaches the post-peak region accompanied by the buckling of longitudinal reinforcement and the spalling of cover concrete. In the analytical result (shown in **Figure 4.3b**), the behavior of the RC bridge pier is found to be close to the experimental result. The comparison of two results indicates that the analytical method is applicable to the prediction of the initial stiffness, the load carrying capacity, and the cyclic behavior of RC bridge piers after the yielding of longitudinal reinforcement. The behavior can be successfully predicted. However, it is also confirmed that further softening behavior in the post-peak region is not properly predicted by the analysis.

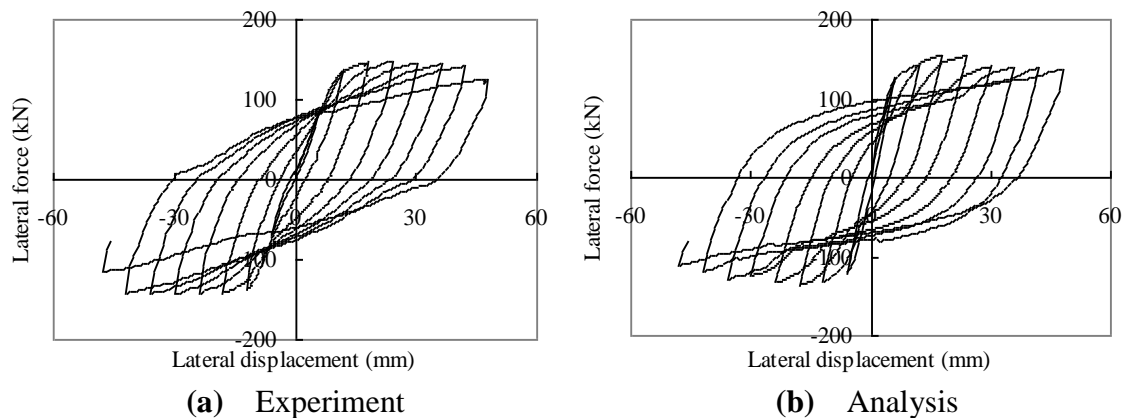


**Figure 4.3** Lateral force and lateral displacement relationships

## 2.7. Static Analysis of RC Columns Subjected to Bilateral Loading Using 3D Lattice Model

The 3D lattice model has been developed based on the 2D lattice model as previously stated. One of the new and key features of analysis in 3D space is that the assumption of plane stress is no longer used and therefore the bilateral loading of RC columns can be used to verify the expansion of scope of 3D lattice model from 2D case. In that sense, to show the consequent extension from 2D analysis to 3D analysis using the lattice model, static analysis of RC columns subjected to bilateral loading is performed. The analysis previously carried out by Miki (2004) in his work is used.

### 2.7.1. Outline of experiment and analysis

A set of experiments were carried out by Kawashima et al. (1991, 1993) on RC bridge piers subjected to static reversed cyclic loading. In these experiments in order to investigate the effect of biaxial loading, the test was conducted for RC bridge piers subjected to bending from the diagonal direction of the section. The tests were for the square sectional piers. The dimensions and reinforcement arrangement of the specimen are illustrated in **Figure 4.4** and loading directions in **Figure 4.5**.

The piers were three RC bridge cantilevers with a square cross section of 500 mm × 500 mm. All reinforcing bars had a minimum of 35 mm of concrete cover. The diameter of longitudinal reinforcing bars was 13 mm, and consequently the longitudinal reinforcement ratio was 2.03 %.

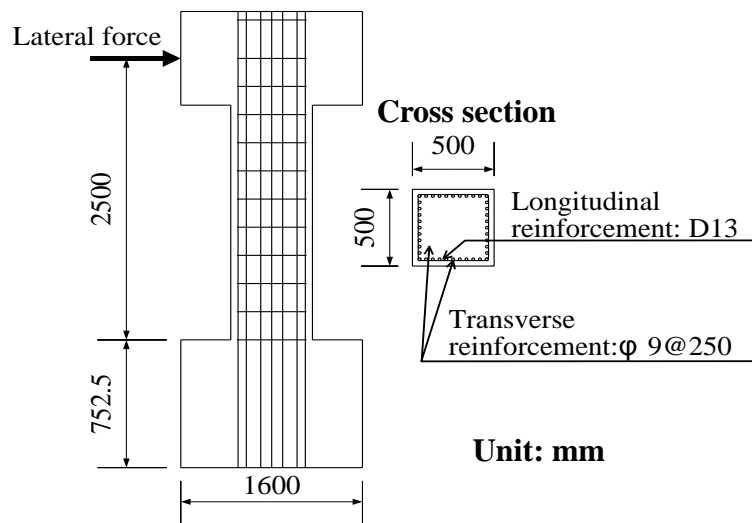


**Figure 4.4** Details and arrangement of specimen

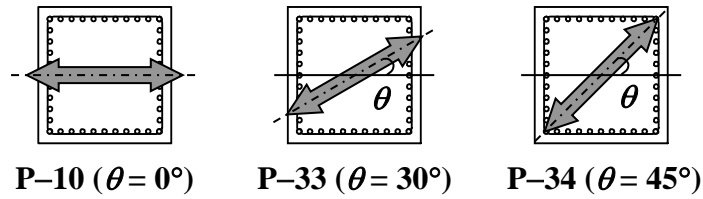


**Figure 4.5** Loading condition

The transverse reinforcements were 9 mm diameter round bars with 250 mm spacing. Hence, the transverse reinforcement ratio was 0.10 %. The longitudinal reinforcement in all piers had the nominal yield strength of 295 N/mm<sup>2</sup>, while the transverse reinforcement had nominal yield strength of 235 N/mm<sup>2</sup>. The average compressive strength of concrete was 31.3 N/mm<sup>2</sup> in the column P-10 and 39.8 N/mm<sup>2</sup> in columns P-33 and P-34. The piers had an identical dimension and arrangement of reinforcement, while the loading direction is different each other. In the column P-10, the lateral load was provided along the principal axis, while in the columns P-33 and P-34, the load was provided in the direction of a diagonal of the pier cross section. For the specimens of P-33 and P-34, the loading stub at the top portion of the pier was inclined from the principal axis as were 30 and 45, respectively.

In the experiment, the displacement amplitude was increased step wisely in increments of  $n \cdot \delta_y$  ( $n = 1, 2, 3 \dots$ ) at each loading step. Here,  $\delta_y$  was determined as the lateral displacement when the measured strain of the longitudinal reinforcement at the bottom of the pier firstly reached the yield strain of  $1,800\mu$ , and was taken as  $\delta_y = 13$  mm in the column P-10. The yield displacement was used to control the displacement in both columns P-33 and P-34. The loading cycles were controlled of ten each cycle at the same amplitude.

### 2.7.2. Analytical results and discussion

The experimental lateral load-lateral displacement relationships at the top of the pier for each specimen are shown in **Figure 4.6**. In all specimens, similar behavior was observed while the development of damage was significantly different. However in analysis For the specimen P-10, the analytical and experimental results are found to show the good agreement with each other.

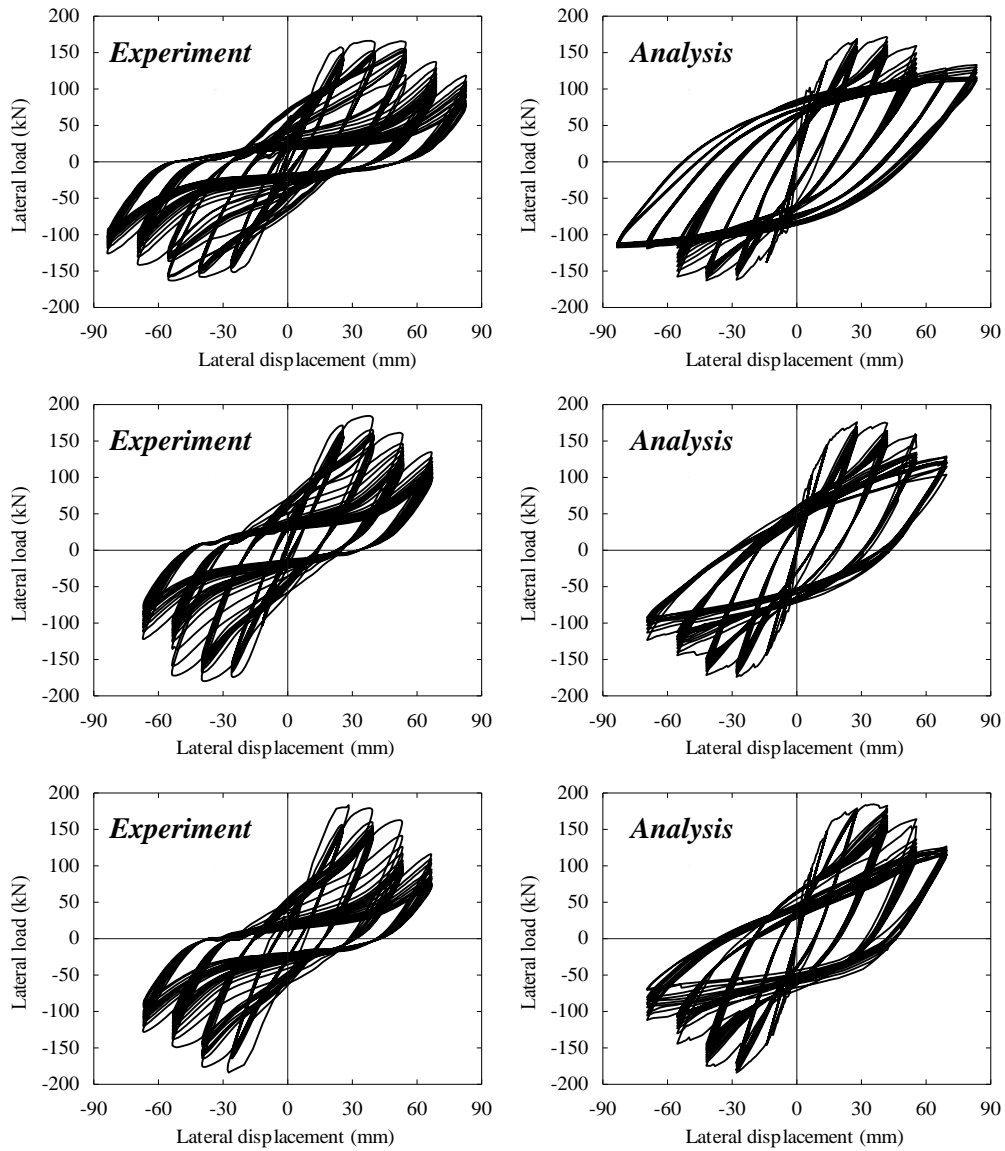


**Figure 4.6** Lateral load-lateral displacement relationships obtained by the cyclic loading test and static 3D lattice model

Matching with experimental observation, the buckling behavior of longitudinal reinforcement is predicted at the lateral displacement of more than 55 mm. However, the divergence of analytical results from the experimental results is observed at the large deformation range. This is because that the fracture of longitudinal reinforcing bars due to the low-cycle fatigue is not incorporated in the analysis.

In the specimen P-33, the analytical load-displacement relationship is also found to be close to the experimental result. It is found that the flexural ductility of these square

piers subjected to bending from the direction of section diagonal is almost similar to that for bending from the direction of a principal axis of the section. In both the experiment and analysis, the slight increase in the load carrying capacity is observed. After the analytical displacement exceeded around 40 mm, the gradual decrease in the lateral force can be observed in the post-peak region of load-displacement relationship. That is similar to the experimental observation. This point is corresponding to the compressive softening of concrete at the base of the pier and the initiation of the buckling of longitudinal reinforcement.

For specimen P-34, it can be observed that the experimental and analytical load-displacement curves and its envelope curves are very close to each other. The analytical and experimental comparison of the load carrying capacity of RC piers indicates that there is slight difference with the load carrying capacity if the lateral load is applied from the direction of a principal axis of the section. The tenth cycle for the same displacement produced nearly the same response and the degradation of stiffness cannot be observed until the lateral displacement reached at 50 mm.

## References of Chapter 2

Fukuura, N. and Maekawa, K. (1997): Computational model of reinforcing bar under reversed cyclic loading for RC nonlinear analysis, *Journal of Materials, Concrete Structures and Pavements*, JSCE, Vol. 564, No.35, pp.291-295.

Kawashima, K. (1991): Effect of Oblique Excitation on Dynamic Strength and Ductility of Reinforced Concrete Bridge Piers, *Civil Engineering Journal*, Public Works Research Center (PWRC), No.33, Vol.8, pp.27-33. (in Japanese)

Kawashima, K., Hasegawa, K., Nagashima, H., Koyama, H., and Yoshida, T. (1993): Seismic Design Method of Reinforced Concrete Bridge Piers Based on Dynamic Strength and Ductility, *Journal of Research PWRI*, No.190, pp.51-57, May. (in Japanese)

Mander, J. B., Priestley, M. J. and Park, R. (1988): Theoretical stress-strain model for confined concrete, *Journal of Structural Engineering*, ASCE, Vol. 114, No(8), pp. 1804-1826.

Miki, T. (2004): *Nonlinear Analysis of Reinforced Concrete Structures Subjected to Seismic Loading by Using Three-dimensional Lattice Model*, Doctoral thesis, Tokyo Institute of Technology, February.

Miki, T. and Niwa, J. (2004): Nonlinear Analysis of RC Structural Members Using 3D Lattice Model, *Journal of Advanced Concrete Technology*, JCI, Vol. 2, No.3, pp.343-358, October.

Miki, T., Niwa, J., and Lertsamattiyakul, M. (2003a): Earthquake Response Analysis for RC Bridge Piers Considering Reinforcement Buckling Behavior, *Journal of Materials, Concrete Structures and Pavements*, JSCE, No.732/V-59, pp.225-239, May. (in Japanese)

Miki, T., Niwa, J., and Lertsamattiyakul, M. (2003b): Numerical Evaluation of Seismic Performance of Reinforced Concrete Bridge Piers Using Dynamic Lattice Model, *Concrete Library of JSCE*, Vol.41, pp.49-64, June.



Niwa, J., Choi, I. C., and Tanabe, T. (1995): Analytical Study for Shear Resisting Mechanism Using Lattice Model, Concrete Library of JSCE, No.26, pp.95-109, December.

Takemura, K. and Kawashima, K. (1997): Effect of Loading Hysteresis on Ductility Capacity of Reinforced Concrete Bridge Piers, *Journal of Structural Engineering*, JSCE, Vol.43A, pp.849-858, March. (in Japanese)

Vecchio, F. J. and Collins, M. P. (1986): The Modified Compression Field Theory for Reinforced Concrete Elements Subjected to Shear, *ACI Journal*, Vol.83, No.2, pp.219-231, March/April.

### **3. DEVELOPMENT AND APPLICATION OF MULTI-DIRECTIONAL POLYGONAL 3D LATTICE MODEL**

#### **3.1. Introduction**

Circular cross-sectional RC columns are favored for bridge piers, because of relative simplicity of construction as well as omnidirectional strength characteristics under wind and seismic loads (Ang et al. 1989). Under those conditions, some very important issues arise: the first one is related to the ability of the column shear resistance considering that the design procedures and formulas that are adopted are based on experimental work performed essentially of rectangular shaped cross-sections. Therefore it is important to consider the particular case of circular cross-sectional geometry in RC columns.

Based on previous studies (Miki and Niwa 2004), the 3D lattice model has shown capabilities of prediction of shear behavior of RC structural members with relative simplicity of analytical procedure. Because of that, an analysis mechanism has been developed for circular cross-section RC columns using the 3D lattice model based on the concept of a more realistic multi-directional polygonal discretization. The 3D lattice model for a circular column is named multi-directional polygonal 3D lattice model (Simão and Miki 2015).

#### **3.2. Modeling and Geometry of Members**

In the multi-directional polygonal 3D lattice model, the discretization of the circular column from solid concrete to the 3D lattice model is performed so that the actual cross-sectional diameter,  $D$  of the analytical model corresponds to that of the original target which means that target diameter defines mesh size and model height, or geometry of the model.

The arch and truss discretization is shown in **Figure 3.1**. The arch action is defined by four arch members, as shown in **Figure 3.2**, connected from the loading point to opposite bottom of the column which is representative of internal stress flow. This is largely a simplification from the general 3D lattice model case where it is assumed that the compressive portion in arch action is sufficiently represented in the pair of arch members. Along the principal axis, after the loading is reversed, the direction of the compressive stress changes to the orthogonal direction, this is a fundamental for the representation of symmetrical pairs of arch members. The representation of the truss action, schematically represented in **Figure 3.3**, is performed on a 3D space.

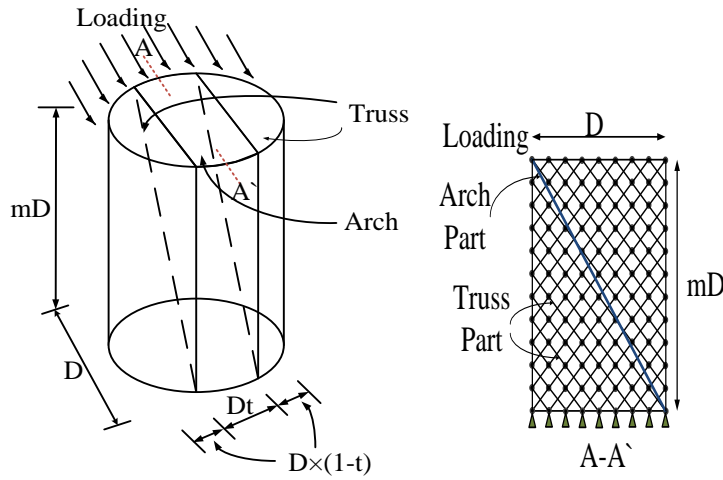


**Fig.3.1** 3D lattice model for a circular column

In the 3D space, the representation of the truss elements is divided in three parts as shown in **Figure 3.3**, which are inner diagonal members (IDM) in **Figure 3.3 (a)**, surface diagonal members (SDM) in **Figure 3.3 (b)** and diagonal members in transverse direction (DMT) in **Figure 3.3 (c)**, respectively. The modeling of diagonal members is preceded by the distribution of sixteen peripheral nodes for every horizontal layer. The distance between two successive layers is equal to half of the diameter i.e.  $0.5D$ , the in-plane nodal positions are set according to their polar coordinates defined by  $x = r \cos\phi$  and  $y = r \sin\phi$  in an orthogonal system, where  $r$  is the radius and  $\phi$  is the internal angle defined by a triangle formed by joining two successive node to each other and the center node. In the case of inner diagonal members, each node at the surface is directly

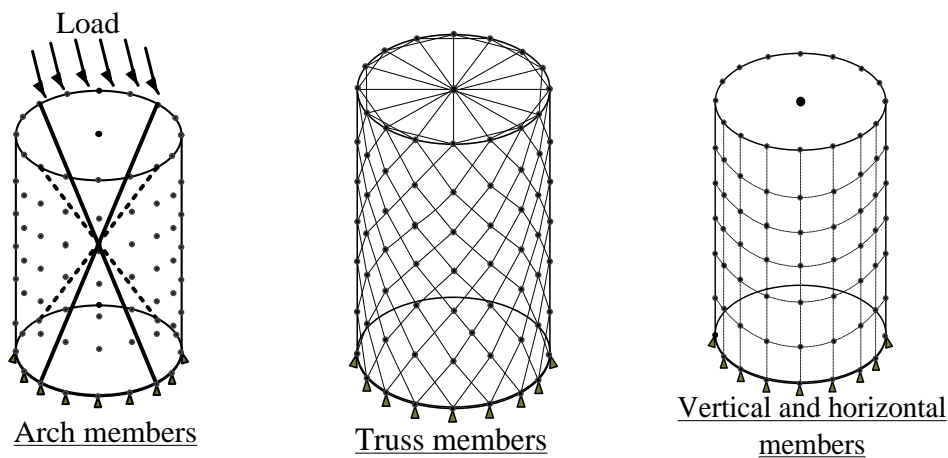


**Figure 3.2** Schematic Diagram of multi-directional polygonal 3D lattice model

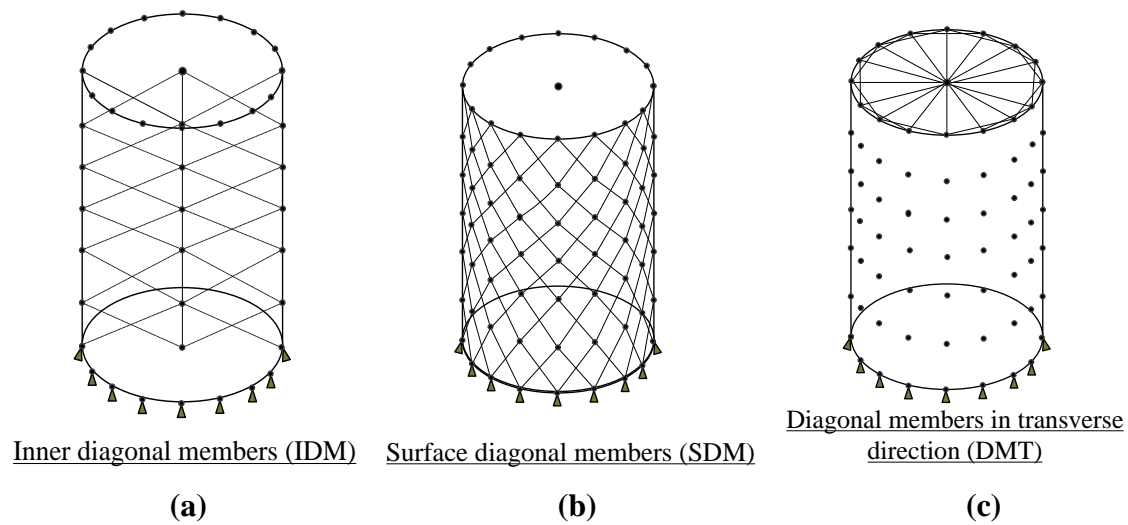


**Figure 3.3** Representation of the truss elements

connected to the lower or upper node in the central group on nodes.

For the surface diagonal members the nodes are connected successively along the surface area and in the case of diagonal members in transverse direction as shown in **Figure 3.3 (b)**, sixteen peripheral nodes are connected to a center node for every layer of nodes as shown in **Figure 3.3 (c)**, and every node is connected to the second following node. In the lattice model, the height of the analytical model does not always correspond to the height of the target, but rather the closest dimension. This is due to the fact that distance between two nodes in vertical direction is fixed as half of the diameter. Longitudinal reinforcement is represented as vertical reinforcement member along the sixteen nodes defining the geometry of the model. Regarding transverse reinforcement, it is represented in the form of horizontal reinforcement members uniformly distributed at intervals of  $0.5D$  throughout the model as the intervals of arrangement are not taken into account. In the model it considered that concrete and steel are perfectly bonded and no bond degradation is observed for simplicity in analysis.

### 3.3. Cross-Sectional Area of Lattice Members

The process of determination of cross-sectional area of arch and diagonal members in the multi-directional 3D lattice model is performed considering the particularities of the cross section of the analytical target. As previously stated, the diameter of the model is invariant for the definition of geometry of the analytical model. Previous researches (Pique and Burgos 2008, Merta and Kolbitsch 2006) refer to the fact that under severe seismic loading inelastic response and cracking of concrete is observed. Under those conditions, the shear resisting area of concrete and the structural stiffness conditions

will be affected. In order to take those conditions into account in analysis the notion of analytical diameter is introduced in order to facilitate the calculation of the cross-sectional area of lattice members considering the effects of such conditions and generally improve the performance of the analytical model. With that, analytical diameter is defined as the diameter obtained from analytical conditions to calculate the cross-sectional area of arch and truss members.

With that, the transformation from solid concrete to truss and arch members analogy tries to offer a more realistic discretization of RC columns. In the 3D lattice model, material nonlinearity is already considered; however in this study reduction factors are used to better consider material nonlinearity, especially reduction of cross-sectional area of trusses to account the effect of cracking. Based on that, in this research two different approaches are studied: the first one is the shear resisting capacity of concrete as discussed by Merta and Kolbitsch (2006). In their work they derived the effective shear area of circular cross-section columns purely analytically. The ratio of the effective shear area to gross section area was expressed as a function of the neutral axis depth for different values of the concrete cover. For a typical value of neutral axis depth, it was shown that the effective shear area ranges between 0.6 and 0.8 times the sections gross area depending on the depth of the concrete cover.

A second approach used to consider the change in mechanical properties after cracking of concrete is the degradation of stiffness  $EI$ . Pique and Burgos (2008) extensively studied the effective rigidity of reinforced concrete elements in seismic analysis and observed in their work that stiffness degradation can be observed along the element length after cracking of concrete. However it is not practical to evaluate the stiffness degradation in various cross-sectional portions individually, because of that reasonable average reduction factor values must be adopted. Reduction factors of moment of inertia to consider the averaged effect of stiffness degradation ranging from 0.4 to 0.7 times gross moment of inertia are considered in the pre-analysis in this study based on the work presented by the previous study by Pique and Burgos (2008).

### **3.3.1. Cross-sectional area of arch members**

For the determination of the stiffness matrix in the arch members, it is assumed that a single arch member is representative of the stress flow for analysis purposes. The equivalence of global stiffness of structural systems in 2D and 3D is assumed. The

geometrical properties of the circular cross section column are considered the same in the transverse plane directions.

The structural stiffness matrices for the 2D and 3D lattice model,  $K_{2D}$  and  $K_{3D}$ , are expressed using the direct stiffness method as follows:

$$\mathbf{K}_{2D} = \frac{\gamma_{2D}}{1+m^2} \begin{bmatrix} 1 & m & 0 & -1 & -m & 0 \\ & m^2 & 0 & -m & -m^2 & 0 \\ & & 0 & 0 & 0 & 0 \\ & & & 1 & m & 0 \\ sym. & & & & m^2 & 0 \\ & & & & & 0 \end{bmatrix} \quad (3.1)$$

$$\mathbf{K}_{3D} = \frac{\gamma_{3D}}{2+m^2} \begin{bmatrix} 1 & m & 1 & -1 & -m & -1 \\ & m^2 & m & -m & -m^2 & -m \\ & & 1 & -1 & -m^2 & -1 \\ & & & 1 & m & 1 \\ sym. & & & & m^2 & m \\ & & & & & 1 \end{bmatrix} \quad (3.2)$$

In this case,

$$\gamma_{2D} = \frac{E_c A_{arch-2D}}{l_{arch-2D}} = \frac{E_c A_{arch-2D}}{\sqrt{D^2_{ana}(1+m^2)}} \quad (3.3a)$$

$$\gamma_{3D} = \frac{E_c A_{arch-3D}}{l_{arch-3D}} = \frac{E_c A_{arch-3D}}{\sqrt{D^2_{ana}(2+m^2)}} \quad (3.3b)$$

where,  $A_{arch-2D}$  and  $A_{arch-3D}$  are representatives of the cross-sectional areas of arch members for both the 2D and 3D lattice models.  $l_{arch-2D}$  and  $l_{arch-3D}$  are the lengths of arch members in the 2D and 3D lattice models.  $E_c$  is the Young's modulus of concrete.  $m$  is set so that that  $mD_{ana}$  corresponds to the height model, furthermore  $D$  is the diameter of cross section of the column.

Regarding the cross-sectional area of an arch member of concrete in the 3D lattice model, the equivalence in global stiffness is used for the computation of the relationship between the arch members in 2D and in 3D assuming a single representation of the stress flow in the arch part and expressed by **Equation 3.4**.

$$A_{arch-3D} = \left( \frac{2+m^2}{1+m^2} \right)^{3/2} \cdot A_{arch-2D} \quad (3.4)$$

$$A_{arch-2D} = D_{ana}^2 t \cdot \sin \theta \quad (3.5)$$

where, in the 2D case it is assumed that the length of the arch band corresponds to the full length of diameter for simplicity, and  $\theta$  is the inclination of the arch member in the 2D lattice model.

### 3.3.2. Cross-sectional area of truss members

The determination of the truss action in the multi-directional polygonal 3D lattice model is performed based on the omnidirectional nature of the circular cross section. Therefore, the cross sectional area of diagonal truss members will be determined according to the formulas shown in **Equations 3.6, 3.7** and **3.8**, respectively. Because of the high-contribution to stiffness that the IDM have in response, a stiffness adjusting factor  $\beta$  empirically determined in pre-analysis between 0.5 and 0.9 is necessary in the calculation of the cross-sectional area of the IDM.

$$A_{IDM} = \beta \frac{D_{ana}(1-t)}{2} \cdot \frac{D_{ana}}{2} \sin 45^\circ \quad (3.6)$$

$$A_{SDM} = \frac{D_{ana}(1-t)}{2} \cdot \frac{D_{ana}}{2} \sin 45^\circ \quad (3.7)$$

$$A_{DMT} = \frac{a}{2m} \cdot \frac{D_{ana}}{2} \sin 45^\circ \quad (3.8)$$

where  $A_{IDM}$ ,  $A_{SDM}$  and  $A_{DMT}$ , represent the cross-sectional areas of the inner diagonal members, surface diagonal members and diagonal members in transverse direction in the 3D space. Here  $a$  represents the shear span,  $D_{ana}$  is the analytical diameter,  $m$  is set so that that  $mD_{ana}$  corresponds to the height model.

### 3.4. Parametric Analysis of Relationship between Arch and Truss Members

#### 3.4.1. Introduction

In the modeling of RC structures using the multi-directional polygonal 3D lattice model, a certain level of uncertainty can be observed due to the interaction between the arch and truss analogy and the use of reduction factors as well as multiple other analogies. In order to extend the arch and truss analogy to a 3D case using the multi-directional polygonal 3D lattice model, it is important to understand first how much the response of the analytical target is affected by using different relationships between the arch and truss members through the value of  $t$ . From that a clear tendency in behavior can be grasped and the use of reduction factors can be done much more effectively.

#### 3.4.2. Effect of value of $t$

In order to investigate the effect of value of  $t$  fundamental 2D lattice model analysis of rectangular cross-section RC column is presented. The arch and truss analogy used in the multi-directional polygonal 3D lattice model is largely an extension of the approach proposed in previous studies (Miki and Niwa 2004), therefore using a 2D approach allows a simple and clear validation of the assumption. The analysis presented has been conducted by Miki (2004) and is here used. The analytical target is shown in **Figure 3.4**. The parameters of the column are as follows:  $f_c' = 27.0 \text{ N/mm}^2$ ,  $f_y = 380 \text{ N/mm}^2$ ,  $E_s = 72 \text{ kN/mm}^2$ ,  $f_{wy} = 360 \text{ N/mm}^2$ , and  $E_{sw} = 175 \text{ kN/mm}^2$ . The longitudinal and transverse reinforcement ratios are set as 2.38 % and 0.056 %, respectively. The Constant compressive axial force of 79.7 kN is applied at the top of the column.

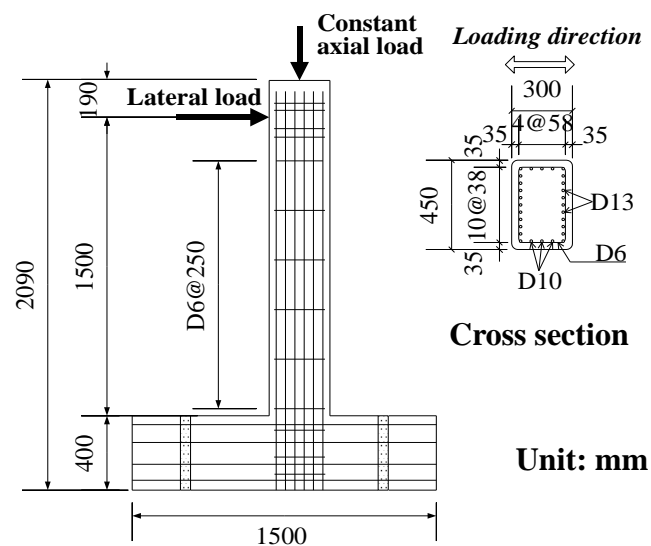


**Figure 3.4** Experimental setup (Miki 2004)



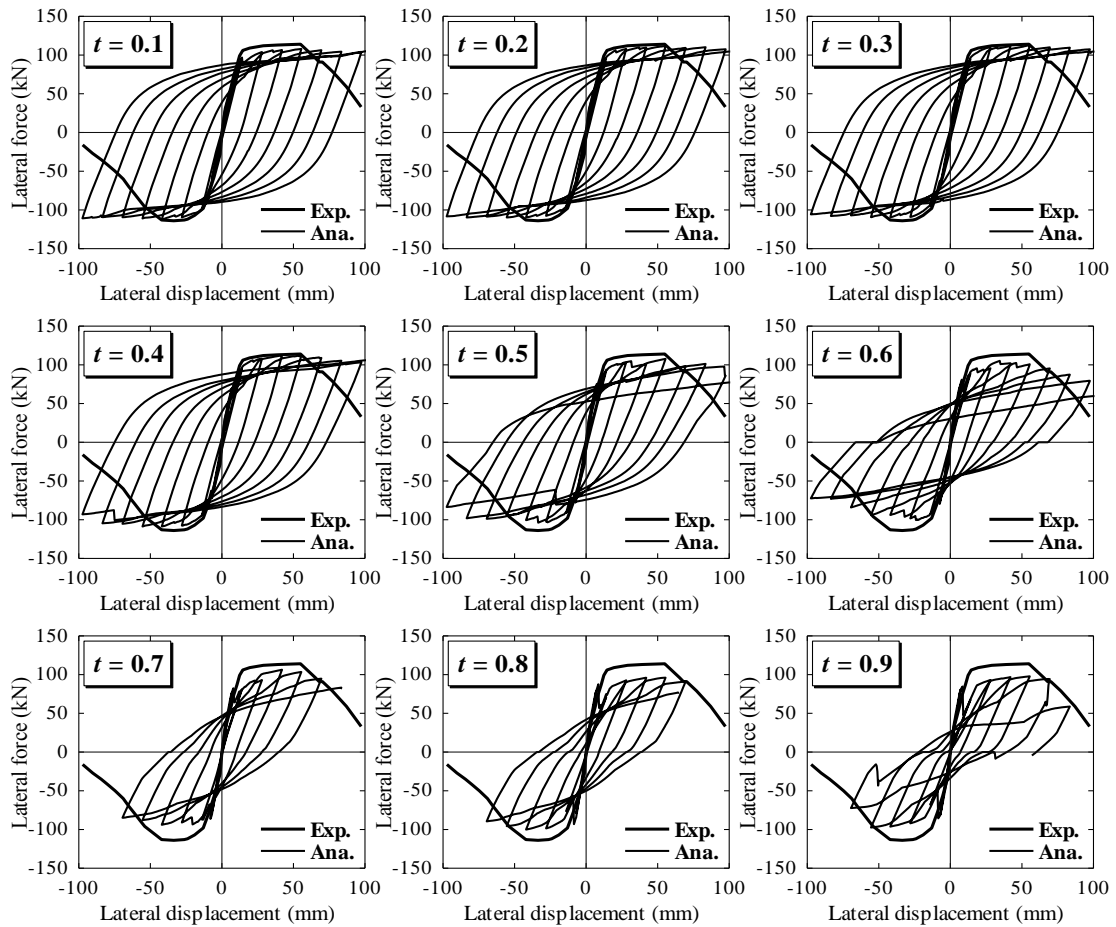


**Figure 3.5** Effect of value of  $t$

The analytical results are shown in **Figure 3.5**. In his calculation, Miki (2004) determined the value of  $t$  based on the theorem of minimization of total potential energy as 0.2. However by extending the limits from 0.1 to 0.9 it is visible that the smaller values show a higher energy dissipation capacity up to the large deformation range. With the increase of  $t$  the maximum force is slightly increased. Based on that, it is possible to assume that in the multi-directional 3D lattice model, any changes in the relationship between arch and truss part will likely affect the energy dissipation capacity based on visible changes in the maximum displacement while changes in the maximum force are marginal in their contribution. In the modeling of RC structures using the proposed analytical model it becomes then necessary to pay attention at all steps to the energy dissipation capacity. It remains to be studied to real arch effect in circular RC columns, however this analysis gives a valuable benchmark to be used in circular columns in conjunction with reduction factors.

### 3.5. Linear-Elastic Analysis of Circular-Cross Section RC Columns

#### 3.5.1. Introduction

In order to verify the applicability of the two analytical cases previously discussed, one related to the hypothesis of reduction of shear area of concrete and a second one related to degradation of stiffness  $EI$ , linear-elastic analysis will be conducted on a circular cross-section column and the analytical results compared to a linear-elastic curve response determined by the elasticity theory. Here the analysis is centered in stress conditions that will not produce any yielding in the target column. The analytical relationship that has been applied the determination of the load-displacement relationship in elastic range is presented in **Equation 3.9**.

$$d = \frac{Pl^3}{3EI} \quad (3.9)$$

where  $d$  is the displacement,  $P$  represents the load,  $l$  represents the length of the column,  $E$  is the Young's modulus and  $I$  the moment of Inertia.

#### 3.5.2. Outline of analytical target

The analytical target is a circular cross sectional column tested by E-Defense. The target of this study is the C1-5 column (Kawashima et al.2010). The detailed description of the target of analysis, including arrangement of reinforcement is shown in **Figure 3.4**. The specimen C1-5 is a cantilever circular column with diameter 2000 mm. The heights of the column and footing correspond to 7500 mm and 1800 mm respectively. The longitudinal and transverse reinforcement have a nominal strength of 345 MPa and the design concrete strength of 27 MPa. Sixty four deformed 35 mm diameter longitudinal bars are presented in two layers, while deformed 22 mm circular ties are set at 150 mm and 300 mm intervals in the outer and inner longitudinal bars.

#### 3.5.3. Discretization of target

In order to analyze the target presented in **Figure 3.6**, two analytical cases are set for static analysis. For analytical case one (AC-1) and analytical case two (AC-2) the multi-directional polygonal 3D lattice model is used. In the modeling for AC-1 and AC-2 geometrical properties defined by the mesh size and height of the models are precisely the same.

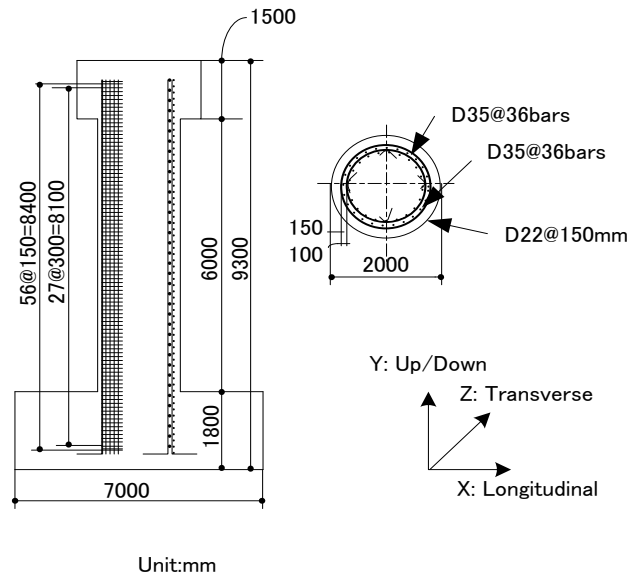


**Figure 3.6** C1-5 specimen details (Kawashima et al.2010)

The geometry of AC-1 and AC-2 is shown in **Figure 3.7**. The dimension of the truss members and arch members differ between AC-1 and AC-2. In the AC-1  $D_{ana}$  is obtained from effective shear area of concrete determined to be a value corresponding to 0.7 of the gross area of concrete. In the AC-2,  $D_{ana}$  is derived from the flexural stiffness  $EI$ , and corresponds to 0.5 of the gross moment of Inertia. These reduction factor values were obtained in pre-analysis by calibrating the analysis each time until satisfactory load-displacement curve was obtained. However the benchmarks used are those referred by the literature (Pique and Burgos 2008, Merta and Kolbitsch 2006). The analytical diameters obtained for analysis are 1673.32 mm for AC-1 and 1829.38 mm for AC-2.

#### 3.5.4. Analytical results and discussion

The analytical results of the load-displacement for the target column C1-5 are presented and subjected to discussion for the proposed analytical cases. The results for analytical case AC-1 **Figure 3.7 (a)** and analytical case AC-2 are presented in **Figure 3.7 (b)**. The analytical results of AC-1 shows acceptable degree of agreement between the analysis and the linear-elastic theory plot regarding elastic stiffness. The proposed cases capture the elastic stiffness in elastic phase both acceptably. AC-1 produced a slightly bigger analytical diameter than AC-2. One of the key issues during the development process of the multi-directional polygonal 3D lattice model was a tendency to overestimate plastic stiffness. These two approaches for all their merits also address this issue.

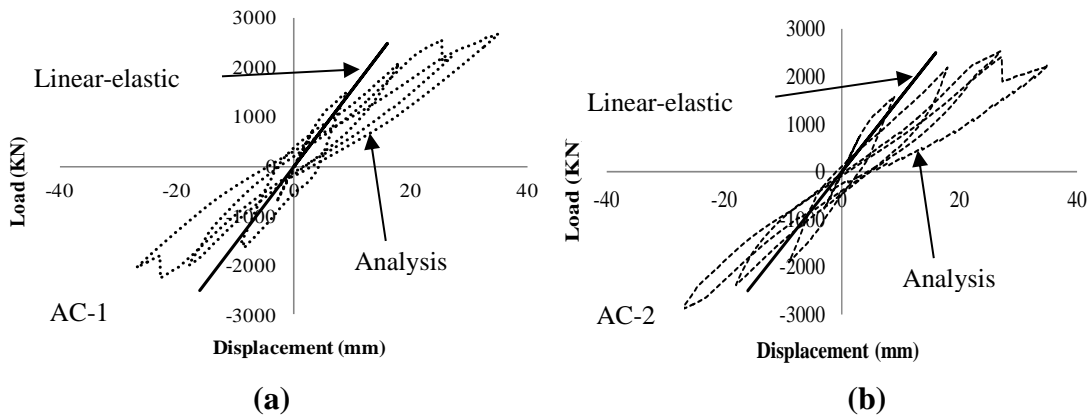


**Figure 3.7** Load-displacement of AC-1 and AC-2

With the above results it is confirmed the validity of the effective shear hypothesis and the effective stiffness hypothesis based on comparison with the elastic stiffness obtained from the elastic theory. Since the results are quite similar, one of the conclusions that can be drawn is that both approaches can equally be applied to discretize a circular cross-section column using the multi-directional polygonal 3D lattice model.

### 3.6. Static Analysis of Circular RC Columns Subjected to Cyclic Loading

#### 3.6.1. Outline of analysis

In order to further confirm the performance of the multi-directional 3D lattice model, the model was verified by the simulation of RC column that has been subjected to cyclic loading experimentally. The target is a circular cross section column tested named C-29 (Hoshikuma et al. 2013). In previous sub-chapter a discussion on the hypothesis of effective shear area and effective flexural area was introduced. One of the conclusions at that level was that these two approaches could equally be applied in the multi-directional polygonal 3D lattice model. Based on that, a more detailed look will be presented here on the sensitivity analysis of reduction factor based on degradation of stiffness. In other words in this study, the stiffness degradation is analyzed considering the applicability of stiffness reduction factors to represent the effect that a cracked section has in the actual design and response of RC columns. To perform the analysis, the focus will be on the degradation of flexural stiffness. In a more specific way, parametric analysis was conducted in order to verify the effective applicability of moment of inertia (second moment area) reduction factors. The assessment of stiffness

degradation induced by seismic damage is verified by the simulation of RC column that has been subjected to monotonic loading experimentally.

Column C-29 details are shown in **Figure 3.8**. The cross section is circular with diameter of 600 mm and column height of 3410 mm, respectively. The compressive strength and Young's modulus of concrete are 31.8 N/mm<sup>2</sup> and 28000 N/mm<sup>2</sup>, respectively. The longitudinal reinforcement of D10 has yield strength of 397 N/mm<sup>2</sup> and the transverse reinforcement D6 has yield strength of 397 N/mm<sup>2</sup>, respectively

The benchmark inertia reduction factors suggested by previous studies range from 0.4 to 0.8 times gross moment of inertia (Pique and Burgos 2008, Paulay and Priestley 1992) and were considered in pre-analysis. However, during the pre-analysis, the decision was made to select three analytical cases, each corresponding to a specific reduction factor of inertia that presented the most effective demonstration of the effect of inertia reduction factors. In that way analytical case one denoted as C-29(1) corresponds to an effective inertia of concrete of 0.8 times the gross moment of inertia of concrete, analytical case two denoted as C-29(2) corresponds to the effective moment of inertia of 0.6 times the gross moment of inertia, and analytical case three denoted as C-29(3) corresponds to an effective inertia of 0.4 times the gross moment of inertia. The obtained effective moments of inertias were the used to calculate analytical diameter used to discretize the RC column in the multi-directional 3D lattice model. In all analytical cases the value of  $t$  is set as 0.4.

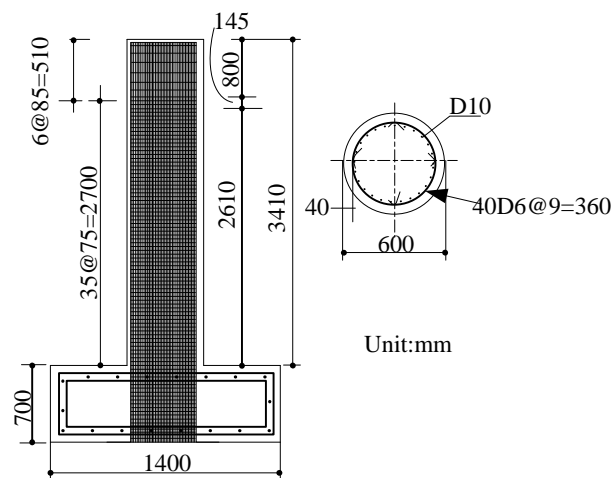


**Figure 3.8** C-29 specimen details (Hoshikuma et al. 2013)

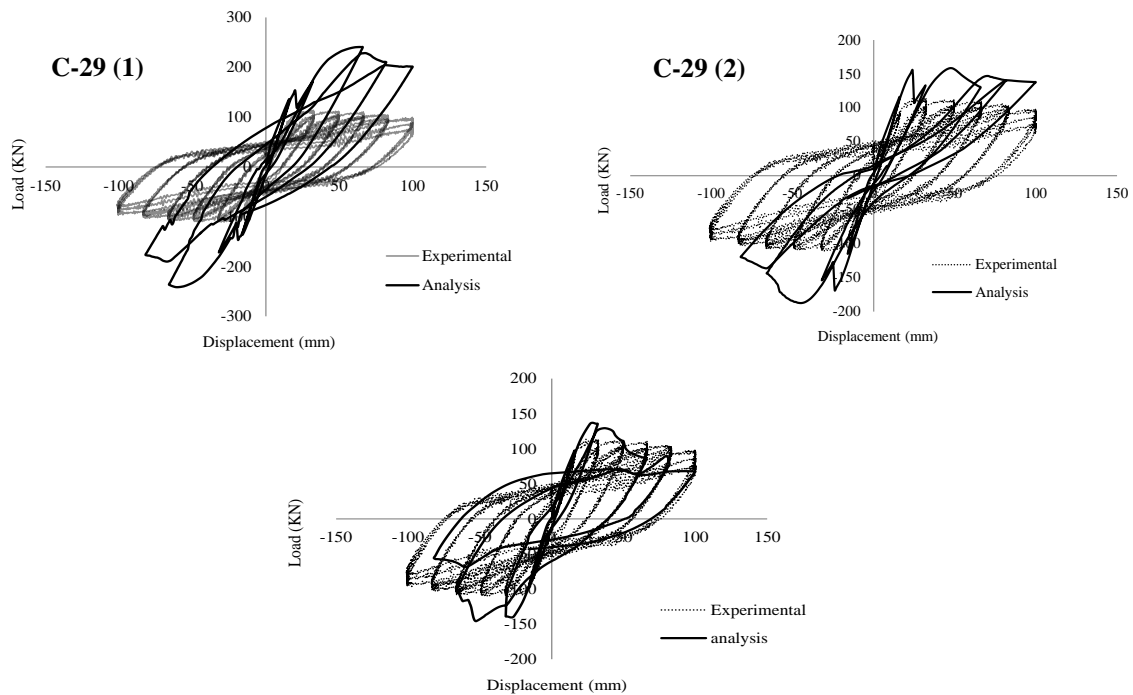


**Figure 3.9** C-29 load-displacement relationships

### 3.6.2. Analytical results and discussion

The analytical results presented in **Figure 3.9** show that there is a considerable difference in the load-displacement relationships for the analytical cases. Based on hysteretic agreement, C-29(3) presents more agreement between the analysis and the experiment, while C-29(1) presents less agreeability regarding the predicted the hysteresis of the target.

Looking at the results, it is possible to infer that that in the case of AC1 and AC2, the tendency is to underestimate the displacement and overestimate the lateral load. The case of AC3 shows that actually a more significant reduction in effective inertia is necessary in analysis, when compared to the literature, to more accurately represent the response. One of the reasons behind it is related to how reinforcement is treated. In the discussion about reduction factors proposed, Pique and Burgos (2008) mention that in their analysis there is no special consideration on the effects of reinforcement ratio, meaning that reinforcement is treated as a typical reinforcement ratio; i.e. it is not given special attention to the ratio between confined concrete and the amount of reinforcement. However, the pre-analysis of the target column C-29 in this study proved that the dominance of concrete part of the column cannot be neglected, and one of the effects is the need to further decrease the reduction factors in order to account for this effect.

In terms of hysteretic energy dissipation capacity, it is valuable to focus first on cases C-29(2) and C-29(3) because they produce close values of energy dissipation, and compare them to the energy dissipation produced by the experimental results. The experimental hysteretic energy dissipation corresponds to 27.5 KN-m while AC2 corresponds to 30.2 KN-m and C-29(3) corresponds to 30.5 KN-m. However, looking at the load-displacement relationships presented in **Figure 3.9**, it is clear that although C-29(2) and C-29(3) present very similar hysteretic energy dissipation, the distribution of energy based on hysteretic response of C-29(3) is far more agreeable with the experiment than C-29(2). In other words the hysteric response similarity between C-29(3) and the experiment suggests a much more similar mechanism of energy dissipation than that of C-29(2) and the experiment. On the other hand the tendency of C-29(1) is to overestimate energy dissipation capacity. Here the hysteretic energy dissipation of AC1 corresponds to 47.9 KN-m.

### **3.7. Discretization Method Analysis of Circular RC Columns**

#### **3.7.1. Introduction**

The highly nonlinear behavior that reinforced concrete (RC) structures exhibit in the occurrence of an earthquake is at the top of priorities in the analytical development of numerical techniques to study seismic behavior. Many techniques are available to perform seismic analysis of RC columns. Columns are especially vulnerable against lateral loads induced by seismic action result in many times in shear failure as a dominant mode of failure. In seismic design of RC columns, the geometry of the section has a strong influence on the shear capacity of the member. However the majority of the codes simply assume that the shear capacity of a circular cross section equals the capacity of an equivalent rectangular section (Merta 2004). With that in mind, it is important to evaluate the merits of treating a circular column just as an equivalent cross-sectional area rectangular column against a more realistic discretization of circular cross-section.

#### **3.7.2. Outline of analysis**

In order to analyze the applicability of circular-rectangular equivalence against a more direct discretization, the analytical target is a circular cross section column named C1-5 tested using a shake-table by E-Defense (Kawashima et al. 2013) which has been previously introduced in Sub-chapter 3.4.3 and specimen details in **Figure 3.6**.

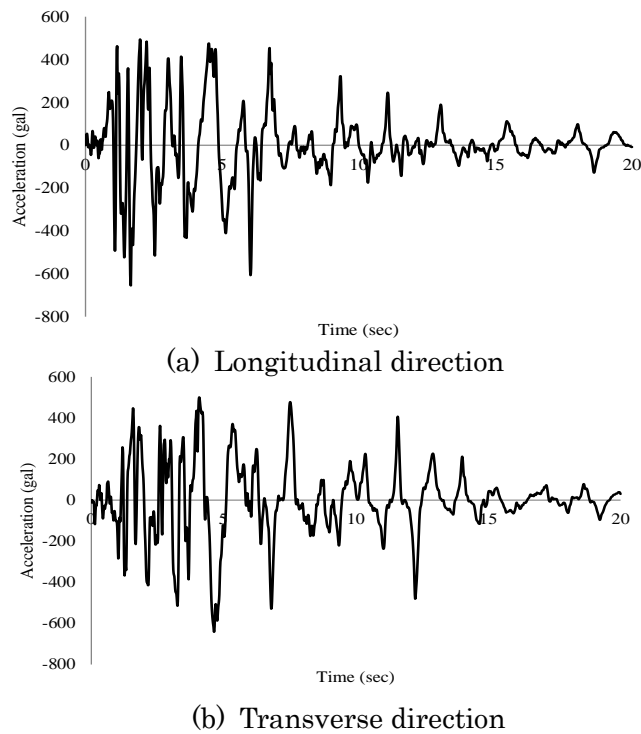


**Figure 3.10** 100% E-Takatori ground motion (Kawashima et al. 2010)

Column C1-5 was designed according to the 2002 JRA Design Specifications of Highway Bridges (JRA 2002), based on the design response spectrum (Kawashima et al. 2002), based on the design response spectrum (Kawashima et al. 2002). The specimen is a cantilever circular column with diameter 2000 mm. The heights of the column and footing correspond to 7500 mm and 1800 mm respectively. Column C1-5 was excited using a near-field ground motion which was recorded at the JR Takatori Station during the 1995 Kobe earthquake. Taking into account the soil/structure interaction, a ground motion with 80% of the original intensity of JR Takatori was imposed as command to the table in the experiment. In the experimental program, C1-5 has been excited under different conditions, however in this study the analysis will focus on C1-5(1) which corresponds to the first excitation. The ground motion corresponding to 100% E-Takatori in longitudinal and transverse directions is shown in **Figure 3.10**.

In order to analyze column C1-5 two analytical situations have been set. First is the conversion of circular cross sectional shape into an equivalent rectangular cross sectional shape, based on the fact that most design methods for shear and flexure of RC members are mainly based on the rectangular cross-sectional shape for the analysis.



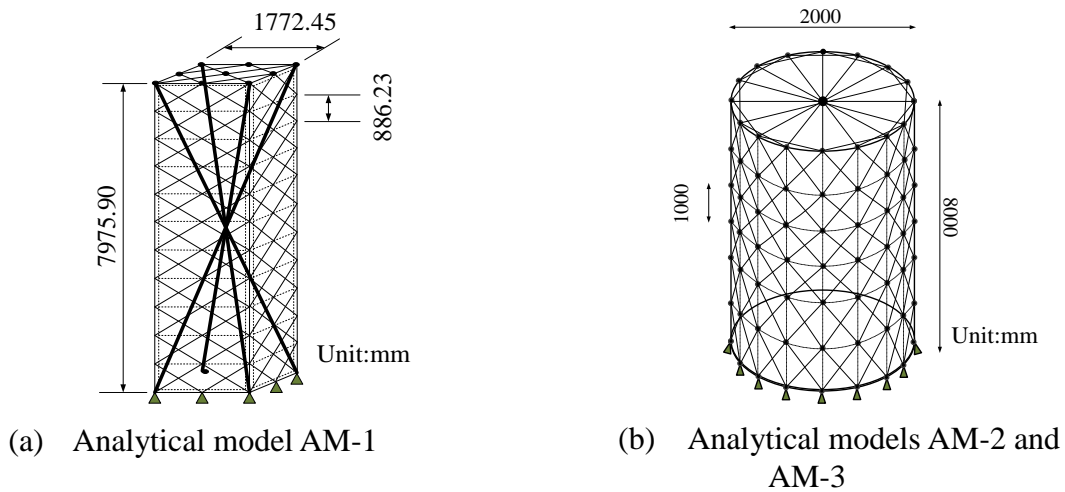


**Figure 3.11** Analytical models

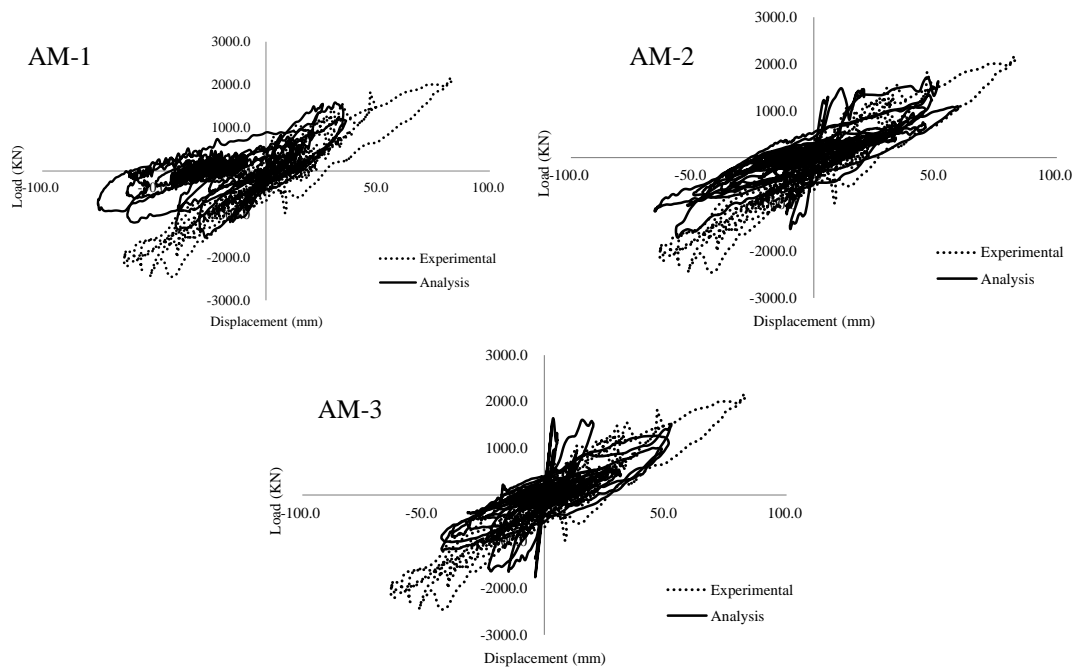
Upon this, the 3D lattice model as developed in previous studies (Miki and Niwa 2004) is used in an analytical model further addressed as AM-1 shown in **Figure 3.11 (a)**.

The second analysis corresponds to the application of the multi-directional polygonal 3D lattice model, newly developed for circular cross section columns. Here, the shear capacity of reinforced concrete is considered by assuming that of the actual resisting area of concrete is reduced in seismic response. It is in that way that an analytical model addressed as the AM-2 is developed, where an effective area of concrete corresponding to 0.7 of the gross area of concrete is assumed to determine the cross-sectional area of the lattice members.

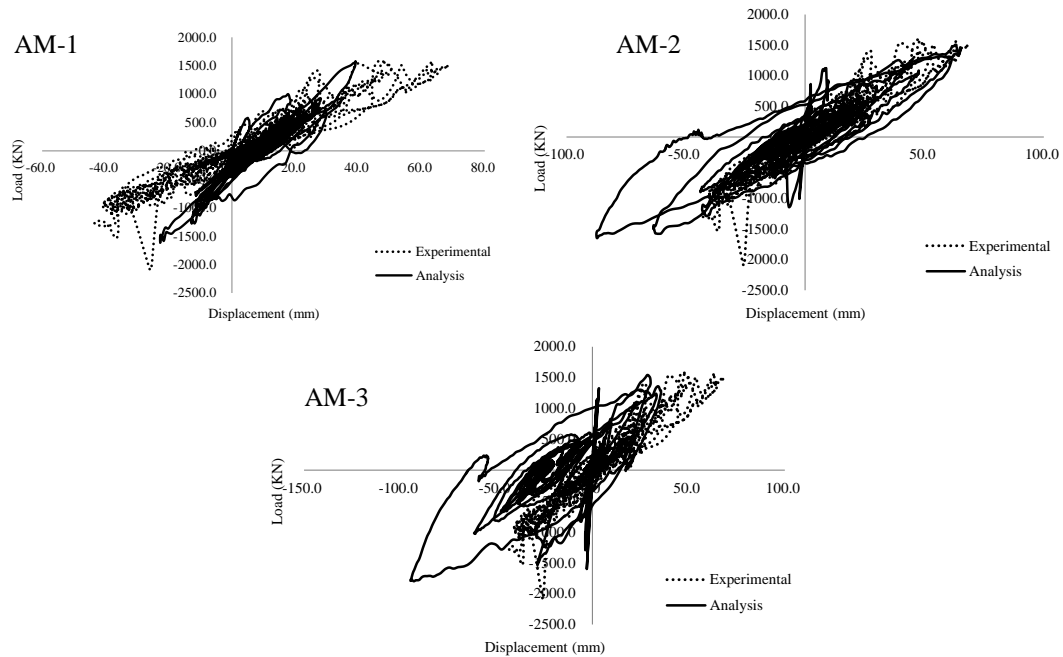
The reduction in flexural stiffness is considered to perform analysis. Assuming that there is stiffness degradation in seismic response, an analytical model AM-3 is developed; where in the case effective area moment of inertia corresponding to 0.7 of the gross moment area of inertia is assumed for the analytical diameter used to determine the cross-sectional area of lattice model elements. It should be noted that the general geometry of AM-2 and AM-3 is the same as detailed in **Figure 3.11 (b)**.

### 3.7.3. Analytical results and discussion

The analytical results using analytical models AM-1, AM-2 and AM-3 are shown in **Figure 3.12** and **Figure 3.13** respectively, and compared to the experimental results.



(a) Longitudinal direction



(b) Transverse direction

**Figure 3.12** Load-displacement relationships computed using analytical models

The analytical response using AM-1 shows reasonable agreement with the experiment before cracking occurs; the initial stiffness is very consistent in both directions, however, it is in the longitudinal direction that the after cracking behavior differ visible, but while in the transverse direction the hysteretic response though is agreeable underestimates

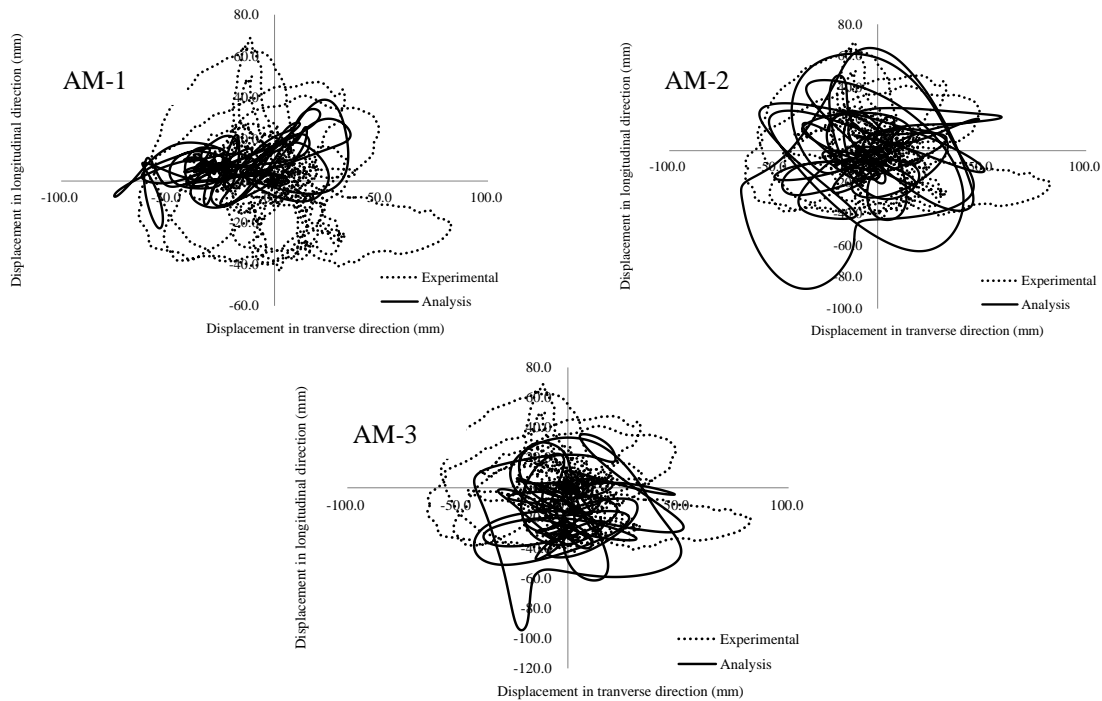


**Figure 3.13** Displacement relationships computed using analytical models

maximum force as well as displacement. Thus supporting that, the assumption of equivalence of responses between a rectangular cross sectional member and circular cross section member has large limitation in inelastic phase.

The analysis performed using the multi- directional polygonal lattice model, in both proposals presented in this paper show that largely better hysteretic agreement is obtained. Looking at the response using AM-2 when consideration for reduction of shear area of concrete is used, it is visible that the prediction of maximum displacement and force is reasonably performed, especially in the longitudinal direction. However in the transverse direction the hysteretic response overestimates the deformation capacity.

On the other hand, AM-3 shows the most acceptable prediction of response when compared to the other models presented. This suggests that consideration for an equivalent flexural stiffness in the analysis proved more accurate than for shear area of concrete. It is nonetheless important to mention that using the multi-directional polygonal lattice models the initial stiffness is highly estimated.

The reason behind that is the elevated number of elements necessary to describe the element, when compared to the rectangular lattice model. The consequence of this is

that at the beginning, regardless of the approach chosen, that is AM-2 and AM-3, the model consistently has large initial stiffness. This shortcoming should be object of attention in further research on the topic. A detailed look at Fig.10 allows the comparison of displacement capacity prediction in longitudinal and diagonal directions. Comparing the analytical models to the experiment, AM-2 and AM-3 present more acceptable agreement with the experiment in comparison to AM-1; this is a fundamental outcome that comes from the more realistic discretization of target that AM-2 and AM-3 propose.

### **3.8. Cumulative Seismic Damage Assessment in Circular RC Columns**

#### **3.8.1. Introduction**

Experimental and field evidence indicates that the strength, stiffness and ultimate deformation capacity of reinforced concrete (RC) elements and structures deteriorate during excursions into the plastic range (Teran-Gilmore and Jirsa 2005).

Furthermore, a number of seismic events such as the Loma Prieta earthquake in 1989, and more recently Kumamoto earthquake in 2016 are evidence that RC structures and specially columns are in a relatively short time-period subjected to strong plastic deformation due to the sequence of earthquakes` foreshock, main shock and after-shock in one hand, and on the other hand the great Tohoku earthquake in 2011, the strongest ever recorded in Japan proved that RC structures can be hit by a very powerful earthquake followed by numerous strong after-shocks.

It is fundamental that in seismic damage and seismic performance analyses of RC structures, the cumulative effect that an earthquake`s main shock and after-shocks have on the behaviour of RC members, especially columns, is considered, in order to improve the understanding of the real structural behaviour under seismic loading, especially the cumulative effect on the stiffness degradation, energy dissipation as well as parameters related to strength and displacement on RC members.

With the above in mind, this study is focused on the applicability of the multi-directional polygonal 3D lattice model to perform cumulative seismic damage evaluation in circular cross section RC Columns (Simão and Miki 2016).

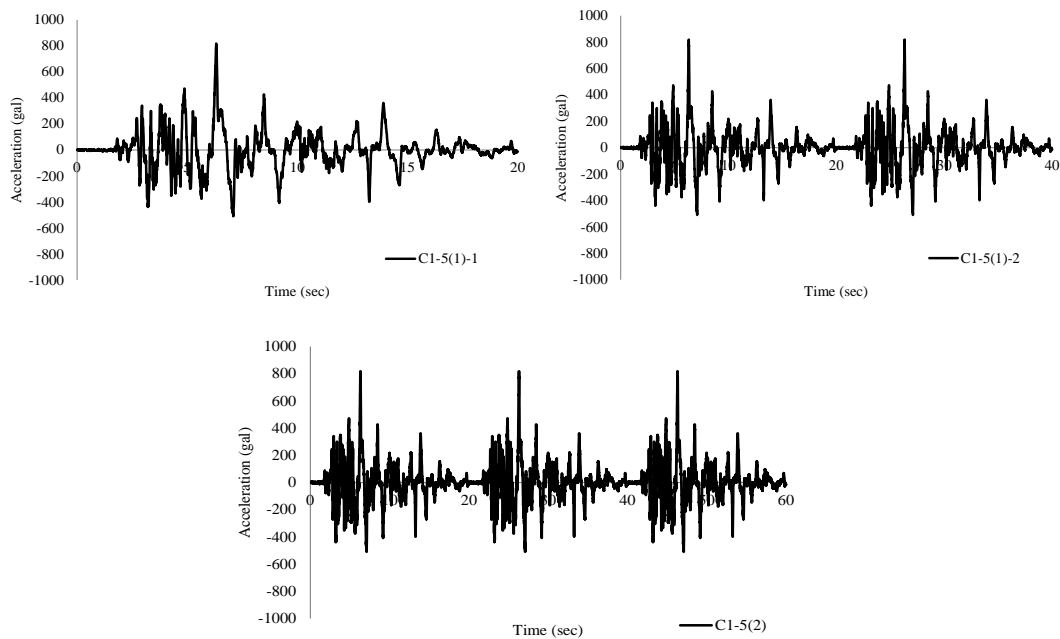


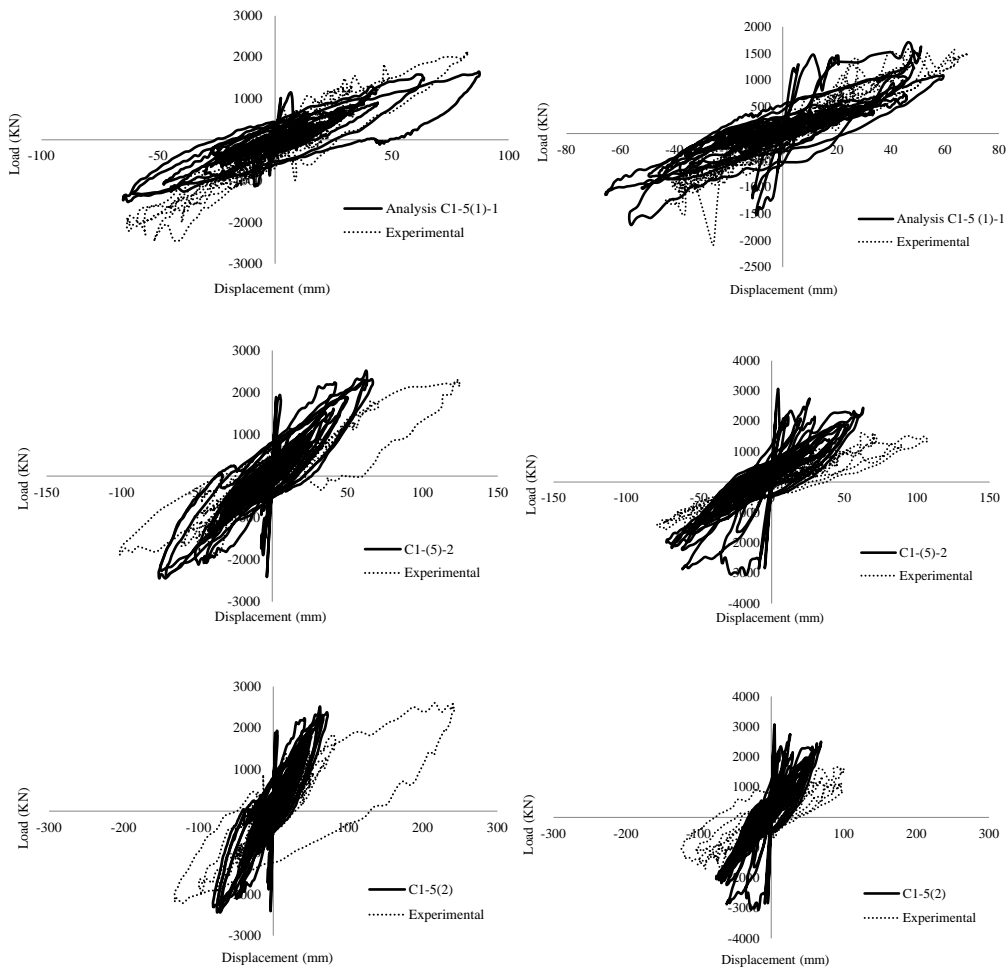
**Figure 3.14** Sequential loading in longitudinal direction for column C1-5

### 3.8.2. Outline of analysis

The analytical target is a circular cross section column named C1-5 tested using a shake-table by the E-Defense presented in Sub-chapter 3.4.3 and specimen details in **Figure 3.6**. In the experiment Vertical load is in the form of tributary mass to the column by two decks including four weights of 307 ton and 215 ton in the longitudinal and transverse directions, respectively. The geometry of the model corresponds to the same geometry presented in **Figure 3.11(b)**. For reduction factors, Pique and Burgos (2008) suggest that for typical columns in order to balance precision and simplicity based on studies previously presented, reduction factor of 0.7 to the gross flexural stiffness is applied in this analysis. The analytical diameter corresponds to 1825.85 mm.

According to Kawashima et al. (2010) column C1-5 was excited in longitudinal, transverse and vertical direction. However this study will neglect vertical direction to focus on the principal directions. The convention and loading sequences used in the experiment are also applied in the analysis.

With that C1-5(1)-1 corresponds to one 100% E-Takatori to a time of 20 seconds of loading, C1-5(1)-2 to two 100% E-Takatori corresponding to 40 seconds of aggregate



(a) Longitudinal direction

(b) Transverse direction

**Figure 3.15** Load-displacement relationships for C1-5 analytical cases

loading, and after 21% increase in the tributal mass at the top of the pier, from 307 ton to 372 ton, C1-5(2) was excited to three 100% E-Takatori corresponding to 60 seconds of aggregate loading. In the experiment, column C1-5 was subjected to further loading. However, for the scope of this study, the focus will be on the three initial loading sequences as explained, because it was concluded during the pre-analysis, that on further loadings, the nonlinear behavior of the column became much more difficult to describe. The loading sequences for longitudinal direction for C1-5(1)-1, C1-5(1)-2 and C1-5(2) are shown in **Figure 3.14**, respectively.

### 3.8.3. Analytical results and discussion

The analytical results for load-displacement relationships are shown in **Figure 3.15** and the results for time-history are shown in **Figure 3.16**, for both longitudinal and transverse direction. Looking at Fig. 6, generally the comparison of hysteresis response between the analytical cases and the experiment shows the highly nonlinear behaviour that accumulated damage causes in the response of the RC column, and this complexity in response calls for a very detailed analysis of the response. It is noticeable that case C1-5(1)-1 shows the best agreement in hysteresis between analysis and the experiment for both directions, when compared to cases C1-5(1)-2 and C1-5(2). Overall the strength capacity prediction is considered to be acceptable in both directions for the three analytical cases.

On the other hand, with increase in the number of loading sequences, going to cases C1-5(1)-2 and C1-5(2), there is a visible tendency to underestimate the maximum displacement capacity due to overestimation of stiffness in response in the longitudinal direction, especially in the quadrant corresponding to positive displacement and positive load. This situation is directly related to the high initial stiffness that is observed in the analytical response of all analytical cases, and according to results previously reported by Simão and Miki (2015), by modelling a circular column using the multi directional polygonal 3D lattice model, elastic stiffness is by tendency overestimated due to the increased number of diagonal members used to discretize a circular column into polygonal 3D lattice model, which increases the size of the stiffness matrix.

In the analytical results, it is visible that after cracking, for the longitudinal direction, the response continues to underestimate the stiffness degradation, thus the response fails to reach the maximum displacement capacity, remaining stiffer than the experiment. This is a point that should be addressed in further stages of this study. However in the transverse direction the response better captured the strength and stiffness degradation going from case C1-5(1)-1 to C1-5(1)-2 and C1-5(2).

The interpretation of analytical results can be further performed by evaluating the hysteretic energy dissipation capacity of all cases. Hereafter, the hysteretic energy dissipation corresponds to the enclosed area of the load-displacement relationships, calculated for analytical response and experimental cases. The energy dissipation is calculated at the end of each analytical cycle, corresponding to total loading time. The analytical calculated energy dissipation for C1-5(1)-1 at 20 seconds of total loading

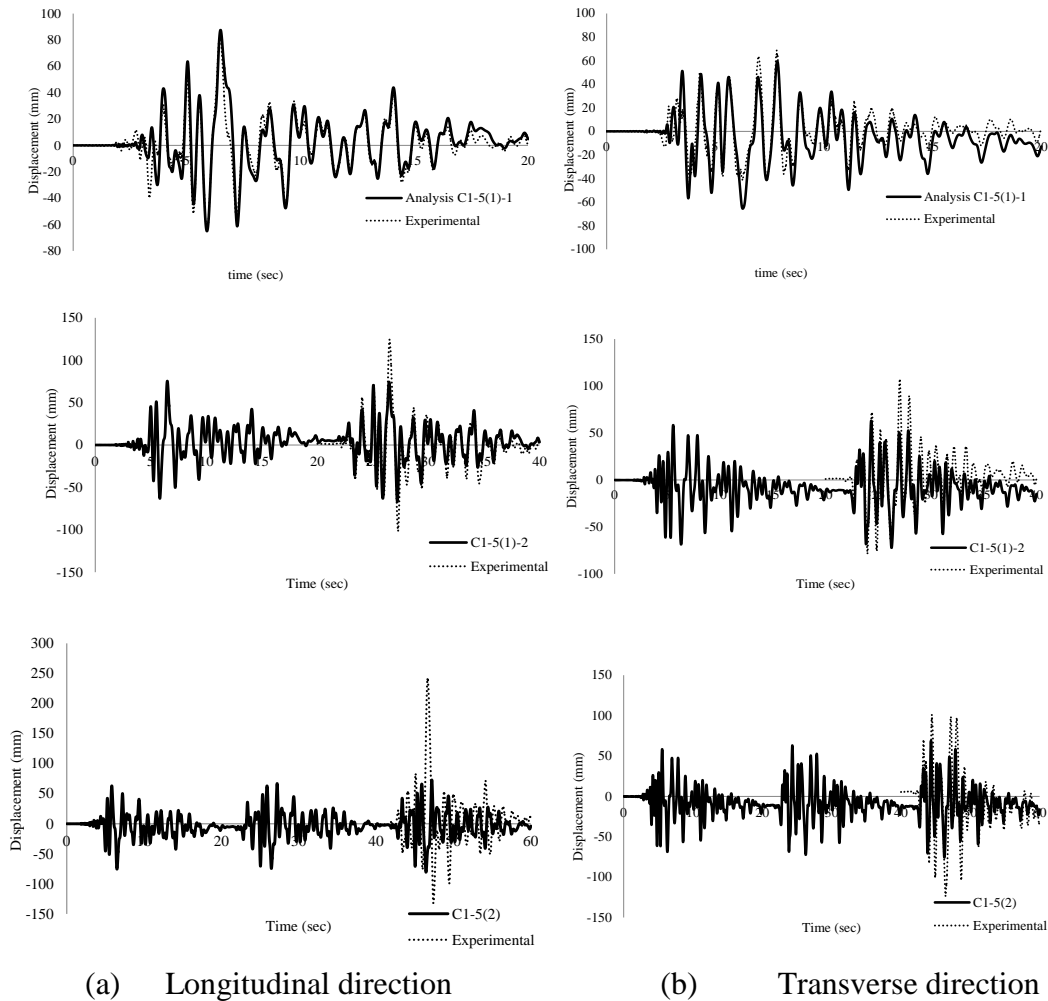


**Figure 3.16** Time-history relationships for C1-5 analytical cases

time correspond to 174 KNm for longitudinal direction and 181 KNm in transverse direction. The calculated values of experimental energy dissipation for C1-5(1)-1 correspond to 180 KNm for longitudinal direction and 140 KNm for transverse direction. In this case, comparing the values of energy dissipation for analysis and experiment it is clear that the analysis acceptably predicts the level of energy dissipated by the column, although it is slightly overestimated in transverse direction.

Looking at the cases of C1-5(1)-2 at 40 seconds of loading time and C1-5(2) at 60 seconds of loading time, in transverse direction the values or energy dissipation of analysis and experiment are somehow close to each other. In case C1-5(1)-2, analytical energy dissipation corresponds to 275 KNm while experimental corresponds



to 318 KNm. In case C1-5(2), analytical energy dissipation corresponds to 376 KNm and experimental energy dissipation corresponds to 409 KNm.

On the other hand, for longitudinal direction, although some portions of the hysteretic response are acceptably described, the failure to accurately grasp the maximum displacement in the analysis for C1-5(1)-2 and C1-5(2), produces an important underestimation in the analytical energy dissipation in this direction. With that, in the case of C1-5(1)-2, analytical energy dissipation corresponds to 219 KNm while experimental corresponds to 281 KNm. For C1-5(2), analytical energy dissipation corresponds to 292 KNm and experimental energy dissipation corresponds to 497 KNm.

The interpretation of analytical results can be further performed by evaluating the hysteretic energy dissipation capacity of all cases. Hereafter, the hysteretic energy dissipation corresponds to the enclosed area of the load-displacement relationships, calculated for analytical response and experimental cases. The energy dissipation is calculated at the end of each analytical cycle, corresponding to total loading time. The analytical calculated energy dissipation for C1-5(1)-1 at 20 seconds of total loading time correspond to 174 KNm for longitudinal direction and 181 KNm in transverse direction. The calculated values of experimental energy dissipation for C1-5(1)-1 correspond to 180 KNm for longitudinal direction and 140 KNm for transverse direction. In this case, comparing the values of energy dissipation for analysis and experiment it is clear that the analysis acceptably predicts the level of energy dissipated by the column, although it is slightly overestimated in transverse direction.

Looking at the cases of C1-5(1)-2 at 40 seconds of loading time and C1-5(2) at 60 seconds of loading time, in transverse direction the values or energy dissipation of analysis and experiment are somehow close to each other. In case C1-5(1)-2, analytical energy dissipation corresponds to 275 KNm while experimental corresponds to 318 KNm. In case C1-5(2), analytical energy dissipation corresponds to 376 KNm and experimental energy dissipation corresponds to 409 KNm.

On the other hand, for longitudinal direction, although some portions of the hysteretic response are acceptably described, the failure to accurately grasp the maximum displacement in the analysis for C1-5(1)-2 and C1-5(2), produces an important underestimation in the analytical energy dissipation in this direction. With that, in the case of C1-5(1)-2, analytical energy dissipation corresponds to 219 KNm while

experimental corresponds to 281 KNm. For C1-5(2), analytical energy dissipation corresponds to 292 KNm and experimental energy dissipation corresponds to 497 KNm.

Looking at Fig. 7, the time-histories are presented for the analysis. In case C1-5(1)-1 the results correspond to a one 100% E-Takatori corresponding to 20 seconds, while in C1-5(1)-2 are two 100% E-Takatori corresponding to 40 seconds and in C1-5(2) are three 100% E-Takatori corresponding to 60 seconds. In the case of C1-5(1)-2 and C1-5(2) the last 20 seconds are compared to the experiment, which performed accumulation of damage by loading separately each case in sequences of 20 seconds (Kawashima et al. 2010), and since in the analysis the loading sequences are continuous, the last 20 seconds correspond to the displacement-time relationship that is co-related to damage accumulation or cumulative damage.

In these results, the longitudinal direction shows acceptable capability of predicting the residual displacement from all three cases. Case C1-5(1)-1 in longitudinal direction shows the best agreement between analysis and experiment among all the cases. The effect of accumulation of damage is acceptably described for longitudinal direction, in the transition from first to second loading in case C1-5(1)-2 and from second to third loading in case C1-5(2), as shown by the analytical and experimental displacements in those portions. The transverse direction however came short in accurately describing this transition.

### References of Chapter 3

- Ang, B. G., Priestley, M. J. N. and Paulay, T. (1989): Seismic Shear Strength of Circular RC Columns, *ACI structural journal*, Vol. 86, No.1, pp. 45-59,
- Hoshikuma, K., Sakai, J., Komori, N. and Sakayanagi, N. (2013): Evaluation of Limit States of Reinforced Concrete Columns for Seismic Design of Highway Bridges, *Technical Note of PWRI*, No. 4262,
- Merta, I. (2004): Shear Strength Model of Reinforced Concrete Circular Cross-Section Members, *Proc. of 5th International Conference on Fracture Mechanics of Concrete and Concrete Structures*, pp. 1297-1302,
- Merta, I. and Kolbitsch, A.: Shear Area of RC Circular Cross-Section Members, *proc. of 31<sup>st</sup> Conference on our World in Concrete and Structures*, 2006.
- Miki, T. and Niwa, J. (2004): Nonlinear Analysis of RC Structural Members using 3D Lattice Model, *Journal of advanced concrete technology*, Vol.2, No.3, pp. 343-358,
- Paulay, T, Priestley M. J. N. (1992): *Seismic Design of Reinforced Concrete and Masonry Buildings*, Wiley Interscience, 1992
- Pique, J. R. and Burgos, M. (2008): Effective Rigidity of Reinforced Concrete Elements in Seismic Analysis and Design, *Proceeding of 14<sup>th</sup> World Conference on Earthquake Engineering*, Beijing, China
- Simão, M.R., and Miki, T. (2015): Dynamic Analysis for RC Columns with Circular Cross Section Using Multi-Directional Polygonal 3DLattice Model, *Proceeding of JCI*, No.2 , 757-762
- Simão, M.R., and Miki, T. (2016): Cumulative Seismic Damage Assessment Circular RC Columns Using Multi-Directional Polygonal 3DLattice Model, *Proceeding of fib*, No.2 , 757-762
- Teran-Gilmore, A. and Jirsa, O.J. (2005): A Damage Model for Practical Seismic Design that Accounts for Low Cycle fatigue. *Earthquake spectra*, Vol. 21, No.3

## **4. NUMERICAL VERIFICATION OF SEISMIC PERFORMANCE OF CIRCULAR RC COLUMNS USING MULTI-DIRECTIONAL POLYGONAL 3D LATTICE MODEL**

### **4.1. Introduction**

Reinforced concrete (RC) structures reluctantly exhibit severe damage subjected to a strong earthquake motion. In Japan in the context of seismic performance of RC structures, the assessment of serviceability and reparability is a primary task after a huge earthquake. In most post-earthquake structural damage evaluation, the analysis is qualitative. However, it is important to establish a quantitative correlation between the observed damage state and an applicable damage index, so as to make the post-earthquake evaluation of damage level in structures more reliable and less time-consuming.

The damage index normalizes the damage evaluation criteria and the threshold values influence the decision related to repair and retrofitting, and they should be connected to the damage states, with clear definition of the damage level and failure mechanism. This is specially the case on the context of performance-based design, where performance objectives are set so that the structural capacity for each performance level is related to a state of damage and is quantified using one or more engineering limit states.

With a new focus in seismic design on the performance of reinforced concrete bridges, commonly current seismic design standards for reinforced concrete bridges do not provide adequate performance design requirements. Although previous research on the response of reinforced concrete bridge columns is extensive, these studies are not adequate to develop all aspects of performance-oriented design. Development of performance-based design methods requires further experimental and analytical investigations to evaluate intermediate damage levels and to develop analytical models and appropriate design methodologies (Lehman and Mohele 2000).

Based on the above considerations, the multi-direction polygonal 3D lattice model is proposed to perform the verification of performance level of RC columns from the material point of view based on sustained seismic induced damage (Simão and Miki 2015).

## 4.2. Energy Dissipation Capacity in RC Columns

### 4.2.1. Introduction

In the field of engineering mechanics the evaluation of behavior of structures has traditionally focused on strength and deformation capacity. In those cases to a certain level of applied force, a certain level of displacement is expected and from that the behavior of the structure understood from pure force-deformation criteria. It is nonetheless true that in modern design of structures, the structural members tend to be composite structures. That means that more than one material is used in the same member and thus the global structural response is very much dependent on material behavior. At the material level a division between brittle materials, quasi-brittle material and ductile materials can be found. That is specially the case in RC structures; where concrete is a quasi-brittle material and steel reinforcement a ductile material. At this level the behavior of materials is best understood by looking and the stress and strain conditions, and the criteria that differentiates the material type is the energy dissipation criteria. In this sub-chapter energy capacity of materials will be studied in the context of seismic damage evaluation (Popov 1990).

### 4.2.2. Hysteretic energy dissipation

Tembulkar & Nau (1987) stated that damage attained by a RC member under dynamic loading can be assessed by a well-constructed hysteretic model. Furthermore, with well-defined parameters, energy based hysteresis models may successfully represent seismic response considering the deteriorating behavior of RC members.

On the other hand, Bousias et al. (1995) reported that the strong coupling between the two transverse plane directions of columns produces an apparent reduction of strength and stiffness in each of the two transverse plane directions when considered separately, but also an increase in hysteretic energy.

With that, the cumulative hysteretic energy dissipation is a very important notion in the analysis of cyclic behavior of RC structures, because it relates to the global damage potential and energy capacity. The hysteretic energy is calculated considering the area of each loading cycle in the X (longitudinal) and Y (transverse) direction for the lateral force and displacement relationships, and the total energy dissipation is calculated as the sum of these two parts. **Equations 4.1, 4.2 and 4.3** express the analytical relationships.

$$E_{d-x} = \int F_x d_x \quad (4.1)$$

$$E_{d-y} = \int F_y d_y \quad (4.2)$$

$$E_{d-total} = \int F_x d_x + \int F_y d_y \quad (4.3)$$

where  $E_{d-x}$  is hysteretic energy dissipation in X direction;  $E_{d-y}$  is hysteretic energy dissipation in Y direction;  $E_{d-total}$  is total hysteretic energy dissipation;  $F_x$  is force in X direction and  $F_y$  is force in Y direction

### 4.2.3. Elemental energy dissipation

The 3D lattice model offers some unique characteristics in terms of analytical capacity of the composing analytical elements. Because of the truss and arch analogy, the analytical response is obtained individually for every component of the system. The lattice model comprises several elements, and it is assumed that an average stress and strain relationship governs each one of them. In other words, the stress and strain relationships define the strain energy for each element in the lattice model, that is concrete and reinforcement elements.

This definition can be very useful for the calculation of strain energy after the target of analysis has reached the yielding point, and especially because of highly nonlinear behavior of concrete after cracking. That way, the strain energy density for one element is defined as presented in **Equation 4.4**, and the accumulated strain energy density of a material is shown in **Equation 4.5**.

$$E_{ei} = \frac{1}{2}(\sigma_i(t) + \sigma_i(t-1))(\varepsilon_i(t) - \varepsilon_i(t-1)) \quad (4.4)$$

$$E_{s-mat} = \sum_{t=1}^n E_e(t) \quad (4.5)$$

where  $E_{ei}$  is the elemental strain energy density,  $\varepsilon_i(t)$  is strain in element  $i$  at time step  $t$ ,  $\sigma_i(t)$  is the strain in element  $i$  at time step  $t$ ,  $E_{s-mat}$  is the accumulated material strain energy.

By taking into account the energy dissipation in individual elements, the distribution of energy dissipation in a RC column can be evaluated by the lattice model. Based on this assumption the energy dissipated in each element can be calculated from the product of the strain energy dissipated in each element, where the strain energy is the area enclosed by the stress-strain relationship for the unloading and reloading curves, and the elemental volume. RC member accumulated energy dissipation will be the sum of all the elemental energy dissipation histories as shown in **Equation 4.5** below.

$$E_{d-mat} = E_{s-mat} \times V_e \quad (4.5)$$

where  $E_{d-mat}$  is the accumulated energy dissipation of the material in the member  $E_{s-mat}$  is the accumulated strain energy density for all element and  $V_e$  is the Volume of elements which for simplicity is assumed to be constant

### 4.3. Damage Range Evaluation

#### 4.3.1. Introduction

The evaluation of seismic damage of concrete structures is very important in order to take countermeasures, such as repair and strengthening the deteriorated structures after severe earthquakes. In technical literature, a large number of damage indexes have been proposed. Some of them are based on cyclic fatigue concepts (Krawinkler and Zohrei 1983) and others make use of structural mode (Dipassquale and Cakmak 1990,). Furthermore, a group of damage indexes include ductility ratio or plastic deformation (Powell and Allahabadi 1988; Cosenza et al.1988) whilst some concern hysteretic energy absorption (Dipassquale and Cakmak 1989; Fajfar 1992). Other damage indexes are a integration of different parameters. For example, Park's and Ang's model (Park and Ang 1985], and Reinhorn's and Valles's model (Reinhorn and Valles 1995) consist of both deformation and energy terms.

From the material point of view however it is very useful to derive a damage index from the energy criteria point of view, because in that way a useful understanding of the actual damage range capacity of the material can be attained, based on the strain energy density analysis, issues of resilience and toughness can be studied and thus providing a better understanding of the damage distribution in material that is connected to structural performance. However, global damage condition of a structure can only be assessed using energy methods if there is knowledge about the total energy capacity.

Based on the discretization method of the lattice model it is possible to determine from an elemental level the expected energy capacity of single elements and compare them to the response obtained from the analytical results

#### **4.3.2. Evaluation of seismic damage using damage index**

In order to realize the performance evaluation of RC columns under seismic loading, it is very important to quantitatively verify the damage states. In this study, this is performed by looking at the damage level, based on the measured damage range measures at the end of the relevant loading sequence. To do that, damage range evaluation is proposed using a damage index defined from the material point of view based on energy criteria for concrete and steel reinforcement. In order to use the energy dissipated as an indicator of seismic damage in concrete structures, the total energy dissipated must somehow be normalized so as to compare the results of different size specimens (Inoue 1994).

In this study damage index is defined from the energy dissipation point of view. In that way, damage index in material is defined as the ratio between the calculated materials accumulated energy dissipation and the ultimate material energy dissipation. The ultimate material energy dissipation is obtained from the constitutive models for ultimate condition of materials and for concrete for concrete in compression is used the model proposed by Mander et al.(1988), concrete in tension proposed by Uchida et al. (1991) and reinforcement proposed by Fukuura and Maekawa (1997). In the case of concrete the ultimate strain in compression is assumed to be 0.0035 when concrete crushes and the ultimate compressive stress corresponds to 0.002 of compressive strain. The tensile strain is calculated using the 1/4 model (Uchida et al. 1991). The damage index in material is presented as:

$$DI_{mat} = \frac{E_{d-mat}}{E_{d-ultimate}} \quad (4.6)$$

here  $DI_{mat}$  is the damage index of the material,  $E_{d-mat}$  is the accumulated energy dissipation of the material in the member and  $E_{d-ultimate}$  is the ultimate energy dissipation of the material in the member.



## 4.4. Numerical Verification of Seismic Performance

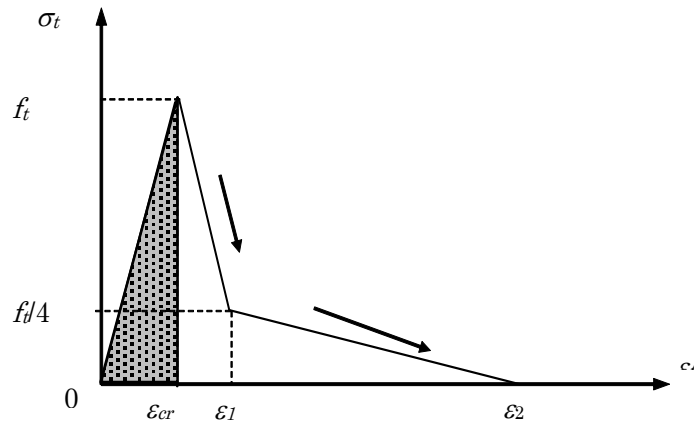
### 4.4.1. Analytical frame-work

In the context of performance-based seismic design most codes define a single level of seismic hazard and a single level of performance that is generally understood to be life-safety i.e. performance objectives other than the life-safety are not evaluated explicitly. As seismic performance objectives can be defined based on expected performance levels, according to Li et al. (2013), structural damage conditions can be assessed from 0-1. Here damage condition 0 means no damage at all, while damage condition 1.0 means total failure of structure. This convention is quite simple and useful to evaluate the damage potential in structures.

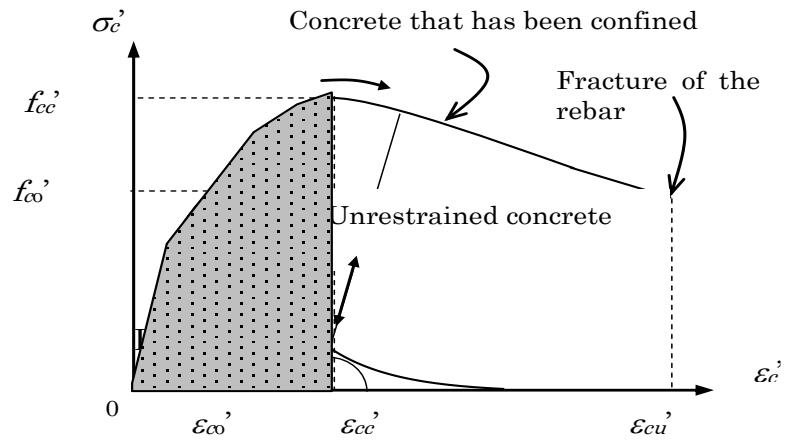
In this study, this convention will be applied at the material level, where to the same extent damage level 0 corresponds to sound material and damage level 1 corresponds to total failure of material. In this study a damage potential separation point named damage limitation point (*DLP*) is proposed. The *DLP* corresponds to the point in the damage scale where damage potential changes from moderate to high. The *DLP* corresponds to a theoretical threshold in the damage scale where damage potential in the material becomes critical under the given loading conditions and is defined for concrete and reinforcement as follows:

To understand this concept it is useful to fall back to classic engineering mechanics of solids and explained by Popov (1990). According to the later resilience corresponds to the ability of material to absorb energy without suffering plastic strain. On a stress-strain diagram of material the area of the elastic region represents the density of strain energy that can be absorbed without any permanent damage to the material or the so called *modulus of resilience*  $U_R$ . On the other hand, toughness corresponds to the ability of the material to absorb energy prior to fracture, and in the stress-strain diagram of the material it is represented by the full area of the enclosure prior to fracture or the so called *modulus of toughness*  $U_T$ . With that two important threshold values are presented: resilience and toughness.

In order to use this analogy and extend these concepts to numerical evaluation of RC structures a few assumptions are important: the first one is that the constitutive models of material used in this study are to be best extent possible representatives of the actual behavior of material is seismic response, and in the analysis process a few simplifications are necessary to ensure practicability of the method.



(a) Concrete in tension



(b) Concrete in compression

**Figure 4.1** Damage limitation points in concrete

Based on the explained, DLP will be the ratio between modulus of resilience and modulus of toughness.

$$DLP_{mat} = \frac{U_{R-mat}}{U_{T-mat}} \quad (4.7)$$

where  $DLP_{mat}$  is the damage limitation point of material,  $U_{R-mat}$  is the *modulus of resilience* of material and  $U_{T-mat}$  is the *modulus of toughness* of material. In concrete the *modulus of toughness* corresponds to the sum of total enclosed area of stress-strain diagram in tension side and in compression side or in other words the ultimate strain energy density in concrete.

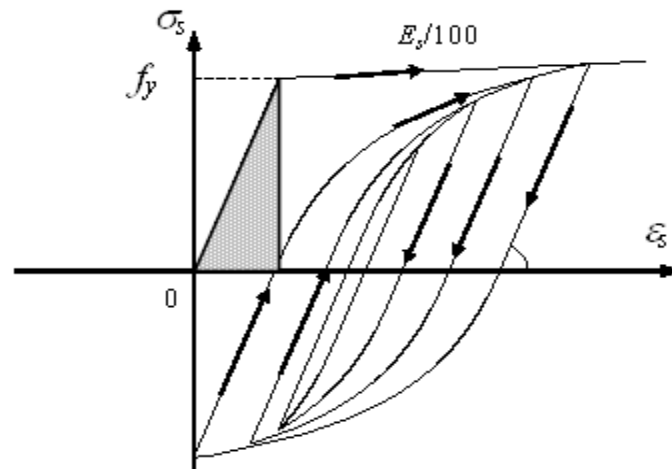


**Figure 4.2** Damage limitation points in steel reinforcement

On the other hand, *modulus of resilience* in tension side is the sum between the tensile strain energy density at cracking of concrete represented by the hatched area in **Figure 4.1(a)** and the compressive strain energy density at maximum stress which is represented by the hatched area in **Figure 4.1(b)**.

The same approach is used for reinforcement. In that case the *modulus of toughness* corresponds to the sum of total enclosed area of stress-strain diagram until fracture of reinforcement or the total strain energy density of reinforcement. On the other hand the *modulus of resilience* corresponds to the an closure represented in hatch in **Figure 4.2**, which is the yielding strain energy density of reinforcement.

In the numerical evaluation of seismic performance the damage index of material is compared to *DLP*. The detailed explanation of the method is shown in the next sub-chapter.

#### **4.4.2. Evaluation of performance states**

In order to establish a co-relation between the analogies describe in sub-chapter 4.4.1, and real structural damage condition and from that derive structural performance of RC member, it is important to look at the JSCE specifications (2002) and experimental evidence to co-relate damage index and observed structural performance.

With that, based on the seismic performance criteria indicated by JSCE (2002) three seismic performance levels of structures are defined. First, the seismic performance that is assumed to correspond to small residual deformation on a structure and in principle yield load of the member is not reached. In the seismic performance II the load carrying capacity does not deteriorate after an earthquake and finally in the seismic performance III it is required that the whole structural system does not collapse.

On the other hand, Kawashima et al. (2010) clearly described the seismic performance of RC columns from the material point of view based on experimental evidence. According to their experimental observations, in this study, the seismic performance of RC columns will be evaluated based on damage index and correlated to structural damage as discussed in the previous research (JSCE specifications 2002; Kawashima et al. 2010)

With that, in order to evaluate the performance, damage range between 0 to  $DLP$  corresponds to a seismic performance category I (SP-I), and damage range between  $DLP$  to 1.0 corresponds to a seismic performance category II (SP-II), respectively. As for the SP-I of concrete, the maximum structural damage corresponds to cracking of cover concrete. For reinforcement the maximum structural damage corresponds to yielding and buckling of reinforcement.

On the other, hand in the SP-II for concrete the maximum structural damage condition is spalling of cover concrete, crushing of concrete and fracture of confined concrete, for reinforcement the maximum structural damage is fracture of reinforcement.

## **4.5. Numerical Verification of Seismic Performance of RC column subjected to Cyclic Loading**

### **4.5.1. Outline of analysis**

The experimental case (Hoshikuma et al. 2013) described in sub-chapter 3.5.1 will be used to perform the numerical verification of seismic performance of RC column that has been subjected to cyclic loading. The target is a circular cross section column named C-29. The cross section of this column is circular with diameter of 600 mm and column height of 3410 mm. The compressive strength and the Young's modulus of concrete are 31.8 N/mm<sup>2</sup> and 28000 N/mm<sup>2</sup>, respectively.

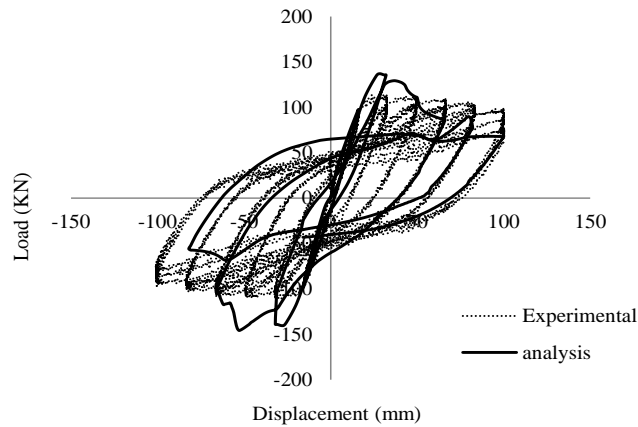


**Figure 4.3** C-29(3) load-displacement

The longitudinal reinforcement of D10 and transverse reinforcement D6 have yield strength of  $397 \text{ N/mm}^2$  and the transverse reinforcement D6 has yield strength of  $397 \text{ N/mm}^2$ , respectively. In order to conduct the analysis, three scenarios related to different inertia reduction factors were studied, corresponding to C-29(1), C-29(3) and C-29(3). In this cub-chapter the focus will be case C-29(3) which offered the best agreement between analysis and experiment in load-displacement curve. Detailed explanation of all the cases can be found in chapter 3.5.1. The load-displacement curve of C-29(3) is shown in **Figure 4.3**.

#### **4.5.2. Analytical results and discussion**

The seismic performance verification of column C-29(3) is presented in **Table 1**. The results show that energy accumulated dissipation of concrete is  $35.4 \text{ kN-m}$  and ultimate energy dissipation of concrete is  $151.1 \text{ kN-m}$ , while in reinforcement the accumulated energy dissipation is  $202 \text{ kN-m}$  and ultimate energy dissipation is  $6072 \text{ kN-m}$ . This means that by large in the given conditions, the damage potential is bigger in concrete than in steel as and also the idea that energy the energy dissipation potential of steel reinforcement is by large most significant than that of concrete in damage resistance capacity due to higher ductility of steel reinforcement.

Looking at the seismic performance of materials, it can be assessed that the damage index of concrete corresponds to 0.59 and is placed between the *DLP* and 1, and the damage index of steel reinforcement is 0.00008 and is placed between 0 and *DLP*.

**Table 1:** seismic performance verification of column C-29(3)

Material		Concrete	Steel
Energy dissipation KN-m	Accumulated	35.4	202
	Ultimate	151.1	3036
DLP		0.40	0.004
Damage index		0.59	0.00008
Seismic performance		SP-II	SP-I

With that, the concrete performance is that of SP-II and the performance of reinforcement is that of SP-I. In terms of structural seismic performance it is important to correlate the observed structural damage reported by the experiment. Based on the definition provided, analytical seismic performance criteria concrete has been affected by cracking followed by spalling of cover concrete. Reinforcement on the other hand, has been affected by yielding of reinforcement at the plastic hinge followed by localized buckling.

Sensitivity analysis of concrete suggests that because the damage index is not far from the value of *DLP* perhaps the sustained damage is not critical. On the other hand, reinforcement is less affected by the seismic action based on the calculated damage index, which is confirmed by visual inspection of the experimental target (Hoshikuma et al. 2013).

The report on the experimental results, clearly show the progress of damage in the column C-29. The mechanism of failure is flexural, and flexural cracking developed along the column, with visible concentration on the plastic hinge. The observed damage condition of concrete in experiment corresponds to cracking and some spalling, which is predicted by the analytical model. In reinforcement only yielding is observed in the experiment, which corresponds to SP-I in the analytical performance verification method proposed.

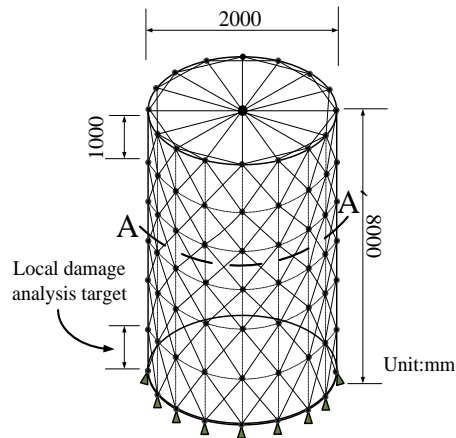


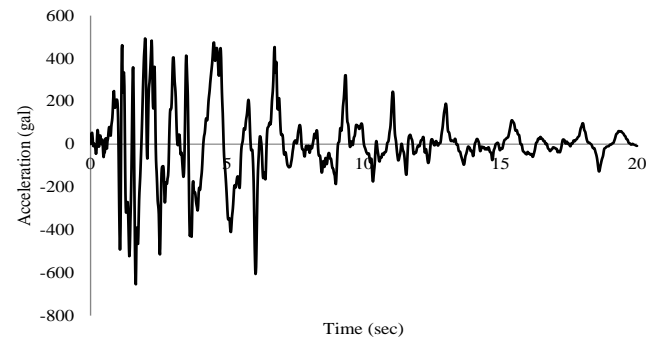
**Figure 4.4** C1-5 Analytical model

## **4.6. Performance Evaluation of RC Columns Subjected to Seismic Motion Designed according to 2002 JRA Specifications**

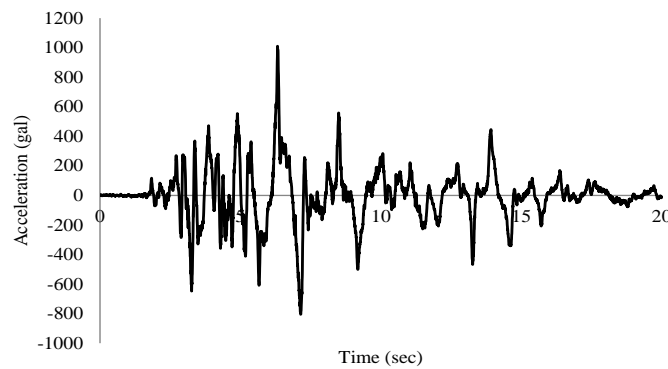
### **4.6.1. Outlines of Analysis**

In order to perform the analysis the analytical target is a circular cross section column named C1-5 tested using a shake-table by E-Defense. The complete detailing of column C1-5 is shown in sub-chapter 3.4.2. The specimen is a cantilever circular column with diameter 2000 mm. The heights of the column and footing correspond to 7500 mm and 1800 mm respectively. The analytical model is shown in shown in **Figure 4.4**. Column C1-5 was excited using a near-field ground motion which was recorded at the JR Takatori Station during the 1995 Kobe earthquake. Taking into account the soil/structure interaction, a ground motion with 80% of the original intensity of JR Takatori name E-Takatori was imposed as command to the table in the experiment and corresponds to 100% E-Takatori. In this study the analysis will focus on C1-5(1) corresponding to 100% E-Takatori and C1-5(3) corresponding to 125% E-Takatori and 21% top mass increase, respectively. The input accelerations are shown in **Figure 4.5** for longitudinal direction.

Simão & Miki (2014) reported that on a cantilever bridge column, about 50% of damage is concentrated below the column mid-height. Based on that, it is reasonable to assume that the most significant concentration of damage at the bottom is very representative of damage condition. In order to analyze Localized damage evaluation, numerical verification of damage concentration is performed in case C1-5(1). The height at the bottom of the column portion where it is assumed that the plastic hinge



(a) 100% E-Takatori



(b) 125% E-Takatori

**Figure 4.5** E-Takatori acceleration - longitudinal direction (Kawashima et al. 2010)

will develop and thus numerical verification of damage concentration is performed is 1000 mm corresponding to the first layer of lattice model elements as shown in **Figure 4.4**.

#### 4.6.2. Analytical results and discussion

The results of analysis are presented for C1-5(1) and C1-5(3) regarding the load-displacement relationships in **Figure 4.6**. The calculated analytical and experimental hysteretic energy dissipations are presented in **Table 2**. In **Table 3** is presented the analysis on levels of performance for C1-5(1) for concrete and steel reinforcement.

A detailed look at **Figure 4.6** shows that for both C1-5(1) and C1-5(3) the multi-directional polygonal 3D lattice model acceptably shows the hysteretic behavior, comparing the analytical response and the experiment in longitudinal and transverse directions. In general, there is an over-estimation in initial stiffness, and this is due to the fact that by discretizing a circular column using the multi-directional polygonal 3D lattice model, more elements are needed to accurately describe the detailing of the column as in opposition to a 3D lattice model applied to a rectangular column (Miki and



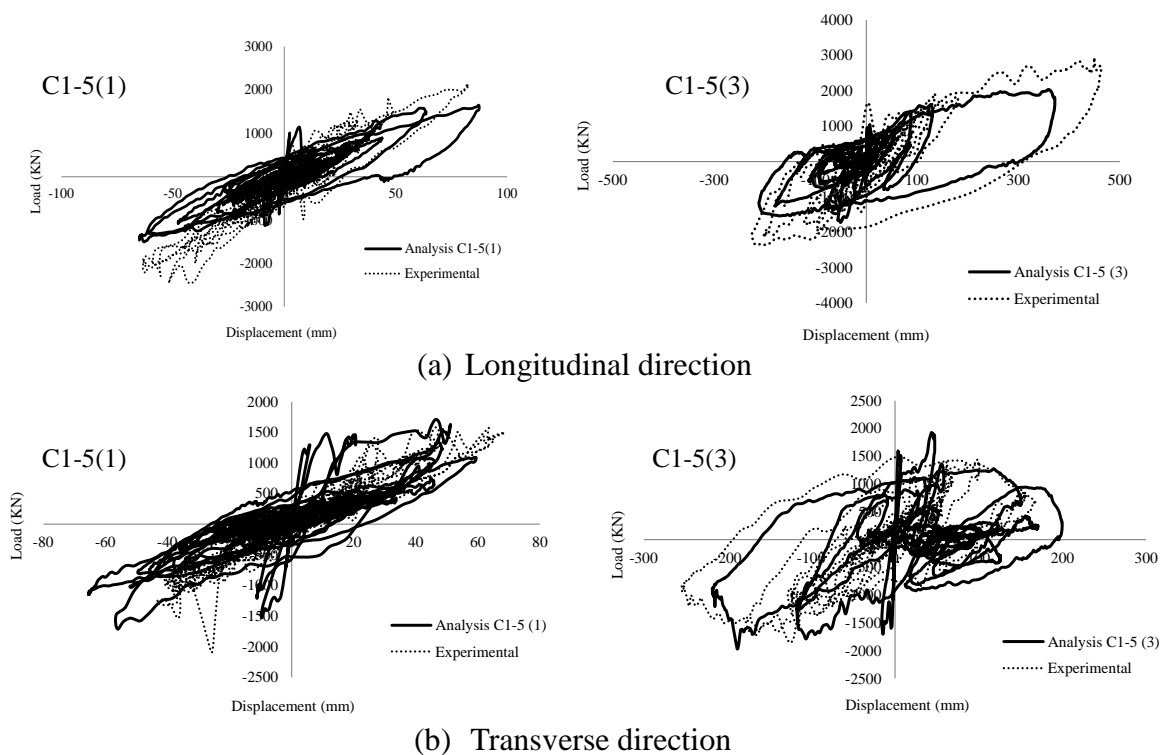


**Figure 4.6** Load-displacement relationship computed using analytical model

Niwa 2004) or representing a circular cross-section column using a circular-rectangular cross-sectional area equivalence. On the other hand the maximum displacement capacity and the strength have acceptable agreement between analysis and experiment.

The hysteretic energy dissipation that has been calculated and shown in **Table 2** for analysis and experiment shows that by looking at the ratios between analysis and experiment, in the case of C1-5(1) corresponds to 1.24 and for C1-5(3) corresponds to 0.87. These values suggest that generally the method grasp the behavior of the column acceptably and furthermore the impact of the slight overestimation if initial stiffness is not very big on energy dissipation capacity.

In **Table 3**, the results for performance level of column are shown. Looking at the analytical results, in concrete the response strain energy corresponds to  $3.60 \text{ N/mm}^2$  while the total strain energy corresponds to  $8.91 \text{ N/mm}^2$ . Furthermore accumulated response energy dissipation corresponds to  $12.05 \text{ KN-m}$  while total energy dissipation corresponds to  $41.87 \text{ KN-m}$ . Furthermore accumulated response energy dissipation corresponds to  $12.05 \text{ KN-m}$  while total energy dissipation corresponds to  $41.87 \text{ KN-m}$ . For steel reinforcement on the other hand, response strain energy is equal to  $12.13 \text{ N/mm}^2$  while the total strain energy is equal to  $316.02 \text{ N/mm}^2$ .

**Table 2:** Hysteretic energy dissipation of column C1-5

Hysteretic Energy dissipation (KN-m)	C1-5(1)	C1-5(3)
Analysis (1)	353	2466
Experimental (2)	283	2808
(1)/(2)	1.24	0.87

**Table 3:** Concentrated seismic performance evaluation of C1-5(1)

Material		Concrete	Steel
Strain energy N/mm <sup>2</sup>	Accumulated	3.60	12.13
	Ultimate	8.91	316.02
Energy dissipation KN-m	Accumulated	12.05	20.75
	Ultimate	41.87	201.9
Damage limitation point (DLP)		0.39	0.43
Damage index		0.33	0.04
Performance Level		SP-I	SP-I

On the accumulated material energy dissipation, response energy dissipation is equal to 20.75 KN-m while total accumulated energy dissipation is equal to 201.9 KN-m. These results show that by a large margin steel reinforcement is more ductile than concrete in one hand, and also based on energy dissipation levels, in concrete the C1-5(1) case produced almost a quarter of total energy dissipation capacity, while in reinforcement it had a small significance. The objective of assessing seismic performance levels in material in this study is realized comparing the damage index of material to the damage scale previously explained. In that manner, for concrete the damage index calculated corresponds to 0.33, which falls between 0 and *DLP* that corresponds to 0.39. This corresponds to performance level SP-I. On the other hand, in the case of steel reinforcement, the calculated damage index is 0.04 and that corresponds to performance level SP-I. For both materials based on the performance levels, the damage range corresponding is moderate. However a more detailed look at both damage indexes suggests that concrete by far as been more exposed to greater damage such as occurrence of some level of cracking because it's damage index of 0.33 is close to the threshold *DLP* value of 0.39. This is further confirmed by the report on the experimental program (Kawashima et al. 2010) which states that after the first shaking corresponding to C1-5(1) concrete shows some visible damage cracks.

#### References of Chapter 4

Cosenza, E, Manfredi, G, Ramasco, R. (1988): The Use of Damage Functionals in Earthquake Engineering: A Comparison Between Different Methods, *Journal of Earthquake Engineering and Structural Dynamics*, Vol.22, No.10, pp. 855-868

Dipasquale, E., Cakmak, A. S. (1989): *On the Relation between Local and Global Damage Indices*, Technical Report No. NCEER- 89/34, National Centre for Earthquake Engineering Research, State University of New York at Buffalo, NY

Dipasquale, E, Cakmak, A. S. (1990): Seismic Damage Assessment Using Linear Models, *Journal of Soil Dynamics and Earthquake Engineering*, Vol.9, No.4, pp.194-215

Fajfar, P. (1992): Equivalent Ductility Factors Taking into Account Low Cycle Fatigue, *Journal of Soil Dynamics and Earthquake Engineering*, Vol.21, No.10), pp.837-848.

Fukuura, N. and Maekawa, K. (1997): Computational Model of Reinforcing Bar Under Reversed Cyclic Loading for RC Nonlinear Analysis. *Journal of Materials, Concrete Structures and Pavements*, JSCE, Vol. 564, No.35, pp.291-295.

Hoshikuma, K., Sakai, J., Komori, N. and Sakayanagi, N., (2013): *Evaluation of Limit States of Reinforced Concrete Columns for seismic Design of Highway Bridges*, Technical Note of PWRI, No. 4262. (in Japanese)

Inoue, S. 1994. *Ductility and energy dissipation of concrete beam members and their damage evaluation based on hysteretic energy dissipation*, Kyoto: Kyoto University Press

JSCE (2002): Standard specifications for concrete structures-2002, Seismic Performance Verification, December.

Kawashima, K., Sasaki, T., Ukon, H., Kajiwara, K., Unjoh, S., Sakai, J., Kosa, k., Takahashi, Y., Yabe, M., and Matsuzaki, H. (20010): Evaluation of Seismic Performance of a Circular Reinforced Concrete Bridge Column Designed in Accordance With the Current Design Code Based on E-Defense Excitation, *Journal of JSCE*, vol.66, no.2, pp. 324-343.

Krawinkler, H, Zohrei, M. (1983): Cumulative Damage in Steel Structures Subjected to Earthquake Ground Motions, *Journal of Computers and Structures*, Vol.16, No.1-4, pp.531-541

Li, D. Peng, Y. Ning, M. and Long, G., (2013): A New Strategy to Assess the Seismic Energy Dissipation Safety of Reinforced Concrete Bridge Piers, *International Journal of Energy Engineering*, Vol.3, pp.55-61.

Mander, J. B., Priestley, M. J. and Park, R. (1988): Theoretical Stress-Strain Model for Confined Concrete, *Journal of Structural Engineering*, ASCE, Vol. 114, No.8, pp. 1804-1826.

Park, Y. J., Ang, A. H. S. (1985): Mechanistic Seismic Damage Model for Reinforced Concrete, *Journal of Structural Division (ASCE)*, Vol.111, No.4, pp.722-739

Popov, E. P. (1990): *Engineering Mechanics of Solids*, Prentice –Hall Inc. Vol.2.

Powell, G. H., Allahabadi, R. (1988): Seismic Damage Prediction by Deterministic Methods: Concepts and Procedures, *Journal of Earthquake Engineering and Structural Dynamics*, Vol.16, No.5, pp.719-734

Reinhorn, A. M., and Valles, R. E. (1995): *Damage Evaluation in Inelastic Response of Structures: A Deterministic Approach*, Report No. NCEER-95, National Centre for Earthquake Engineering Research, State University of New York at Buffalo,

Simão, M.R. and Miki, T. (2015): Damage Evaluation of RC Columns Subjected to Seismic Loading by Energy Dissipation Using 3D Lattice Model. *Proceeding of 2015 fib Conference*: Leipzig.

Simão, M.R. and Miki, T. (2014): Seismic Damage Range Evaluation of RC Columns with Circular Cross Section by Energy Dissipation Using 3D Lattice Model. *Proc. 2014 JSCE International Summer symposium*: Osaka.

Uchida, U., Rokugo, K., and Koyanagi, W. (1991): Determination of Tension Softening Diagrams of Concrete by Means of Bending Tests, *Journal of Materials, Concrete Structures and Pavements*, JSCE, No.426, Vol.14: 203-212.

## **5. PERFORMANCE EVALUATION OF RC VIADUCT**

### **5.1. Introduction**

Viaducts as civil structures are in the epicenter of societies. Good and sound viaducts provide the infrastructure from which socio-economic development can be put to place. This is the case especially in Japan, because the country has a very extensive network of elevated viaducts, mainly in urban areas. Whenever an earthquake takes place in Japan, viaducts are very much exposed to seismic induce damage. This was the case with the Hyogo-ken Nanbu earthquake, which cause the collapse and ultimately failure of many reinforced concert structures, but especially viaducts.

The evaluation of damage remains a highly difficult task, because so many factors influence the level of damage and response of an RC (reinforced concrete) structure, even within the same structure with similar arrangements of reinforcement and concrete member's cross sections. Factors such as soil conditions, applied ground motions and other properties of the earthquakes such distance from the fault line and epicenter, material and structural specifications such as strength and stiffness of material and deterioration of concrete and reinforcement based on the age of materials, ensure that this task will remains ever complex. But still, even with the complex nature of the analysis, it is ever important to study the behavior of RC viaducts under seismic loadings, if not for their interesting and challenging analysis process, definitely for their social and economic importance.

In this study, the dynamic lattice model was introduced and used for the evaluation of structural response under cyclic loading. Furthermore, from the dynamic analysis, energy dissipation was proposed as means to evaluate damage range under seismic loading from a RC column, either for the whole target or more specifically the most damaged zone, according to a specific case assessment. On that note, using the concept of energy dissipation presented ion chapter four, this chapter will perform analysis of damage in a RC rigid-frame viaduct that suffered damage during the Hyogo-ken Nanbu earthquake. In this analysis the buckling behavior of reinforcement at the end of columns is taken to account, but the bond-slip behavior of reinforcing bars at the joint portion as well as soil and structure interaction are not considered.

## 5.2. Damage Distribution in RC Viaducts Based on Energy Dissipation

### 5.2.1. Outline of target structure

The seismic performance evaluation is performed for Hansui R5 which is a rigid-frame railroad viaduct. The target is a beam-slab type rigid-frame RC viaduct with three-span. The viaduct was designed according to Structural Design Standards of Japan National Railways enacted in 1970. Here, the viaducts were designed using the seismic intensity method with a design horizontal seismic intensity of 0.2 (Miki, 2004). In the observation of actual structures, the degree of damage was determined according to most heavily damaged members in the viaduct. **Figure 5.1** shows the dimensions and reinforcement arrangement of Hansui R5. In **Figure 5.2**, the ground-motion acceleration for the viaduct in transverse and longitudinal direction is shown.

In the viaduct, the cross section of a column was a square of 900 mm. All reinforcing bars in the columns had a minimum concrete cover of 60 mm. The beams had rectangular cross section with 700 mm width and 1,000 mm depth for the upper portion in transverse direction, while with 700 mm width and 1,100 mm depth for other portions. Heights of columns were 5,000 mm and 4,000 mm in lower and upper portions, respectively. The compressive strength of concrete was 29.1 MPa, while the tensile strength was 1.27 MPa to a Young's modulus of 18.4 GPa. The longitudinal reinforcement had yield strength of 322 MPa, ultimate strength of 521 MPa and Young's modulus of 203 GPa. While the transverse reinforcement had yield strength of 263 MPa, ultimate strength of 380 MPa and Young's modulus of 183 GPa.

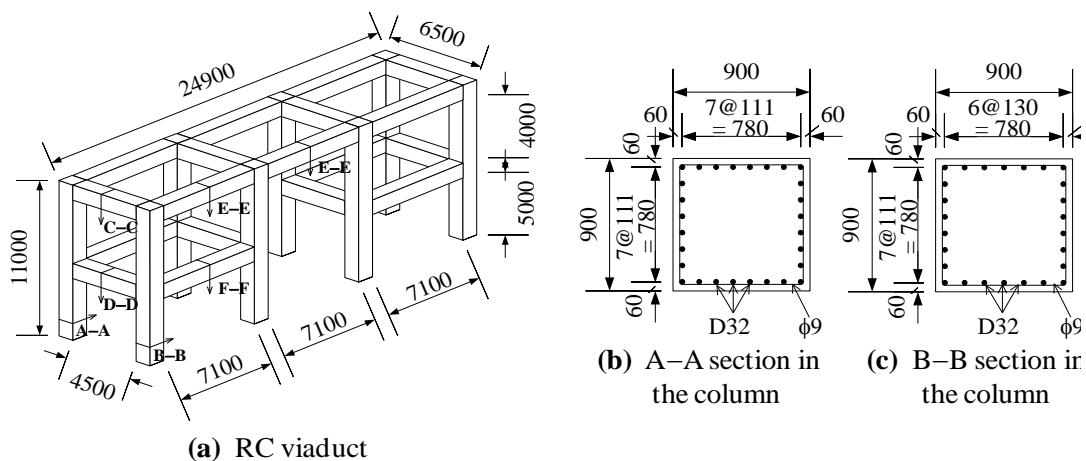
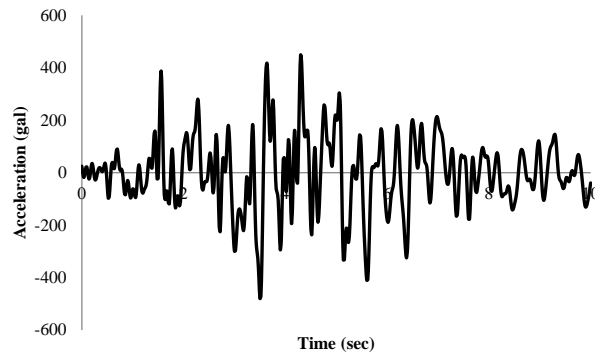
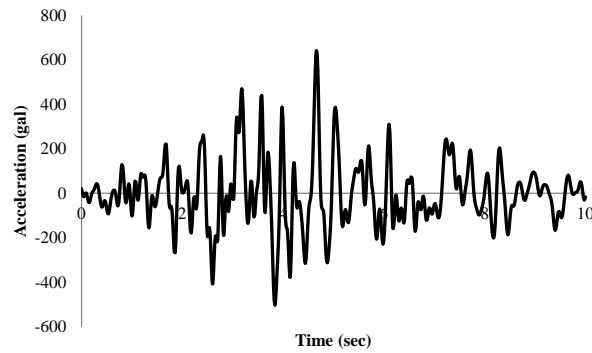


**Figure 5.1** Dimensions and arrangements of reinforcement in Hansui R5 Viaduct (Miki, 2004)



(a) Longitudinal (NS)



(b) Transverse (EW)

**Figure 5.2** Hansui R5 Input ground motion

### 5.2.2. Configuration of lattice model

The 3D dynamic lattice model and the boundary conditions used in the analysis are illustrated in **Figure 5.3**. The three-span viaduct is treated as a unit of the analytical model. As seen in the figure, the model consists of beams and columns, while the slab is not included. In the analysis, it is assumed that the masses corresponding to the self-weight of viaducts are uniformly distributed over all nodal points, using the lumped-mass idealization. It is also assumed that there is a concentrated mass, which is equal to the weight of the superstructure and the slab, acting on the top nodes of columns and beams. It is considered that the joints of each column and beam are rigidly connected between each member. According to the flexural deformation of columns and beams, it is appropriate to provide arch members in two layers along the longitudinal direction of the member axis.

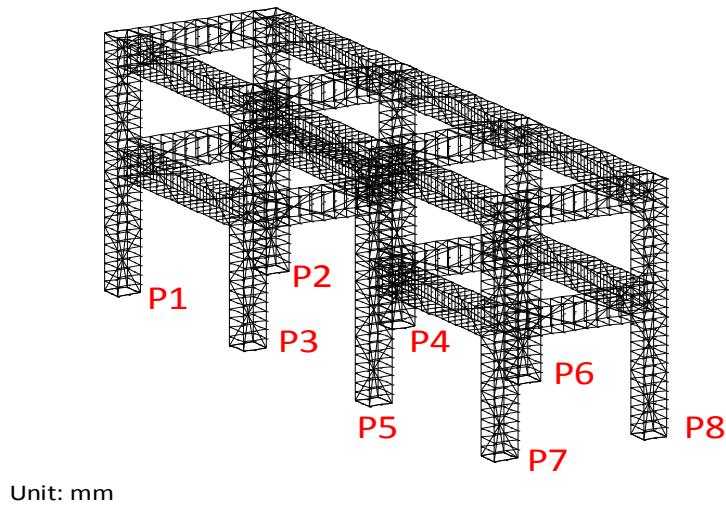


**Figure 5.3** Lattice model of Hansui R5 Viaduct (Miki.2004)

Hence, the arch members in both columns and beams are modeled into eight concrete members. Similarly, at the column-beam joint portion, four arch members are modeled as. In order to determine the cross-sectional area of arch members in the 3D lattice model, the values of  $t_b$  and  $t_d$  are determined based on the theorem of minimization of the total potential energy. The calculations for the values of  $t_b$  and  $t_d$  are conducted on each structural member individually.

Viaducts are founded on the sufficiently stiff ground; it is assumed that the input ground motion is directly applied to the bottom of each lower column. The 3D lattice model treats the RC viaduct that is disregarded the foundation, and consequently the interaction between the structure and soil is not considered in the analysis. For the boundary between neighboring viaducts in the longitudinal direction, the horizontal direction is assumed to be a free condition.

In the dynamic analysis it is assumed that the viscous damping is neglected ( $h=0$ ) and the numerical damping of the Newmark method with factors  $\beta=0.36$  and  $\gamma=0.70$  is used as time integration. Here a time interval of 0.01 sec. is set, the Newton-Raphson iteration method is used for the calculations until an adequately converged solution is obtained, since the nonlinear responses appear in RC structures when they are subjected to large ground motions.

In order to check the convergence, the out-of-balance force and energy increment are



compared with initial values during the iteration. The convergence tolerances of the out-of-balance force and energy are set to be 0.001 and 0.01, respectively (Miki 2004).

### 5.2.3. Damage distribution of Hansui R5 viaduct

The damage distribution evaluation is performed according to the principle of energy dissipation previously presented. The damage will be focused on the columns of Hansui RC. In order to evaluate the damage, the structure, the elemental stress and strain of the 8 columns that are part of the structure will be used for the calculation of strain energy. This same strain energy will be multiplied by each individual volume, related to each specific elemental stress and strain and thus energy dissipation computed. The analysis will evaluate the amount of damage in terms of energy dissipation for the whole column height, followed by a specific focus on the bottom layer, in which case corresponds to the height of 2100 mm corresponding to six lattice layers. Furthermore, for column P1, the joint between the column and the beam will be object of calculation. The damage range of the pier of the Hansui R5 has been calculated, based on their energy dissipation. The assumption that more energy dissipated means potentially a bigger range and degree of damage allows a clear and practical assessment of damage sustained because of seismic excitation. **Figure 5.4** shows the damage of eight piers that are part of the target.

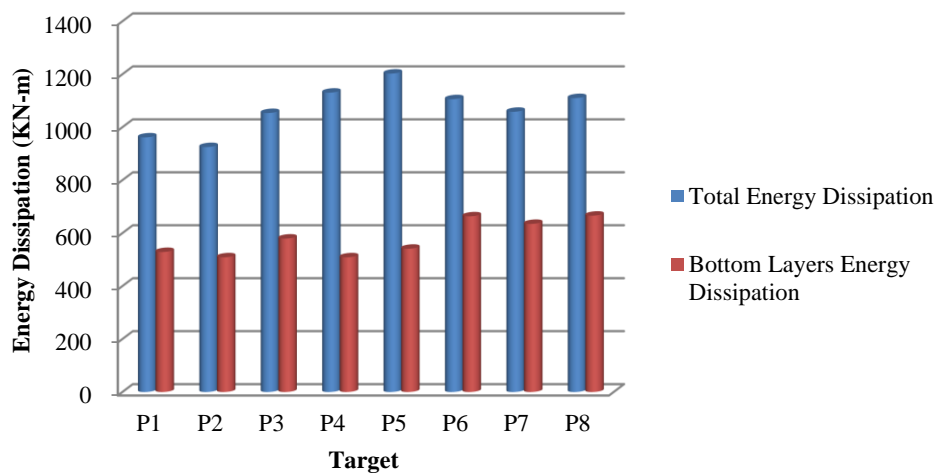


**Figure 5.4** Damage distribution evaluation of Hansui R5 piers

The damaged has been calculated to the full height of the piers, as well as bottom layers corresponding to a height of 2100 mm. from the analysis pier P5 in the presents the biggest damage range equivalent to a energy dissipation of 1203 kN-m, while pier P2 presents the least damage range which is equivalent to 925 kN-m. In general, the region composed by piers P3, P4, P5 and P6 has the biggest damage range, and in the structure this region corresponds to the transition zone from one set of piers to the following, with no stiffness beam connecting them, as visible in Figure 5.3

The calculations of damage range at the bottom of the columns suggest that about 40% to 60% of the total damage was there located. This proved totally independent from the actual total energy dissipation. In other word piers P6 and P8 had about 60% of damage concentrated at the bottom, the maximum percentage, but their total energy dissipation does not correspond to the maximum values if the entire targets are object of comparison, thus proving the complex and nonlinear nature of this estimations.

**Figure 5.5** shows the location of the joint within pier P1. The energy dissipation at the joint has been calculated, in order to understand its contribution to the general state of damage range of P1. The results are presented in **Figure 5.6**. The total energy dissipation at the joint is 147 KN-m which corresponds to 13% of the total energy dissipation of the pier. The energy was calculated considering the four arch members that are part of the joint lattice model structure. The value of energy dissipation at the joint and thus damage range is small when compared to the contribution of the bottom layer.

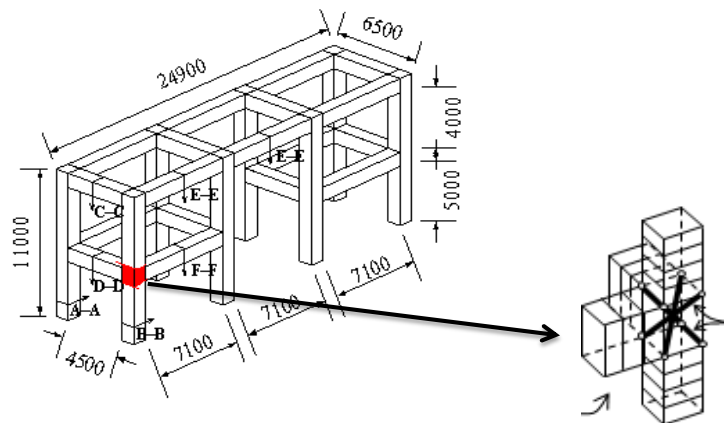


**Figure 5.5** Damage range evaluation of P1 joint

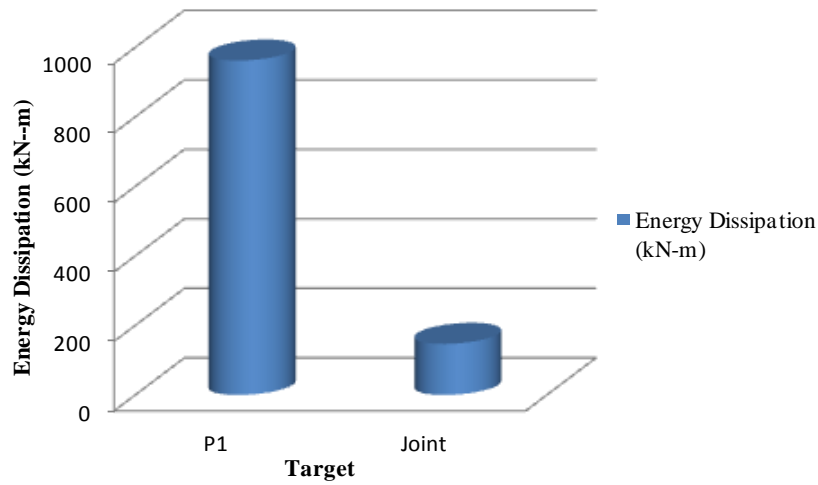


**Figure 5.6** P1 and P1 joint comparative Energy Dissipation

In other words the level of damage range at the top of the column is much less than the level of damage at the bottom, and the joint, although it represents a portion of discontinuity in the columns, that is the behavior is affected by the connection to the beam, showed reduced damage range level. This is most likely related to the stiffness the connection beam introduced to the system at that level.

**Figure 5.7** shows the actual damage conditions of the Hansui R5 viaduct after the earthquake.



**Figure 5.7** Damaged conditions of Hansui R5 (Miki.2004)

It is possible to visualize at first glance that the biggest range of damage is at the bottom of the piers. The damage range analysis based on energy dissipation correctly predicted that this would be the actual damage situation. Looking closer at the joint of the piers, the level of damage is not as elevated as it is at the bottom, and this is related to the decreased level of energy dissipation at this point that was calculated using the 3D lattice model. Although very complex, the level of response and damage was acceptably predicted by the 3D Dynamic Lattice Model, especially the damage range evaluation considering the nonlinearities, by using the stress-strain relationships for the calculation of strain energy, further applied for the estimation of energy dissipation in order to predict damage range.

By comparing between the actual damage condition and the analytical response of RC viaducts, the validity of the 3D dynamic lattice model has been confirmed at the structural system level. The analytical response predicted by the 3D dynamic lattice model is used to evaluate the seismic performance of RC structures.

The maximum displacement during the earthquake and the residual displacement after the earthquake are useful to evaluate the possibility of the restoration or rehabilitation after the earthquake occurs. In order to evaluate the seismic performance of a RC structure, the predicted response, such as the maximum and residual displacements, can be compared with the limiting values determined from the importance of target structures.

### **5.3. Numerical Verification of Seismic Performance of Hansui R5 Viaduct**

In order to perform the numerical verification of seismic performance of Hansui viaduct, the analytical target has been subjected to the motion presented in **Figure 5.2**. In order to perform the simulation, the footing is not modeled and at the bottom of each lower column a fixed support is provided. In this analysis a personal computer Pentium 4 with 1.7 GHz was used and the total computation time is about 3 hours, where the total time and time intervals were set to be 10 sec and 0.01 sec, respectively (Miki 2004).

The numerical verification method fully detailed in Chapter 4, was applied to the columns of Hansui viaduct and the analytical results are described in **Table 4**. The time history is presented in **Figure 5.8**; in the figure it is visible that the calculation fails at 4 seconds of acceleration. Therefore the numerical verification has limited time scope.

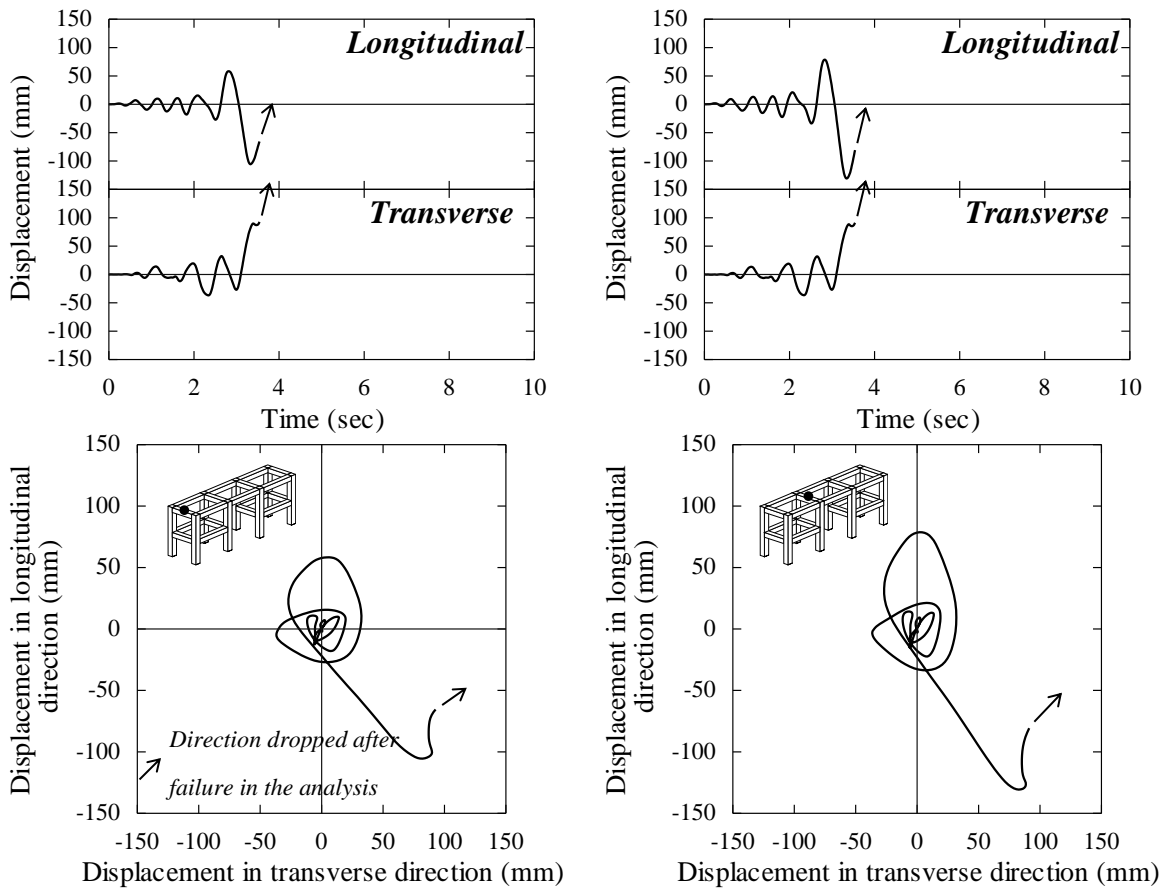


**Figure 5.8** Analytical responses for Hansui R5 Viaduct

The analytical results shown in **Figure 5.8** represent the response obtained at different target points marked in black dot in the figures. From the response, it is possible to observe that the longitudinal direction is dominant in both cases for the target point and in the case represented in the right in the figure, where the target point is an inner beam, the maximum observable displacement is about 100mm compared to the case presented to the left where it is a bit over 50mm. This might be due to the stiffening effect observed in the outer layer members, which present a stiffer response when subjected to seismic motion.

On the other hand, one of the key objectives of this work is to make use of energy dissipation criteria to evaluate the performance of RC structures under seismic motion. With that, the analytical results offer a great chance to understand the performance of the structure from the material point of view up to the moment the calculation is interrupted. The resumed calculations regarding the seismic performance evaluation of the Hansui viaduct from the material point of view are shown in **Table 4**.

**Table 4:** Seismic performance evaluation of Hansui viaduct

Column	Damage Limitation Point		Damage Index (DI)		Seismic Performance	
	Concrete	Steel	Concrete	Steel	Concrete	Steel
P1	0.4	0.0038	0.05	0.00072	SP-I	SP-I
P2	0.4	0.0038	0.06	0.00070	SP-I	SP-I
P3	0.4	0.0038	0.06	0.00078	SP-I	SP-I
P4	0.4	0.0038	0.07	0.00087	SP-I	SP-I
P5	0.4	0.0038	0.08	0.00090	SP-I	SP-I
P6	0.4	0.0038	0.07	0.00089	SP-I	SP-I
P7	0.4	0.0038	0.06	0.00079	SP-I	SP-I
P8	0.4	0.0038	0.07	0.00087	SP-I	SP-I

The columns of Hansui viaduct present the same material properties and distribution of reinforcement and because of that looking at the table the damage limitation point is the same for all the targets. On the other hand the damage index is calculated for each target and compared to the damage limitation point to understand the performance of the materials at 4 seconds of shaking. The overall results suggest that both materials remain structurally sound after the first 4 seconds. For concrete in all 8 peers, the seismic performance level is SP-I, which corresponds to the first level. At the structural damage level in concrete in all 8 peers, cracking of concrete as well as some level of spalling can be expected in visual inspection. On the other hand for the case of steel reinforcement in all 8 peers, the seismic performance category is SP-I. At the material level the maximum observable damage condition expected in yielding of reinforcement.

The analytical method proposed can generally predict the damage states from a numerical point of view. However it is necessary to conduct some sensitive analysis on the values presented by the methods in order to be better informed about the real damage condition of structures. With that, comparing the values of the damage indexes calculated for concrete and for steel with the damage limitation point of each material it is possible to understand that numerically they are considerably apart. In other words, the damage indexes are considerably smaller than the damage limitation points. In the definition of damage limitation point, it has been said that this corresponds to the threshold value where the damage potential of the material changes from moderate to considerable, and based on this definition at 4 seconds of shaking, it is possible to conclude that both material still present a considerable sound state.

#### **5.4. Seismic Design and Retrofit Considerations based on 3D Lattice Model**

The standard goal of every analytical model in seismic analysis is to contribute to a better understanding of the complex factors that affect the behavior of RC structures in seismic events. Miki (2004) states in his doctoral thesis that one of the key concepts the updated JSCE standard specification establish is the concept that inelastic deformation can considerably be observed in RC structures after the longitudinal reinforcement yields, in opposition to the idea that only plastic behavior of structures subjected to strong motion is considered. On the other hand Priestley et al. (1996) stated that the use of elastic design promotes a false sense of the response levels to be expected under seismic attack and typically will result in severely underestimated displacements while encouraging designers to ignore aspects of ductility and rational hierarchy of strengths.

In current design practice a large consideration should be given do ductility aspects. Ductility being defined as: the ability of the structural member to displace inelastically through several cycles of response without significant degradation of strength or stiffness. This is specially the case for bridge columns, where sudden loss of strength or stiffness can have catastrophic results and ultimately lead to structural failure and collapse. In the discussion pertaining ductility, strength, stiffness, energy dissipation and deformation are at the center of discussion. Although mathematically ductility is defined as the ration between deformation at a certain level of response to the level of deformation at yielding, understanding strength, stiffness, energy dissipation and deformation allows a much more informed decision on design aspects of RC bridge elements, especially columns

The contribution of the 3D lattice model for the design and retrofit of RC structures can be seen from a multitude of approaches. Recent development in earthquake engineering allow the improved estimation of earthquake input ground motions and thus allowing the dynamic analysis using input ground motion that has been recorded during actual earthquakes to be used in the performance evaluation of RC structures. With a discretization method that is simplified, the 3D lattice model allows the typical use of dynamic analysis using actual ground motion to relatively easily estimate the seismic performance of existing RC structures while retaining reasonable computational time.

On the other hand, aspects of design can be seen through the lenses of Priestley et al. (1996). According to their discussion, in design several different measures of strength must be considered. They discuss required strength, nominal strength, expected strength,

dependable strength, extreme strength, ideal strength and according to their discussion, in design, the presented strength characteristics follow a Gaussian or bell shaped distribution, on a relationship between strength and frequency. That evaluation shows how important it is to correctly grasp the response strength of a structure under seismic loading. Throughout the analysis the 3D lattice model has shown consistency in correctly predicting the strength to a certain load. The evidence of that is the extensive comparison between analytical results and experimental information to give proof or reliability. In that sense it can be useful to use to 3D lattice model to evaluate the strength of RC structural members.

The contribution of the 3D lattice model can be extended to aspects of retrofit as well. It is commonplace that still existing RC bridges have been designed without clear understanding of performance states or performance demand in actual seismic events. The result of that is that many RC bridges have been designed to substandard codes and so in seismic events, their performance is not to be taken for granted and it is necessary to go back and verify the expected levels of performance under seismic loading so that appropriate retrofitting action can be taken.

With a better understanding of site seismicity, which might be the single most important aspect in retrofit consideration, the modeling and simulation of existing RC bridges can easily be performed under dynamic analysis using the 3D lattice model. A simple example of the applicability of the 3D lattice model is in the retrofitting of RC Columns. In many cases they are retrofitted using steel jackets, which act as an extremely efficient transverse reinforcement. In that manner it is possible to simulate different transverse reinforcement ratios using the 3D lattice model to make a more informed decision on the steel jacketing to be used.

## **References in Chapter 5**

Miki, T.(2004): Nonlinear Analysis of Reinforced Concrete Structures Subjected to Seismic Loads by Using Three-Dimensional Lattice model, Tokyo Institute of Technology, Doctoral Thesis, March

Priestley, M.J.N., Seibe, F. and Calvi, G.M.(1996): Seismic Design and Retrofit of Bridges, Willey and sons, March



## **6. CONCLUSIONS AND RECOMMENDATIONS FOR FUTURE RESEARCH**

### **6.1. General Conclusions**

This study presented the performance evaluation of reinforced concrete (RC) structures subjected to seismic loading using 3D lattice model. The concept of 3D lattice model defines the shear resisting mechanism in terms of arch and truss actions in RC structural member. The truss action is comprised of an orthogonal coordinate system defined by three planes, as for the arch part, the internal stress flow is idealized as the compressive strut. The fundamental 3D lattice model has been developed for a quadrangular cross section target structure. In this study an expansion of scope is presented, with the development of 3D lattice model that targets circular cross section columns. Furthermore the damage analysis is performed and taken further by proposing a seismic performance evaluation method. With that a few important conclusions may be taken.

The applicability of the 3D lattice model to perform static analysis on reinforced concrete columns with circular cross section is verified through the application of the 3D lattice model previously developed, to a circular cross section column, considering equivalence in cross-sectional area in geometry to a rectangular cross section. A second and new approach is proposed, the multi-directional polygonal 3D lattice model, with more realistic geometrical discretization.

Looking at the analytical results, the circular to rectangular equivalence in cross sectional area shows acceptable performance in response prediction based on initial stiffness, however its applicability has a larger scope in 2D analysis, in 3D analysis a more realistic discretization is obtained using the multi-directional polygonal 3D lattice model. The performance of the multi-directional polygonal 3D lattice model is considered acceptable both in terms of general response prediction of the envelope curve comparing initially to linear-elastic curve obtained from analysis of large-scale bridge pier followed by analysis performed on a column subjected to monotonic loading test. In both cases good agreement was observed in initial stiffness of the columns when reduction factors of cross-section area of concrete part of RC column are used. However, comparing analysis to the experimental results it was observed that the initial response strength is slightly overestimated.

The applicability of the 3D lattice model to perform dynamic analysis for reinforced concrete columns with circular cross section is proposed. The analytical results show

that before cracking, the geometrical equivalence between circular and square cross sectional areas produces softer and more acceptable results, especially with relation to initial stiffness. On the other hand, in the inelastic range, the multi-directional polygonal 3D lattice model shows reasonable accuracy in hysteresis analysis, either considering the reduction of shear resisting area of concrete or reduction in the flexural stiffness that occurs in seismic response of RC members.

In this research the multi-directional polygonal 3D lattice model is proposed in order to perform cumulative seismic damage evaluation of circular cross section RC columns under multiple loading sequences. The analytical results suggest that after the first shake the model works in an acceptable way to predict the transition from one loading sequence to the following, as well as residual displacement in longitudinal direction, and the energy dissipation capacity for one, two or three of loading sequences in transverse direction.

In the analysis, the hysteretic response should be conjugated with the energy dissipation capacity and the residual displacement in order to have a more complete evaluation of the response. This need is proved by the increased complexity in the nonlinear behavior that is introduced by shaking the analytical target to more than one excitation.

The applicability of this model to perform cumulative damage analysis is verified under a limited scope. Based on that, for further stages of this study, the research should focus on reducing the intrinsic initial high initial stiffness observed in elastic response, as it influenced the stiffness degradation in inelastic phase in some cases. Furthermore, underestimation of response displacement in higher order shaking sequences should also be closely looked at.

The applicability of the 3D lattice model to perform damage evaluation of reinforced concrete columns with circular cross section is proposed using the multi-directional polygonal 3D lattice model. The analytical results confirm the applicability of the model, especially the hysteretic response after cracking of concrete. Damage evaluation has been proposed from the material point of view considering the accumulated energy dissipation of concrete and reinforcement, which are dependent on strain energy. Analytical results show that by large scale, steel reinforcement is the most dominant material in seismic resistance capacity.

The analysis of damage considering the critical damage condition point (CDP), allowed the reasonable prediction of real structure damage condition. At this point in this research, suffices to assume that damage range potential between 0 and CDP is moderate, while damage range from CDP to 1 is consistent with more severe damage potential, especially for concrete which presents less ductility capacity when compared to steel reinforcement.

In this study, numerical verification of seismic for circular RC columns using multi-directional polygonal 3D lattice model is proposed. From the analysis, it is verified that based on static analysis, it is possible to acceptably reduce the high elastic stiffness observed in the modeling previously proposed based on the dynamic analysis. This suggests that a more fundamental treatment using static analysis should be given to the analytical target when the main focus of analysis is the elastic range.

The damage index and seismic performance categories, allows the numerical evaluation of performance of material based on the seismic performance criteria broadly described by JSCE and fundamental experimental work performed by Kawashima et al. (2010) which are the basis considered in this study to co-relate damage index and structural performance evaluation from the material point of view.

Furthermore a full framed rail road viaduct was subject to damage analysis using energy dissipation developed from 3D dynamic analysis. The target structure was Hansui R5 viaduct. The results from the analysis have good level of agreement with the actual damage structure when compared. From the analysis the bottom layer was the most damaged position of the piers, very much visible in the post-damage figure presented. Furthermore, the joint of pier P1 was subjected to analysis, and based on its energy dissipation which was about 13% of the total for the pier, it was concluded that it presented a very small level of damage when compared to the remaining parts of the structure, especially the bottom.

## **6.2. Recommendations for Future Research**

While conducting this research the complex nature of the issues studied was always present and throughout the study, decision on simplification of procedure and assumptions had to be made. With that certain aspects remain to be further researched to achieve better results.

In the modeling of RC columns using the multi-directional polygonal 3D lattice model there should be a profound experimental study to clarify the arch action in circular columns. In this study although an analytical approach was presented using the direct stiffness method, a more fundamental experimental and analytical research on the arch action in circular columns is needed to reduce the degree of uncertainty.

In the discretization of circular columns using the multi-directional polygonal 3D lattice model for the truss part, a separation between Inner Diagonal Members (IDM), Surface Diagonal Members (SDM) and Diagonal Members in Transverse direction (DMT) has been used. This was the geometry that was found to best work at this stage and stable enough to conduct the analysis. However other geometries should be further investigated and in the current research elemental cross section of diagonal members in the multi-directional polygonal 3D lattice model has been proposed using simplified formulas, but the calculation of their cross sectional area can be better achieved using more sophisticated formulation.

Still regarding the modeling using the multi-directional polygonal 3D lattice model, in the case of dynamic analysis, high plastic stiffness is observed in the response. In this study the applicability of the dynamic analysis was focused on the inelastic range and thus the initial stiffness of the model overestimation was not profoundly investigated. On further research some investigation on how to reduce the elastic stiffness should be performed, especially if the focus is the elastic design of RC members.

One of the key features of the 3D lattice model is the reduced need for computational time due to the reduced number of degrees of freedom. So with that in analysis, especially the geometrical modeling it is important to keep in mind that choices have to be made so that the computational requirements of the analysis will not grow at a very fast pace, and it is also recommendable that computers with strong memory are used for analysis, especially for the analysis of viaducts.

### **6.3. Further Contributions and Discussion**

Based on the discussions and recommendations from the thesis defense sessions, a number of points for further contribution and discussion in the refinement of scope of this research have been presented. From a general point of view, it is important to clearly understand the scopes of the analytical contributions of the study based on a

laboratory controlled environment to a more practical design environment. In this study, in order to confirm the applicability of the procedures proposed, the analytical information is compared to experimental information. However, in an actual RC structural member, the degree of complexity in response is potentially larger than the observed in laboratory environment, therefore it is important to effectively conduct sensitivity analysis in the interpretation of the analytical and experimental in order to extend the applicability to real RC structures.

Furthermore from a general point of view, there is a big trend in the use of Finite Elements Methods (FEM) as well as others such as the fiber model, already described in this thesis and the Distinctive Elements Methods (DEM). All these analytical models have strong points and weak points, but one of the successes that the Lattice Model achieves when compared to them is the ability to give good prediction of flexural and shear behavior and obtain the appropriate failure mode, which can be verified experimentally while allowing the discretization of RC structural members with a reduced number of degrees of freedom. The consequences of that are that in one hand, the calculation time is greatly reduced. For example for a typical column in this study, the calculation time took more than only a couple of minutes. On the other hand the understanding of the failure mode appropriately allows a much more efficient application of the Lattice Model in the damage evaluation of RC structures, which is based on the understanding of failure modes and grasping real damage progress in structure.

From a specific point of view, another important contribution has been offered. In the comparison between analytical results and the experimental results it is important to keep in the interpretation the effect of pull-out of longitudinal rebar in the footing. The question is that there is a size-dependency in the sense that in smaller column samples, the effect is much more severe than in larger samples. Therefore on a case-by-case basis, it is important to analyze carefully this effect, especially in the case where there is underestimation of the effect such as in smaller column samples.

The lattice model showed good ability to discretize circular columns. Based on that, a further extension of scope would be to study its applicability to study RC piles. Based on the geometry alone, the multi-directional polygonal 3D lattice model can discretize RC piles, however, further research is need in the constitutive modeling as well as soil and structure interaction models.